Mechanics and Assessment of Shoe Tread Wear – Replacement Strategies for Preventing Slips

by

Sarah Louise Hemler

Bachelor of Science in Mechanical Engineering, University of Maryland, Baltimore County, 2015

Submitted to the Graduate Faculty of the

Swanson School of Engineering in partial fulfillment

of the requirements for the degree of

Doctor of Philosophy

University of Pittsburgh

2021

UNIVERSITY OF PITTSBURGH

SWANSON SCHOOL OF ENGINEERING

This dissertation was presented

by

Sarah L. Hemler

It was defended on

May 11, 2021

and approved by

Mark Redfern, Ph.D., William Kepler Whiteford Professor, Bioengineering Department

Brian Moyer, Ph.D., Associate Professor, Department of Mechanical Engineering

Carolyn Sommerich, Ph.D., Associate Professor, Department of Integrated Systems Engineering, The Ohio State University

Rakié Cham, Ph.D., Associate Professor, Bioengineering Department

Dissertation Director: Kurt Beschorner, Ph.D., Associate Professor, Bioengineering Department

Copyright © by Sarah L. Hemler

2021

Mechanics and Assessment of Shoe Tread Wear:
Replacement Strategies for Preventing Slips

Sarah L. Hemler, PhD

University of Pittsburgh, 2021

Slips and falls are a major cause of injury in the workplace. Slips often occur due to insufficient friction and fluid drainage (traction performance) between footwear and a contaminated flooring. Shoe tread is designed to increase traction performance to prevent slipping. As shoe tread wears down, however, the risk of slipping increases. This dissertation examined changes and causes of progressive shoe tread wear and developed shoe replacement strategies to reduce the occurrence of slips. Aim 1 assessed the traction performance changes of shoes worn artificially and naturally through two longitudinal studies. Under-shoe friction and fluid drainage ability decreased with wear. The largest continuous worn region size of the tread was applied to a hydrodynamic model to predict the film thickness between the shoe and flooring. These findings provide knowledge for how traction performance changes across the life of a shoe. This knowledge may help guide shoe testing standards and guide metrics such as the worn region size to recommend replacement. Aim 2 determined the impact of gait kinetics and shoe outsole hardness on tread wear rate. Peak shear forces and the required coefficient of friction were positively correlated with wear rate, but normal force and hardness were not associated with wear rate. This work shows that footwear and replacement strategies could be designed to accommodate individual kinetics. Aim 3 focused on the development of a low-cost tool to scan the shoe tread, determine the worn region size, and predict slip risk. User-centered design techniques were used to incorporate potential users throughout the product design process. The developed scanner was

able to accurately determine the shoe worn region size and subsequently predict slip risk. The tool received a satisfactory approval score from the potential users. Findings from Aim 3 will guide future tool iterations and present important insights for involving potential users in the design of products for preventing falls. Overall, this dissertation quantified changes in shoe traction performance with tread wear, identified factors influencing tread wear, and described the development of a tool to recommend shoe replacement to prevent slip and fall injuries.

Table of Contents

List of Tables

List of Figures

Preface

Acknowledgements

This work was not a singular effort, but rather performed through supported effort. There is no way to list everyone in my village and the giants on whose shoulders I have stood, but I will attempt to express my immense gratitude to those who have championed me in this research, academic, professional, and personal journey.

First, I would like to thank my Heavenly Father who has been my best support, friend, and guide, and has provided incredible friends and colleagues for this journey. He has helped me to *be joyful in hope, patient in hardship, and faithful in prayer* (Romans 12:12).

I would like to express deep gratitude to my Ph.D. adviser and dissertation chair, Dr. Kurt Beschorner, who kindly encouraged me to think deeper, stay curious, and reach higher. He cared for my academic, professional, and personal advancement in these past years for which I am extraordinarily grateful. Second, thank you to my dissertation committee: Dr. Mark Redfern, who has always supported and challenged me to think and write boldly, Dr. Brian Moyer, for his detailed contributions and for making much of this research possible through the robotic slip tester (affectionately called, 'Ivan the Terrible'), Dr. Carolyn Sommerich, who taught me so much of the importance of designing with the user in mind, and Dr. Rakié Cham for her steady support, especially at the end. This work was also supported by the devoted faculty, staff (especially Jenna Trout), graduate and undergraduate students at the University of Pittsburgh Human Movement and Balance Lab; thank you for supporting me to become a better teammate, leader, and friend.

I would like to thank my faithful parents, Pat and Joy, who prayed for me relentlessly and have paved the way for me in countless ways to be able to pursue this education and experience.

A special thank you to my siblings, Ruthie, PJ, Dave, and Jessica, and all my extended family for their faithful support in doing their best to understand my work and relentlessly encourage me. Also, a special thanks to the University of Maryland, Baltimore County (UMBC) Meyerhoff Scholars Program – shout-out to all my M23 family. Thank you to the UMBC Mechanical Engineering Department faculty and staff – especially Drs. Anne Spence, Taryn Bayles, Jamie Gurganus, Marc Zupan, and Neil Rothman, and all the friends who encouraged me to pursue higher education. Thank you to all my friends-turned-family at Allison Park Church for walking alongside this endeavor and holding up my arms to keep me going. A special thanks to Pastor Jeff and Melodie Leake who not only facilitated a church family for growth but encouraged me and fought with me through so many challenging times. I would be remiss if I did not thank a few other key people who encouraged me deeply and prayed with me through these challenging and rewarding years; thank you, India Awes, Dayna Azevedo, Milana Ballard, Kelli Brownlee, Sarah Graefe, Sarah McAtee, Melissa Miller, Nicole Racine, Greta Schaltenbrand, Kyler and Becky Sederwall, Lori Steinsdoerfer, and Barb Trbusich. Also, thank you to my graduate student family at the University of Pittsburgh, especially Erika Pliner, Stephanie Joslyn, Julie Rekant, and Anna Bailes. Thanks to all my amazing friends and family in the Pittsburgh area, across the USA, and globally who have helped me grow and pursue well-roundedness in these last several years.

This work was supported by the National Science Foundation Graduate Research Fellowship Program (NSF GRFP 1747452), the National Institute for Occupational Safety & Health (NIOSH R01 OH 010940), the National Center for Research Resources (NCRR S10RR027102), and the National Institute of Arthritis and Musculoskeletal and Skin Diseases (R43AR064111).

Nomenclature

ACOF – available coefficient of friction

AW1 – accelerated wear experiment #1

AW2 – accelerated wear experiment #2

$\boldsymbol{b}$ – width of the wedge/worn region

$\boldsymbol{F}$ – applied normal force

FFT – fluid force threshold

$\boldsymbol{F_{fluid}}$ – fluid force

FTIR – frustrated total internal reflection

$\boldsymbol{F_x}$ – force in x-direction (shear)

$\boldsymbol{F_y}$ – force in y-direction (shear)

$\boldsymbol{F_z}$ – force in z-direction (normal)

$\boldsymbol{h}$ – film thickness

$\boldsymbol{h_0}$ – minimum film thickness

$\boldsymbol{K_p}$ – wedge incline correction coefficient

$\boldsymbol{l}$ – length of the wedge/worn region

NW – natural wear experiment

$\boldsymbol{p}$ – fluid pressure

PFT – predicted film thickness

PSS – peak slipping speed

SME – subject matter expert

SR – slip-resistant

$\boldsymbol{R_a}$ – arithmetic average roughness

RCOF – required coefficient of friction

$\boldsymbol{R_q}$ – root mean square deviation roughness

$\boldsymbol{R_z}$ – average peak-to-valley roughness

UCD – user-centered design

UCOF – utilized coefficient of friction

UUD – usability, usefulness, desirability

$\Delta \boldsymbol{t}$ – time between frames

$\boldsymbol{v}$ – sliding velocity

WRS – worn region size

$\Delta \boldsymbol{x}$ – distance between scans

$\boldsymbol{\mu}$ - viscosity

$\boldsymbol{\lambda}$ – lambda ratio

$\boldsymbol{\eta}$ – geometry-dependent wedge coefficient

1.0 Introduction

1.1 Motivation

Slips and falls are a leading cause of injury in the workplace. Slips resulting in falls often occur when there is insufficient friction at the shoe-floor interface. Research has shown that shoe outsole (bottom exterior) design and wear influence slip risk. Specifically, increased shoe outsole wear leads to increased slip risk. However, there is a gap in the literature quantifying the changes in traction performance (friction and under-shoe fluid drainage) during progressive shoe wear. Although wear theories have been applied to a variety of conditions for elastomers, of which shoe outsoles are often comprised, there is a paucity of research exploring shoe wear mechanisms. Moreover, there is need for an effective tool to quantify shoe wear in the workplace to inform shoe replacement.

The goal of this project is to quantify shoe traction performance, determine shoe wear mechanisms, and develop a new assessment tool for shoe outsole wear. Quantifying changes in shoe traction performance will create novel understanding of shoe wear progression. This knowledge will inform the testing of wear model mechanisms which will assess the impact of gait kinetics and outsole hardness on shoe wear rate. These factors will guide the development of a tool that will assess shoe outsole wear and guide a shoe replacement recommendation.

The *innovations* of this study arise from a multi-disciplinary (tribology, biomechanics, and user-centered design) approach for reducing the rate of slips and falls:
1) Measure traction performance for shoes progressively worn via accelerated and natural wear, **2)** Model under-shoe fluid films based on shoe tread wear geometry, **3)** Assess the worn condition

of shoes based on the worn region size, **4)** Apply elastomeric wear theory to gait biomechanics and shoe design, and **5)** Develop a low-cost, portable tool to evaluate shoe outsole wear and determine slip risk. The *long-term goal* of providing knowledge and strategies to reduce the number of slips and falls in the workplace will be achieved through the following three specific aims.

1.2 Specific Aims

Aim 1: *Quantify traction performance changes for progressively worn shoes.*

Factors related to slip risk – available coefficient of friction (ACOF) and under-shoe fluid forces – will be quantified for shoes worn via accelerated and natural wear procedures. ACOF and fluid forces will be measured at specific wear/time points for each set of shoes. The size of the worn region on the shoes will be measured and applied to a tapered-wedge solution to determine the predicted film thickness between the shoe and contaminated floor.

Hypothesis 1.1: ACOF will decrease, and fluid force will increase as shoes are worn.

Hypothesis 1.2: Under-shoe fluid dynamics will be predicted from the size of the worn region using thin-film solutions.

Aim 2: *Identify the impact of gait kinetics and shoe outsole hardness on shoe wear rate.*

Wear rate for shoes worn via accelerated and natural wear procedures will be quantified. Gait kinetics for participants wearing naturally worn shoes and shoe outsole hardness for shoes worn via natural and accelerated wear will be assessed. Shoe wear rate will be tested against these kinetic parameters and shoe outsole design factors to determine potential relationships.

Hypothesis 2.1: Higher peak RCOF and higher peak normal forces will accompany higher wear rates.

Hypothesis 2.2: Lower outsole hardness will accompany higher wear rates.

Aim 3: *Develop a low-cost tool to assess the shoe outsole worn region size and determine slip risk.* The wear assessment tool will scan the shoe outsole and determine the size of the worn region. A user-centered design approach will be used to iteratively design, produce, and evaluate the tool for use in service-providing industries.

Objective 3.1: Root mean square error of the tool's measurement for size of the worn region will be below 10%.

Objective 3.2: The tool will achieve a user experience score equal to or greater than 80% based on tool usability, usefulness, and desirability.

Hypothesis 3.1: The tool will predict slips based on the worn region size.

Hypothesis 3.2: The tool will predict under-shoe fluid pressure during slipping based on the worn region size.

1.3 Dissertation Structure

This dissertation is structured in seven chapters:

1. Chapter 1.0 contains the motivations, innovations, and specific aims of the dissertation.
2. Chapter 2.0 addresses previous work and research findings relevant to this work in addition to the theories necessary that serve as the foundation to analyses presented in the dissertation.
3. Chapter 3.0 presents data from a simulated wear experiment and applies a hydrodynamic model to this experimental data (Aim 1).
4. Chapter 4.0 presents a natural wear experiment that occurred in the workplace (Aim 1).
5. Chapter 5.0 presents work on the impact of gait kinetics and shoe outsole hardness on shoe wear rate (Aim 2).
6. Chapter 6.0 describes the development of a tool that assesses shoe outsole wear and predicts slip risk (Aim 3).
7. Chapter 7.0 addresses implications and proposed future work from this dissertation.

2.0 Background

2.1 Slips & Falls

Slips, trips, and falls are a major cause of occupational injuries. In 2019, they accounted for 27.6% of all nonfatal occupational injuries in the United States (U.S. Department of Labor - Bureau of Labor Statistics, 2021) (Figure 2.1). This percentage is consistent with the prior eight years with about 300,000 incidences yearly (U.S. Department of Labor - Bureau of Labor Statistics, 2021) (Figure 2.1). Furthermore, slip, trip, and fall injuries represent 32% of the Workers' Compensation financial burden with a cost of almost $19 billion annually (Liberty Mutual Insurance, 2020).

According to the U.S. Bureau of Labor Statistics, slips, trips, and falls can be separated into three main categories: 1) fall on the same level, 2) fall to a lower level, and 3) slip or trip without a fall (U.S. Department of Labor - Bureau of Labor Statistics, 2021) (Figure 2.1). In 2019, sixty-four percent of the 300,000 injuries due to slips, trips, and falls, were classified as falls on the same level (U.S. Department of Labor - Bureau of Labor Statistics, 2021). These falls on the same level cost almost $11 billion each year with a single fall costing an average of almost $12,000 (Liberty Mutual Insurance, 2018; Washington State Department of Labor & Industries, 2020) (Figure 2.1). The prevalence and cost of these falls signals a continuing need to research methods and developing practical tools for understanding and preventing falls on the same level.

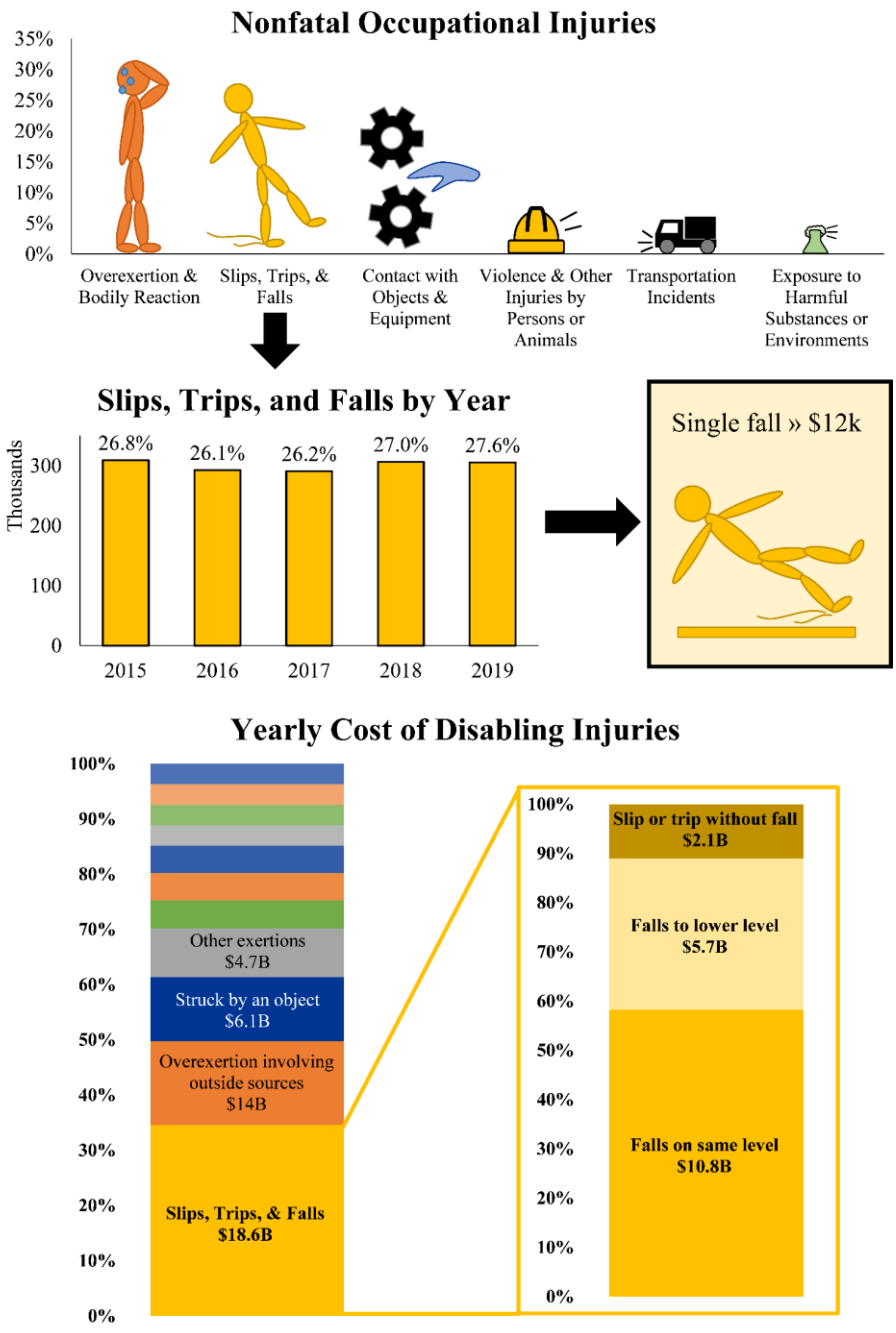

Figure 2.1 Nonfatal Occupational Injuries Summary

(Top) Nonfatal occupational injuries by category (U.S. Department of Labor - Bureau of Labor Statistics, 2021). (Middle) Yearly slips, trips, and falls with respective percentage of nonfatal occupational injuries (U.S. Department of Labor - Bureau of Labor Statistics, 2021) and average cost for a single fall (Washington State Department of Labor & Industries, 2020). (Bottom) Yearly cost of disabling injuries separated by category. Slips, trips, and falls are separated into three main sub-categories (Liberty Mutual Insurance, 2020).

Slipping is a major cause of same level falls. Research has shown that 40-50% of all falls are due to slipping (Courtney, Sorock, Manning, Collins, & Holbein-Jenny, 2001). A slip may be defined as unintentionally sliding of a shoe or foot across a surface after losing static contact during gait. Past research has identified three categories of slipping based on the length of the slip: a 'microslip' is designated as a slip shorter than 3 cm, a slip is generally between 3-10 cm, and a slide describes an uncontrollable movement of the heel generally longer than 10 cm (Leamon & Li, 1990). A microslip is generally unnoticed. A slip will often result in attempting to regain postural control, and a slide is most likely to result in a loss of balance and fall (Chang, Leclercq, Lockhart, & Haslam, 2016). Other research has defined slipping using other metrics such as the peak speed during a slip with a peak slipping speed exceeding 0.2 m/s considered a slip event (Cham & Redfern, 2002; V.H. Sundaram et al., 2020). Across these slip categories, slip initiation is consistently caused by insufficient friction between the shoe and floor. This insufficient friction can be quantified as when the measure of friction available between a shoe and flooring, often termed the available coefficient of friction (ACOF), is less than the friction required for dry walking – required coefficient of friction (RCOF) (Hanson, Redfern, & Mazumdar, 1999) (These friction metrics will be further discussed in Section 2.2.1.). Given variability in ACOF and RCOF between and within a step, this relationship between measured friction and slipping is not deterministic.

This chapter serves to give background to the key themes included in this dissertation. To understand the importance of analyzing shoe-floor interfaces regarding slipping, a deeper analysis of surface interactions is necessary (Section 2.2 – Tribology). The applications of tribology to footwear are presented with corresponding analysis of footwear design and replacement strategies (Section 2.3 – Footwear). Developing informative methods and tools for preventing slips and falls

is an important aspect for implementing change; involving the end user in the design process to produce efficacious methods and tools is subsequently discussed (Section 2.4 – User-Centered Design). Lastly, the gaps in the literature that are addressed by this dissertation are presented (Section 2.5 – Gaps in the Literature).

2.2 Tribology

Tribology is generally the study of the friction, wear, and lubrication between interacting surfaces in relative motion (Stachowiak & Batchelor, 2013). This dissertation focuses on the interaction between shoes and flooring. The outsoles (bottom) of shoes are often comprised of elastomers (i.e., rubber-like polymers). Therefore, this section will focus on elastomeric friction and wear. Applicable lubrication concepts will also be addressed in this section.

2.2.1 Friction

According to the encyclopedia of tribology, friction is "the resisting force tangential to the common boundary between two bodies, when under the action of an external force, one body moves or tends to move relative to the surface of the other" (Kajdas, Wilusz, & Harvey, 1990). In the context of shoe-floor interactions, friction is the resisting force between a shoe and flooring surface when an individual exerts external forces on the shoe relative to the ground during locomotion. Friction is a complex phenomenon; in this section, two of the primary types of friction between elastomers and hard surfaces will be explored: adhesion and hysteresis (Moore, 1975).

When two surfaces come into contact, inter-molecular forces (primarily electrostatic and van der Waals' forces) bond the two surfaces. However, in the presence of a tangential force that overcomes the surface bond energy, these molecular bonds rupture (Moore, 1975; Savkoor, 1965). This forming and breaking of the bonds explains the physical process of material adhesion which is a molecular application of the dissipative stick-slip process (Chang, Grönqvist, Leclercq, Myung, et al., 2001). Thus, adhesive friction is the resisting force to the shearing of the molecular bonds between two surfaces (Figure 2.2) (Moore, 1975; Zhang, 2004). For elastomers sliding over clean and smooth surfaces, most of the friction force is attributed to this interfacial adhesion (Pascoe & Tabor, 1956).

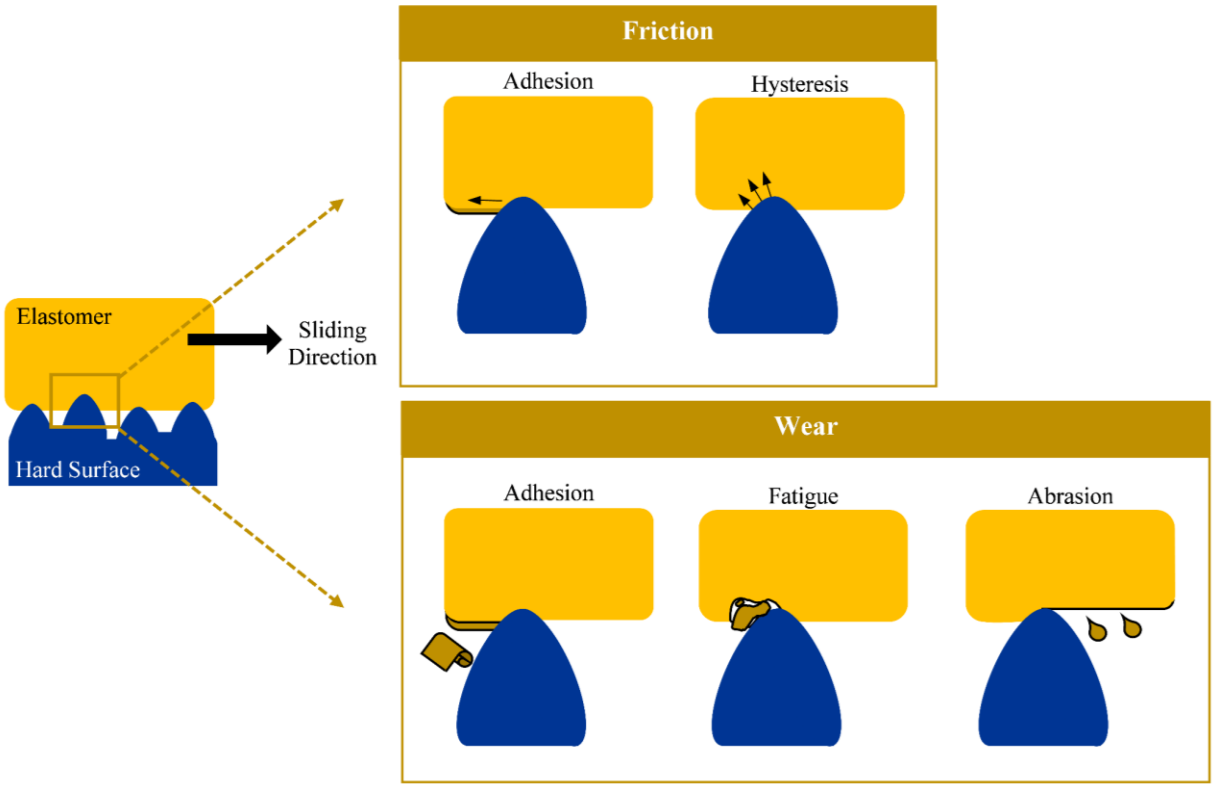

Figure 2.2 Friction and Wear Schematic

Elastomers experience friction (top) and wear (bottom) when sliding across a hard surface with asperities (left). The primary sources of friction are adhesion and hysteresis whereas the sources of wear are mainly adhesion, fatigue, and abrasion.

Adhesive friction acts on the surface of the elastomer whereas hysteresis friction is considered an internal friction (Békési, 2012). Elastomers deform under the application of external loads (Chang, Grönqvist, Leclercq, Myung, et al., 2001; Kummer, 1966). As a periodic rough surface slides relative to an elastomer, stress cycles are induced during which irreversible damping of the material occurs. The damping leads to thermal energy dissipation which can also lead to material deformation (Figure 2.2). This energy dissipation (hysteresis loss) is responsible for hysteresis friction (Chang, Grönqvist, Leclercq, Myung, et al., 2001; Kummer, 1966).

2.2.2 Wear

Wear can be defined as surface material loss that occurs due to the rubbing of solid surfaces (Zhang, 2004). There are many different types of wear including, but not limited to abrasion, adhesion, corrosion, fatigue, and erosion (Zhang, 2004). Of these types of wear, primarily three are believed to be associated with elastomeric wear at the shoe-floor interface: adhesion, fatigue, and abrasion.

As discussed in Section 2.2.1, adhesion is the forming and breaking of molecular bonds (Figure 2.2). When the strength of the adhesion (interfacial) bonds exceeds material cohesion strength (strength of bonds within the material), the rupture of the bonds within the material can lead to a particle detaching from the material. This leads to wear or transfer of the material to the other surface (Myshkin, Petrokovets, & Kovalev, 2006; Zhang, 2004). On smooth surfaces, the adhesion between the surface and elastomer breaks off the elastomer in rolled or waved fragments. This rolling or wave formation is caused by high shear stresses due to the adhesion friction. These stresses can exceed the elastomer cohesion strength during a sliding motion and result in waves of detachment, also known as Schallamach waves (Schallamach, 1971).

Hysteresis deforms the material and when performed cyclically can lead to fatigue of the material. With prolonged load cycling, fatigue failure can cause crack nucleation and subsequent growth leads to cleaving of the material and subsequent wear (Mars & Fatemi, 2004) (Figure 2.2). Further details on fatigue failure of materials are presented in Section 5.1.2.

When a material such as an elastomer contacts the asperities of a rough, rigid surface, the elastomer experiences tractive stresses at these asperities. These stresses can lead to mechanical failure and consequential cutting of the elastomer (softer surface) as the surface asperities break off small fragments of the elastomer. This process is termed abrasion (Gent & Pulford, 1983;

Schallamach, 1958) (Figure 2.2). Further discussion of abrasive wear may be found in Section 5.1.2.

There are many factors that determine the type and rate of wear such as material properties and operating conditions. As mentioned previously, the roughness and shape of the material and surface influence the type of wear. The wear rate of a system is typically measured empirically by the volume and density of the removed material normalized by the sliding distance and, sometimes, the apparent contact area (Meng & Ludema, 1995; Zhang, 2004). The apparent contact area has also been applied as a material property metric in these equations. For example, Archard showed that the wear volume is related to the sliding distance and the apparent contact area which can be measured as the ratio of the applied load to the flow pressure; flow pressure is approximately equal to the material hardness (Archard, 1953; Meng & Ludema, 1995).

2.2.3 Lubrication

Fluid film lubrication, the most applicable type of lubrication to this dissertation, will be discussed in terms of two types of fluid film flow. The Navier-Stokes equations for flow describe these two types of fluid flow: Poiseuille and Couette (Hamrock, 1994) (Figure 2.3). Poiseuille flow occurs when there is a pressure gradient forcing the fluid to flow through the space. The Couette flow occurs when one of the plates is moving relative to the other plate in the absence of a pressure gradient and the fluid is flowing due to the shearing of fluid against the moving plate (Hamrock, 1994). Therefore, Poiseuille flow refers to a pressure-driven profile, and Couette flow refers to a velocity-driven profile.

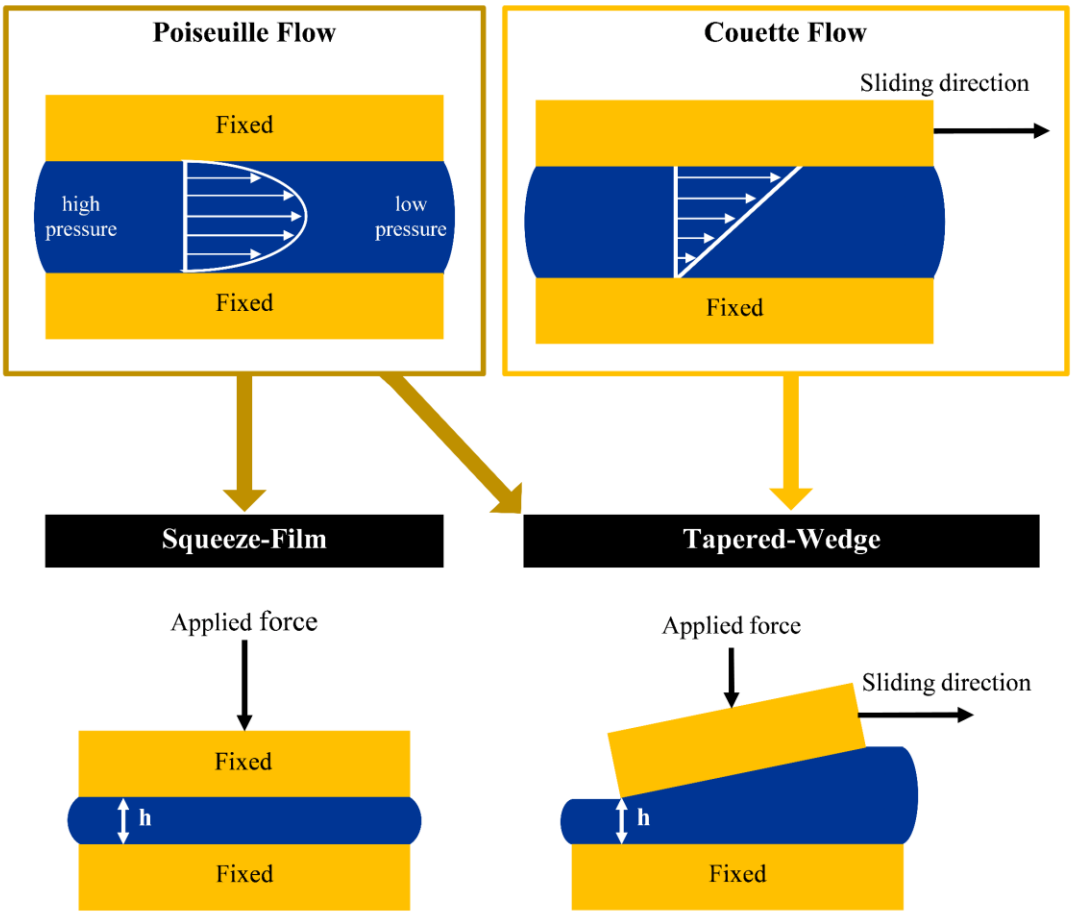

Figure 2.3 Flow Profiles and Lubrication Models

Poiseuille and Couette flow profiles with the white arrows indicating fluid flow (top). The flow profiles may be applied to the squeeze-film and tapered wedge models (bottom). The applied forces, minimum film thickness (*h*), and sliding direction (tapered-wedge) are shown.

There are two primary hydrodynamic phenomena that are applicable to this dissertation and can be explained via Poiseuille and Couette flow: the squeeze-film and tapered-wedge models (Figure 2.3). When a normal force is applied to one of the parallel plates mentioned above, the fluid is forced out from between the plates (Hamrock, 1994). Therefore, a pressure gradient is generated to drive flow of the fluid between the surfaces. This effect explains the relevance of Poiseuille flow to the squeeze-film effect. The film thickness (h) of the fluid between the plates can be determined using derivations of Reynolds equation utilizing the terms that describe the time-dependence of film thickness ($\partial h/\partial t$). The tapered-wedge (also known as the fixed-incline slider bearing) model applies the Couette flow setup described with an angled moving plate. The moving plate generates Couette flow and the angled plate generates Poiseuille flow through the forced pressure gradient. Therefore, the tapered-wedge solution models Poiseuille and Couette flow (Hamrock, 1994). Previous models have been applied to relate the load-carrying capacity of the fluid, the film thickness (h), the dimensions of the bearing, the viscosity of the fluid, and the sliding velocity (Figure 2.3) (Fuller, 1956; Proctor & Coleman, 1988). Further discussion of these models can be found in Sections 2.3.1 and 3.2.4.2.

2.3 Footwear

Footwear design has important implications for safety. The design of surfaces to achieve desirable friction and wear performance is commonly a topic of interest in tribology (Stachowiak & Batchelor, 2013). Applied to shoes, this objective would indicate high friction performance and good wear resistance (Stachowiak & Batchelor, 2013). Therefore, as friction and wear influence slip risk, it is important to understand shoe-floor friction and the way in which shoes wear down.

This section examines tribological principles applied to footwear and the importance of footwear design and replacement for preventing slipping.

2.3.1 Applications of Tribology

Adequate shoe-floor friction is imperative to prevent slips and falls. Many research studies have studied various types of friction. Utilized coefficient of friction (UCOF) often describes the friction (shear forces divided by normal forces) between a shoe and floor during gait. Specifically, the required coefficient of friction (RCOF) is a type of UCOF which is measured between the shoe and dry floor during walking (Chang, Chang, & Matz, 2011; Redfern et al., 2001). The available coefficient of friction (ACOF) is often used to explain the friction between the shoe surface and flooring. Tribometers with a goal to be biofidelic (i.e., simulate the salient conditions of human slips) have often been used to measure ACOF (Aschan, Hirvonen, Mannelin, & Rajamäki, 2005; Beschorner, Redfern, Porter, & Debski, 2007; Chang, Grönqvist, Leclercq, Brungraber, et al., 2001; Grönqvist, 1995; Singh & Beschorner, 2014). Previous research has shown that a slipping incident is likely to occur when the ACOF is less than the RCOF (Burnfield & Powers, 2006; Hanson et al., 1999). For this dissertation, RCOF and ACOF are relevant parameters that will be utilized to describe the kinetics of gait and the measured performance of shoe and floor surfaces, respectively (Figure 2.4).

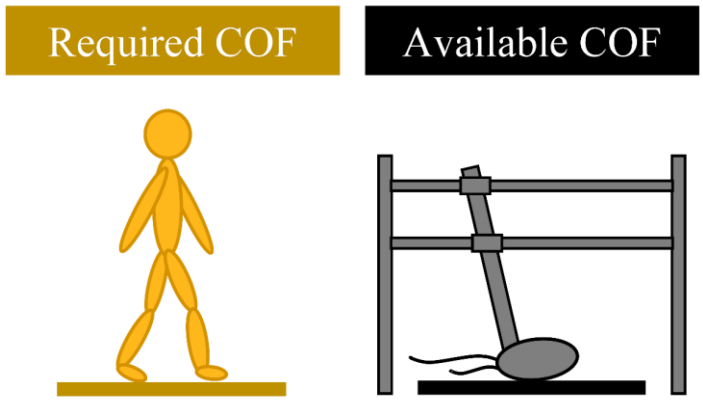

Figure 2.4 Types of Coefficient of Friction

Required COF (RCOF) is measured during dry walking. Available COF (ACOF) is measured using a slip meter or tribometer over a contaminated surface.

Previous research has examined shoe wear and its relation to ACOF. Manning, et al. conducted a longitudinal study where individuals stood on an angled, oily plate. The tangent of the angle at which naturally worn shoes slipped on a surface was calculated as the coefficient of friction (D. Manning, Jones, & Bruce, 1985). Since this inaugural work that indirectly measured friction, shoe wear and friction research have included cross-sectional wear and friction testing of new and naturally worn shoes (Cham & Redfern, 2002; Cook, Hemler, Sundaram, Chanda, & Beschorner, 2021; Grönqvist, 1995; Iraqi & Beschorner, 2017; V.H. Sundaram et al., 2020) and shoes worn via accelerated wear (Walter, Tushak, Hemler, & Beschorner, 2021). These studies have shown that new shoes have a higher ACOF than worn shoes at various stages of wear. However, there is a gap in the literature mapping the changes in under-shoe friction for progressively worn shoes.

Modeling techniques have been useful to understand shoe-floor tribology. Computer finite element modeling has been used to simulate wear of elastomers (Békési, 2012), shoe-floor friction (Moghaddam, Redfern, & Beschorner, 2015) and shoe wear (Moghaddam, Acharya, Redfern, & Beschorner, 2018; Moghaddam, Hemler, Redfern, Jacobs, & Beschorner, 2019). This research has

shown that modeling can be used to calculate shoe-floor friction and simulate shoe wear. However, modeling techniques do not capture all of the nuances of shoe wear in natural environments such as individualized wear patterns and varying types of wear due to different flooring properties.

Previous work has applied lubrication models to footwear. Fuller developed a model that calculated the predicted film thickness for the tapered-wedge bearing solution (1956) which was later applied by Proctor and Coleman (1988). This previous research used the entire shoe outsole in the model and did not account for the individual tread blocks or how wear of these tread blocks could form a worn region. Further discussion and application of the tapered-wedge model can be found in Section 4.1.3.5.

2.3.2 Design

Slip-resistant (SR) shoes are an effective way to reduce occupational slips and falls. SR shoes decrease slip likelihood in the workplace by as much as 54% (Verma et al., 2011) and improve friction and fluid drainage to prevent slipping compared to their non-SR counterparts (Health and Safety Laboratory U.K., 2009; Hemler, Sundaram, & Beschorner, 2019; V.H. Sundaram et al., 2020). The mechanism behind this improved friction and fluid drainage is primarily in the use of small, uniformly sized tread blocks (Figure 2.5). These tread blocks increase friction and increase fluid drainage since under-shoe fluid may be dispersed through the tread channels.

Figure 2.5 Representative Slip-Resistant Shoes

Representative SR shoes with small, uniform tread blocks are shown for three different brands

SR shoes provide improved protection from slipping, though there are limitations. Current standards for labeling shoes as SR only recommend shoe-floor friction thresholds when new (ISO/DIS, 2020) and performance across SR shoes widely varies (Health and Safety Laboratory U.K., 2009; Iraqi, Vidic, Redfern, & Beschorner, 2020; Jones, Iraqi, & Beschorner, 2018). Furthermore, there are no standards to progressively assess safety of naturally worn footwear or recommend replacement.

Previous work has analyzed variations in tread design to prevent slips. Work has found that the ACOF is positively associated with tread surface area (Iraqi et al., 2020), and negatively associated with hardness (Iraqi et al., 2020; Tsai & Powers, 2008). Tread that are oriented 45° to the sliding direction have been shown to have the greatest ACOF (Blanchette & Powers, 2015), though these effects may be dependent on achieving an optimal tread depth and width to increase ACOF (Beschorner & Singh, 2012; Blanchette & Powers, 2015; Li & Chen, 2005; Li, Wu, & Lin, 2006). Outsoles comprised of materials with varying surface roughness may improve ACOF (Yamaguchi & Hokkirigawa, 2014) and a change in heel shape from flat to a beveled (rounded) heel shape has been associated with increased ACOF (Iraqi et al., 2020). All of these factors are especially important at the heel of the outsole as research has shown that 90% of all slips on the

same level occur at heel strike (Strandberg, 1983). Previous work has created models to identify slip risk based on some of these tread features (Iraqi et al., 2020). However, there is a paucity of research identifying how slip risk changes as tread wears down and these factors change.

2.3.3 Replacement Standards

Replacing footwear is an important aspect of reducing slips and falls in the workplace. Previous work has shown that worn shoes experience decreased friction and fluid drainage (Beschorner, Albert, Chambers, & Redfern, 2014; Beschorner & Singh, 2012; Cook et al., 2021; Iraqi, Cham, Redfern, & Beschorner, 2018; V.H. Sundaram et al., 2020). Specifically, these studies analyzed completely worn shoes (Beschorner et al., 2014; Beschorner & Singh, 2012; Iraqi, Cham, Redfern, & Beschorner, 2018) or used broad categories (6-month periods) of wear as reported by participants (Cook et al., 2021; V.H. Sundaram et al., 2020). Qualitative recommendations for when to replace shoes include when “the outsole is worn down”, the outsole separates from the upper, or there are holes in the outsole (Shoes For Crews (Europe), 2019; SR Max Slip Resistant Shoe Company, 2017). Furthermore, many footwear safety guidelines encourage maintaining footwear by cleaning and checking for footwear damage, but there are no specific recommendations for when shoe outsoles may not protect you from slip risk (Occupational Health & Safety, 2018). Previous work has shown that replacing SR shoes after 6 months of wear led to a reduction in workplace slips by 55% (Verma et al., 2014). Footwear companies have similarly supplied quantitative recommendations to replace shoes every 6 months (Shoes For Crews, 2013; Skechers, 2013), or every 6-12 months for “the average work environment” (SR Max Slip Resistant Shoe Company, 2017). The previous research and empirical understanding of footwear

companies shows that wear and slip risk generally increase with time worn, however, there is a lack of research assessing wear condition-specific metrics.

2.4 User-Centered Design

2.4.1 Introduction to UCD

User-centered design (UCD) gained traction in the 1980's stemming from Donald Norman's research group on Human-Machine Interaction at the University of California San Diego. Two books from the group emerged to set the stage for UCD: *User-Centered System Design: New Perspectives on Human-Computer Interaction* (Pea, 1987), and *The Psychology of Everyday Things (POET)* (Norman, 1988). In the latter book, Norman stated that UCD is "a philosophy based on the needs and interests of the user, with an emphasis on making products usable and understandable" (Norman, 1988). He presented four principles of UCD stating that design should (Norman, 1988):

- Clearly define constraints – the user should easily know what to do
- Visibly show the model, alternative actions, and results
- Make evaluation & problem solving easy
- Follow intuitive thought processes

These principles could be summarized as: making it easy for the user to know what to do with the product and outcomes. Norman stated in the book that business and industry understand the importance of pleasing aesthetics for the consumer. However, he also reasoned there are two other important factors without which the attractiveness of the product is unimportant: usefulness

and usability (Norman, 1988). Several years later, Sanders built upon this thought as she presented a new approach by which consumers were involved in the design development process instead of previous design methods that only gathered insight about the consumer (Sanders, 1992). She proposed that for products to be successful, three perspectives would need to be met: Usability (is the product easily used), Usefulness (does the product address a user need), and Desirability (is the product wanted by the user), which were collectively termed, UUD (Sanders, 1992).

2.4.2 Usefulness, Usability, and Desirability

Twelve-to-eighteen-month timelines for product testing in conjunction with high failure rates of new products gave rise to the need to implement UCD and UUD metrics (Power, 1992). A news article in 1992 shared a few ideas for innovating product testing such as sending final products to a few consumers or overseas to test interest, or releasing the products region by region to gauge success (Power, 1992). However, all the presented innovations involved testing the efficacy of products after they had been designed. On the heels of this article, Sanders presented her new approach of using UUD for product development (Sanders, 1992). Sanders stated that in general, consumers do not actually know what they want. However, product developers were often implementing usability testing which affirmed that the product worked as intended but denied any discovery of the actual user needs. Therefore, Sanders argues that usability testing was not enough (Sanders, 1992). Therefore, UUD testing was introduced as an efficacious model for improving the design development process and reducing product failure rates.

The UUD triad addresses the multiplicity of needs according to Maslow's hierarchy of needs (Figure 2.6) (Maslow, 1943). Basic physiological needs such as food and water are the base needs. Once these needs are met, higher levels of need become realized and may be met. Products

are created to meet the vast array of needs within the seven categories. The design development process is often interested in many levels of needs from product safety at the low levels to aesthetic design at the higher levels (Sanders, 1992). Therefore, using customer feedback that addresses the multiple levels of need is essential to implement products that are truly effective. Usability, which assesses if a product can be used immediately or easily learned by the consumer, often addresses more of the middle levels of needs (i.e., belonging and love, esteem, and cognitive needs). For example, a bicycle helmet may address usability needs by how easily the straps around the chin may be buckled and unbuckled by the user. Usefulness, which assesses if a product is needed by the consumer and will be used, often addresses the lower-level needs of the consumer (i.e., physiological and safety needs). For example, the bicycle helmet in the previous example meets usefulness criteria by ensuring adequate protection for an individual's head during a crash. Desirability, which assesses if a product is wanted by the consumer, often addresses the higher-level needs of the consumer (i.e., aesthetic and self-actualization needs). This bicycle helmet may meet aesthetic needs of a certain population with a particular color and design that is independent of the lower levels of needs. Therefore, using UUD metrics is a thorough approach to implement input from the targeted consumer at multiple need levels.

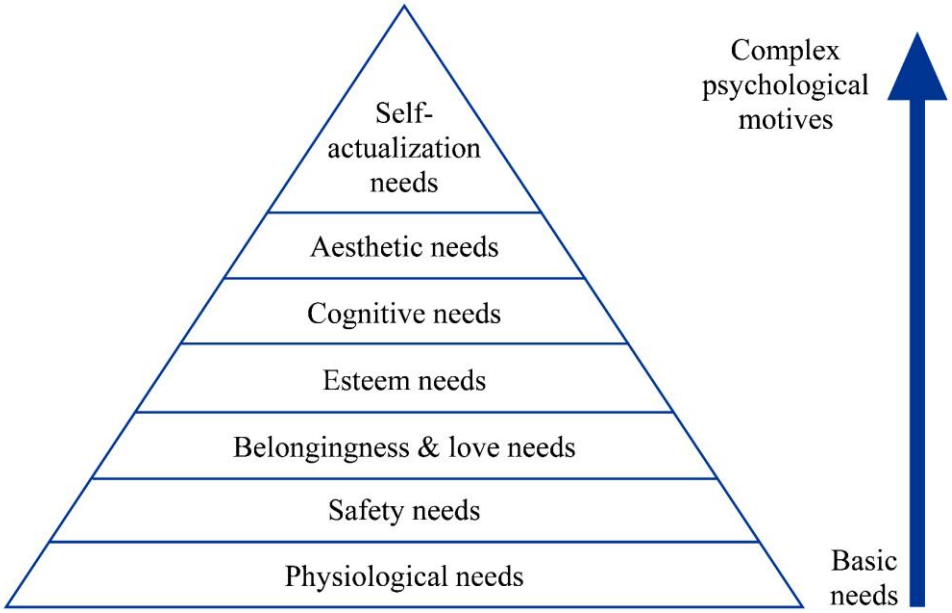

Figure 2.6 Maslow's Hierarchy

Figure adapted from (Sanders, 1992)

Sanders also introduced the use of converging operations within the context of UUD (Sanders, 1992). Converging operations is a multidisciplinary approach by which numerous research methods are used to find overlapping, unbiased information. This concept of including multidisciplinary skills within teams is essential to sufficiently diversify the design and implementation plans. Cagan and Vogel presented a similar strategy of converging operations as a collaboration between design, marketing, and engineering teams to improve the product concept process (Figure 2.7) (Cagan & Vogel; Sanders, 1992). Whether through the different design, engineering, and marketing teams, or through considering strategies that are associated with each area, integration of these areas of expertise is important for developing a good product. Traditionally, the engineering team often develops a product concept based on technological innovation. This team's approach often focuses on the usability and usefulness of the product. The marketing team is often concerned with developing the product concept based on marketing criteria which often leads to a focus on the usefulness and desirability of the product. Finally, the

design team often develops a product concept based on visual appearance or human factors which can be defined as the desirability and usability of the product. The successful integration of these three areas of expertise leads to a customer-driven product concept (Cagan & Vogel).

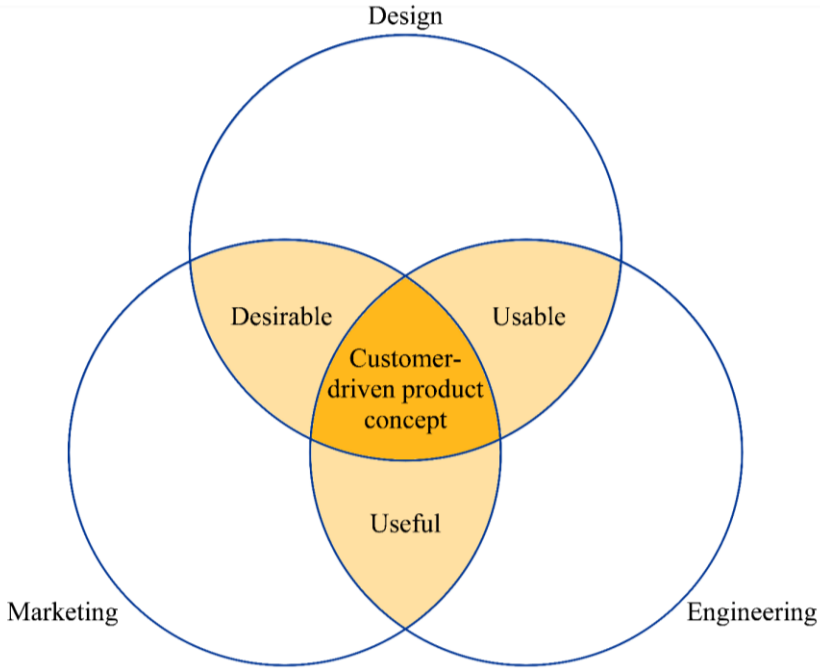

Figure 2.7 Area Integration of UUD

Integrating areas of expertise in design, engineering, and marketing leads to usable, useful, desirable design creating a customer-driven product concept. Figure adapted from (Cagan & Vogel).

2.4.3 Design Process

Understanding the product design process is important to implementing UCD and UUD effectively. Terminology varies, but the general product design process, after identifying the need, consists of the following iterative steps (ISO, 2019; Pahl & Beitz, 2013; U.S. Department of Health & Human Services, 2020) (Figure 2.8):

1) Define the context of use (e.g., consult potential users)

2) Define the design requirements (e.g., identify user needs/requirements)

3) Produce the design (e.g., scenarios of use, low- and high-fidelity prototypes)

4) Evaluate the design (e.g., usability testing, user questionnaires)

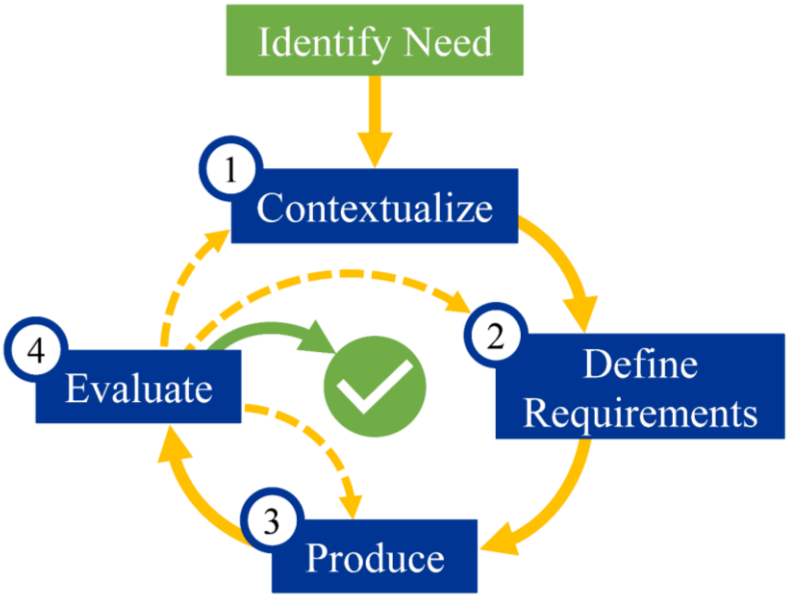

Figure 2.8 Product Design Process

Figure adapted from (ISO, 2019; U.S. Department of Health & Human Services, 2020)

After the evaluation step, the process may return to any of the previously visited steps or it will conclude if the evaluation is successful according to preset goals (Figure 2.8). UCD and UUD may be implemented at almost any of these stages, but primarily at stage 1 (contextualize) to maximize resource efficiency (Cagan & Vogel, 2020). For example, the user feedback may be most valuable to consider when and where the product might be used. At stage 4, user feedback may also be valuable to refine the design and to assess if the iteration's design achieves the set goals (ISO, 2019).

2.4.4 User Feedback Assessments

User feedback assessments are beneficial for budgetary reason at the beginning of the design process (stage 1 of Figure 2.8). These user evaluations can be used to gauge the usability, usefulness, and desirability of a design or product. User evaluations can include, but are not limited to, focus groups, interviews (structured, semi-structured, or unstructured), questionnaires, think aloud protocols, field observations, and controlled experiments (Jordan, 1998). These evaluations can be designed to gather quantitative or qualitative data. Quantitative data may include time on a task, error rate, or quality scale (e.g., 5-point Likert scale). Qualitative data enables the collection of descriptive data which can be used to diagnose problems and prescribe solutions (Jordan, 1998). For example, instead of receiving a low quantitative score from the individual assessing the design without an explanation, the evaluator may receive a qualitative response that states why the assessor found the design unsatisfactory. The evaluator can then use the qualitative response to inform the design.

2.4.5 UCD applied to occupational injuries and workplace slips and falls

Research has applied UCD and UUD for improving health and minimizing injury. UUD assessments have been used to improve worker wellbeing from reducing injuries (Sommerich et al., 2019) to improving home hazard identification (Darragh et al., 2016; Polivka et al., 2019). Such experiments can assess some sort of design or system and gain feedback from the potential user, such as assessing the UUD of a transducer support intervention for medical sonographers to reduce exposure to musculoskeletal injury risk factors (Sommerich et al., 2019). Furthermore,

these experiments show that using UCD and UUD approaches is an effective way to develop user-verified solutions that reduce workplace hazards.

UCD practices can be applied to everyday delivery of information. As shown in the design process, identification of a need is the first step toward providing a solution (ISO, 2019). Increasing awareness of a need is important to engage individuals with prospective solutions. Currently, footwear and safety companies often convey the danger of slips and falls and the need for replacing footwear with high-density wording and few pictures (Brooks Sports, 2020; Nighswonger, 2020; Occupational Health & Safety, 2018; Optimum Safety Management; Shoes For Crews, 2019b; SR Max Slip Resistant Shoe Company, 2017; The Texas Department of Insurance). Incorporating pictures is a more efficient method for conveying information as pictures can be remembered more readily than words (Paivio, Rogers, & Smythe, 1968). Additionally, research has shown that a balanced mixture of wording and pictures is more efficient for retaining information (Unnava & Burnkrant, 1991). Therefore, one way to incorporate UCD practices into slips and falls awareness is through graphic and verbal representation of injury statistics. For example, Liberty Mutual Insurance and the National Occupational Research Agenda have used graphics with few words to disseminate information on workplace safety and injury risk (Liberty Mutual Insurance, 2020; National Occupational Research Agenda (NORA) Traumatic Injury Prevention Cross-Sector Council, 2021). These graphics present the information via a clear image with a key topic, cost, and recommendation. There is a need to convey slips and falls risk and intervention information using UCD approaches to improve understanding and reduce risk of injury.

There are few slip prevention and footwear safety assessment tools that follow UCD guidelines. To the knowledge of the author, there exists only one physical tool to measure shoe wear (Shoes For Crews, 2019a). This tool measures shoe outsole tread depth similar to testing the

tread depth on a car tire (Bridgestone, 2021; Firestone - Complete Auto Care; Goodyear Auto Service, 2021; Tracy, Reeves, Radclyffe, & Longden, 2004). However, previous research has shown that shoe tread wears unevenly across a shoe surface which presents a usefulness limitation to applying tread gauges on footwear (Grönqvist, 1995). In addition to this singular tool, many companies give general time or distance thresholds to recommend shoe replacement – as discussed in Section 2.3.3. However, previous research has shown that shoes may wear down at varying rates that cannot always be predicted by time (Pliner, Hemler, & Beschorner, 2019). Furthermore, distance metrics may be difficult to track without the use of wearable sensor technology. These factors reduce the usability and desirability of these metrics. Other tools for measuring footwear slip risk are slip-meters and tribometers that can measure shoe-floor friction. However, research has shown that these tools are often under-used (14.8%) by safety practitioners compared to easy-to-use safety assessments such as the National Institute for Occupational Safety and Health Lifting Equation (86.9%) and direct measurement techniques such as grip dynamometers (64.9%) (Lowe, Dempsey, & Jones, 2018). Previous findings have shown that footwear safety tools (i.e., replacement recommendations) have often failed to implement UCD principles. Therefore, there is a need for a tool that addresses all the levels of Maslow's hierarchy from basic needs for safety to aesthetic design using UCD and UUD approaches.

2.5 Gaps in the Literature

This dissertation addresses several gaps in previous findings. The primary areas on which this dissertation will focus are how shoes wear down (Aim 1), why shoes wear down (Aim 2), and the lack of a practical tool to inform shoe replacement (Aim 3). Specifically, this dissertation will

seek to inform gaps within a mechanistic model which proposes the pathway from increased footwear usage to increased slip risk (Figure 2.9). This research proposes that increased footwear usage leads to increased tread wear and volume loss (Aim 1). It is proposed that the relationship between footwear usage and tread wear is predicted by gait kinetics (peak normal and shear forces, and RCOF) and shoe material hardness (Aim 1). As tread wears down, it is proposed that a worn region forms and grows (Aims 1 and 3). This worn region formation may then lead to decreased ACOF and increased under-shoe fluid pressures (Aim 1). Furthermore, this research proposes to confirm previous work that showed that increased worn region size is indicative of increased slip risk (Aim 3).

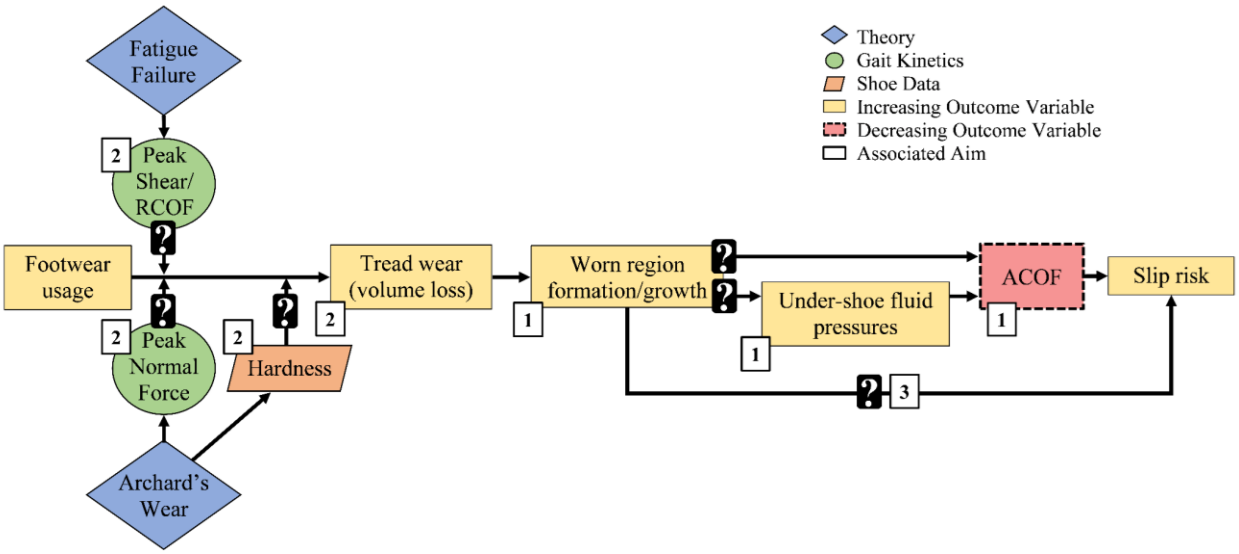

Figure 2.9 Mechanistic Model

In the model, increased footwear usage leads to an increase in slip risk with pathways to be explored labeled with question marks. This model incorporates variables associated with each aim (as labeled) and overall slip risk as related to footwear. This project analyzes the impact of peak RCOF (fatigue failure) and peak normal force (Archard's wear) in green, and shoe hardness in orange on the increases in volumetric tread wear and worn region formation as they relate to under-shoe fluid pressures and decreased ACOF and subsequent increased slip risk.

3.0 Progressive Accelerated Wear – Changes in and Application of Traction Performance and Geometry

This chapter analyzes the influence of progressive accelerated wear on traction performance (friction and under-shoe hydrodynamics) for slip-resistant footwear. Specifically, Section 3.1 discusses traction performance and outsole geometry changes for shoes worn via a simulated wear protocol. Section 3.2 analyzes the application of Section 3.1 findings to lubrication theory to predict film thickness at the shoe-floor interface during slipping. Sections 3.1 (Hemler, Charbonneau, et al., 2019) and 3.2 (Hemler, Charbonneau, & Beschorner, 2020) are adapted from peer-reviewed journal publications for which permission has been granted to be presented in this dissertation (Appendix A). Preliminary results from this chapter have been published as conference abstracts (Hemler & Beschorner, 2019b; Hemler, Charbonneau, & Beschorner, 2017; Hemler, Sundaram, & Beschorner, 2020).

3.1 Accelerated Shoe Wear

3.1.1 Abstract

Shoe wear is known to increase slipping risk, but few studies have systematically studied this relationship. This study investigated the impact of progressive shoe wear on the available coefficient of friction (ACOF) and under-shoe fluid dynamics. Five different slip-resistant shoes were progressively worn using an accelerated, abrasive, wear protocol. The ACOF and fluid forces (the load supported by the fluid) were measured as shoes were slipped across a surface contaminated with a diluted glycerol solution. As the shoes became worn, an initial increase in ACOF was followed by a steady decrease. Low fluid forces were observed prior to wear followed by increased fluid forces as the worn region became larger. Results suggest that traction performance decreases particularly when the heel region without tread exceeds a size of 800mm^2. This study supports the concept of developing shoe replacement guidelines based upon the size of the worn region to reduce occupational slips.

3.1.2 Background

Falls resulting from slipping are among the most common causes of non-fatal injuries in the workplace. In 2016, slips, trips, and falls were the second-leading cause for non-fatal occupational injuries accounting for 26.0% of all injuries (U.S. Department of Labor - Bureau of Labor Statistics, 2020). Of those incidents, over one-third caused workers to be away from work for 31 days or more and 28.3% of the incidences occurred in the service industry (U.S. Department of Labor - Bureau of Labor Statistics, 2020). Furthermore, 40-50% of fall-related injuries have

been found to be attributed to slipping (Courtney et al., 2001). Thus, there is a need to develop prevention strategies for slips and falls.

Slips often occur when there is a reduction in friction between the shoe and floor, particularly when a liquid contaminant is present (Beschorner et al., 2014; Hanson et al., 1999). The friction that prevents slipping between the two surfaces is often measured using the available coefficient of friction (ACOF). A variety of tribometers have been used to measure ACOF (Aschan et al., 2005; Beschorner et al., 2007; Chang, Grönqvist, Leclercq, Brungraber, et al., 2001; Grönqvist, 1995; Singh & Beschorner, 2014). The required coefficient of friction (RCOF) represents friction required for walking (Redfern et al., 2001). A slipping incident is most likely to occur at the shoe-floor interface when the ACOF is less than the RCOF (Burnfield & Powers, 2006; Hanson et al., 1999).

Shoe outsole design is one important factor in friction analysis when liquid contaminants are present on the floor surface. Shoes marketed as slip-resistant (SR) tend to have tread patterns that have an increased ACOF compared to shoes not marketed as slip-resistant (Beschorner, Jones, & Iraqi, 2017). A study conducted in limited-service restaurants showed that SR shoes can reduce the number of slip and falls by as much as 54% (Verma et al., 2011). However, variations in shoe design among SR shoes result in a broad range of ACOF values (Jones et al., 2018).

Variations in tread design (i.e. tread depth and width) have been shown to affect ACOF (Li & Chen, 2004; Li et al., 2006; Yamaguchi, Katsurashima, & Hokkirigawa, 2017). Channels in shoe tread provide fluid dispersion pathways to reduce hydrodynamic pressures (Strandberg, 1985; Tisserand, 1985) and have been shown to reduce the risk of slipping compared to shoes without such channels (Beschorner et al., 2014). Hydrodynamic measurements have shown that under-shoe fluid pressure varies across the contact regions between the shoe sole and floor (Beschorner

et al., 2014; Singh & Beschorner, 2014). Other research has shown increases in ACOF at modest wear levels and a reduction in ACOF for severely worn shoes in some cases (Grönqvist, 1995; I.-J. Kim, 2000). Previous studies have shown that wear tends to be concentrated on the heel sections (Grönqvist, 1995). A recent review article suggested that accelerated wear methodologies should be developed to shorten the observation time in order to assess shoes throughout their life (Chang et al., 2016). Thus, this study aims to detail changes in shoe traction and drainage across the shoe's life using an accelerated wear method to help guide shoe replacement criteria.

Replacement criteria for shoes have not been established. Previous research has shown that shoes worn for less than six months performed better than those worn for more than six months and that changing to a new pair of shoes had a 55% reduction in slip rate (Verma et al., 2014). However, just two states of wear were considered in that study (< 6 months old, > 6 months old). Furthermore, shoe age is an imprecise measure since it does not consider usage or environmental conditions that may influence wear rate. An alternative approach is to develop replacement thresholds using metrics based on the geometry of the worn shoe. This study tracked changes in the geometry of worn shoes to identify wear measures which were correlated to shoe performance changes.

The purpose of this study was to quantify changes in ACOF and under-shoe fluid loading as shoes were progressively worn using a simulated wear protocol. The secondary purpose was to determine a wear replacement threshold based on ACOF and fluid pressure measures.

3.1.3 Methods

3.1.3.1 Summary

A progression of wear-related changes in shoe traction performance was determined via iterations of mechanical testing, mold creation (to capture shoe tread geometry), and abrasion via a simulated wear protocol (Figure 3.1). During mechanical shoe testing, ACOF and under-shoe fluid pressures were measured as a robotic device moved the shoe across a contaminated surface (Figure 3.2). Molds of the heel tread geometry were generated using an apparatus that allowed the mold material to cure while the shoe was held in a fixed and consistent position (Figure 3.4). Shoes were progressively worn using an apparatus with a sliding abrasive belt and a means of adjusting the shoe angle (Hemler et al., 2017) (Figure 3.3).

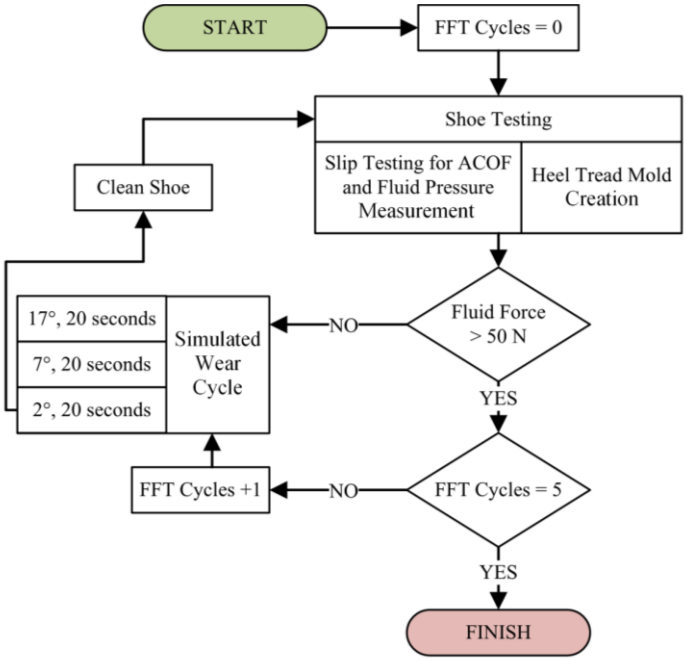

Figure 3.1 Mechanical Testing and Abrasive Wear Protocol

Flowchart of mechanical testing and abrasive wear protocol. The Fluid Force Threshold (FFT) is described in Section 3.1.3.5.

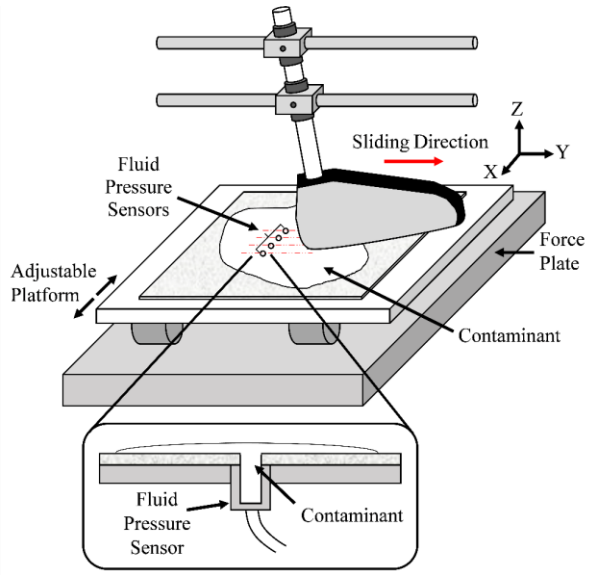

Figure 3.2 Schematic of Robotic Slip Tester

A robotic slip tester used to slide each shoe anteriorly across the contaminated tile along multiple parallel paths. Four fluid pressure sensors mounted above a force plate recorded fluid pressures and shear and normal forces, respectively. Cross-sectional view of contaminant and fluid pressure sensor is shown below the testing apparatus.

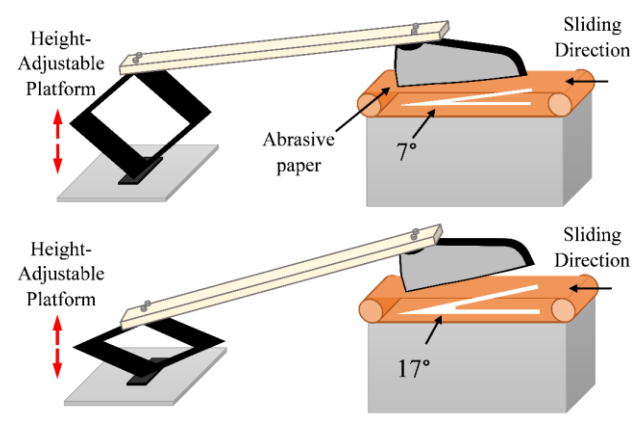

Figure 3.3 Simulated Wear Apparatus

Simulated wear apparatus on which the heel of each shoe was progressively worn at 17°, 7°, and 2°. Examples of wear at 17° and 7° are shown.

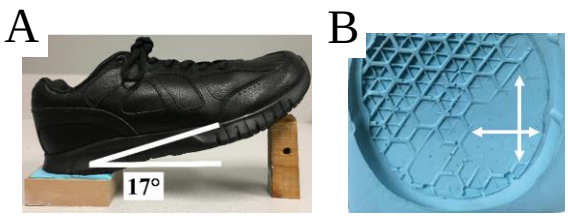

Figure 3.4 Shoe Heel Mold

A) Shoe heel placed in mold compound and frame at 17°, and B) the length and width of the largest wear region indicated with white arrows on the heel tread mold.

3.1.3.2 Simulated Wear Protocol

The accelerated wear apparatus (Figure 3.3), consisting of a linear motion abrasion device (Ryobi BD4601; One World Technologies, Inc.; Anderson, SC, USA) and an angle-adjustable platform, was used to simulate wear of the right heel of the shoes (Hemler et al., 2017). The device slid abrasive paper (180 µm diameter particles) at 9.65 m/s across the heel with a normal force of 40 N, similar to abrasion resistance standards for footwear and previous research for abrasively removing shoe tread (Beschorner et al., 2014; ISO/IEC, 2001; D. P. Manning, Jones, & Bruce, 1990). A normal force lower than that produced during gait was used to reduce heat generation and due to an inability of the device to overcome friction forces when large normal forces were applied. One wear cycle consisted of abrading each shoe for 20 s at three angles (17° ± 1°, 7° ± 1°, and 2° ± 1°). The angles were chosen to simulate angles experienced from initial heel strike to flat foot (Kadaba, Ramakrishnan, & Wootten, 1990). Each wear cycle was equivalent to a total sliding distance of 580 m (193 m at each angle). The angle of the shoe was defined relative to horizontal, which was the orientation of the shoe when it was placed on the floor without an applied external load. Each shoe was abraded until there were five wear cycles for which the fluid force was greater than 50 N (20% of the normal force; described in Section 3.1.3.5). Prior to each accelerated wear iteration, abrasive belt grease (Formax, No. F26) was applied to the abrasive

paper to minimize increases in temperature between the shoe and the paper. After each wear cycle, residual grease was cleaned from the heel section of the tread using detergent and water, and then the heel section was rinsed with water and thoroughly dried.

Five pairs of shoes commonly worn in the service industry were included in the study and the right shoe for each pair was tested (Figure 3.5). All shoes were claimed by their manufacturers to be 'slip-resistant' or 'anti-slip'. Detailed material compound was not available, but shoes were reported as having an outsole composed of 'rubber' or 'rubber compound'. Short-term hardness measurements were recorded at baseline using a Shore A durometer based on ASTM standard D2240 (ASTM, 2015) and the proportion of tread surface area to overall heel surface area, "tread proportion", was recorded (Table 3.1). To determine tread proportion, 3D models of the heel were created based on measurements of heel and tread geometry (ANSYS Design Modeler, ANSYS Inc., Canonsburg, Pennsylvania, USA). The software was then used to sum the areas on the contact surface of the tread as well as the areas in the tread channels that were parallel to the contact surface. The tread proportion was calculated as the ratio of the contact surface area to the total surface area (sum of contact area and tread channel area parallel to contact surface). The roughness of the continuous sections of each tread block (R_z) was characterized by the maximum peak to valley height measurement which was averaged across five scans each using a sampling scan length of 1.6mm and a cutoff frequency of 0.8mm. Measurements were taken at five different locations on the shoe heels for the baseline tread and the fully worn region at final wear using a 2D contact profilometer (Surtronic S-100, Taylor-Hobson, AMETEK, Leicester, England). Portions of this data set were included in a previous publication that compared a shoe wear model to experimental results (Moghaddam et al., 2019).

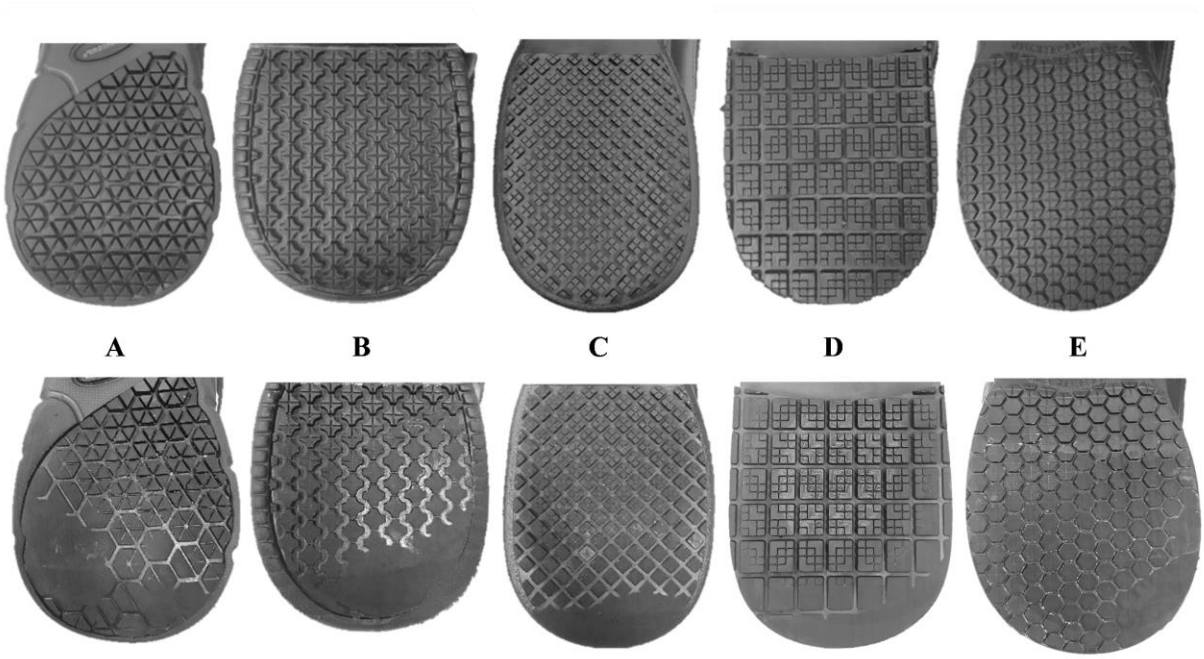

Figure 3.5 Experiment Shoes

Slip-resistant shoe tread at baseline (top) and after completed wear (bottom)

Table 3.1 Experiment Shoes Information

List of shoe code, brand, model, size, short-term hardness, baseline tread depth, initial contact area on the abrasion device at the three angles of wear, proportion of tread surface area to overall heel surface area, and heel edge type.

Shoe Code	Shoe Brand	Shoe Model	Shoe Size (US Men's)	Shore A Hardness	Baseline Tread Depth [mm]	Initial Contact Area [mm^2] (2°/7°/17°)	Tread Proportion	Heel Edge Type
A	Keuka	Galley 55014	9	56.4	3.7	249/180/145	0.48	Beveled
B	safeTstep	Apollo 140060	8.5	63.5	2.7	191/118/91	0.32	Beveled
C	Shoes for Crews	Falcon 6007	9	56.3	3.4	432/266/85	0.41	Square
D	SR Max	SRM 3500	9	50.1	2.8	271/147/44	0.57	Square
E	Tredsafe	M151044BU	9	60.5	2.4	264/325/160	0.66	Beveled

3.1.3.3 Mechanical Testing of Shoes

ACOF and fluid pressure measurements were conducted using a robotic slip tester (Figure 3.2). The slip tester included three electromagnet motors – one motor to control vertical displacement (Z-direction) and two horizontal motors to control horizontal movement (Y-direction) and foot angle, a force plate measuring shear and normal forces (vertical load capacity = 4450 N; BP400600-1K-Q2046, AMTI, Watertown, MA, 02472), and four fluid pressure sensors (Gems ® 3100R10PG08F002) in a linear array in the X-direction of the device (Figure 3.2). A platform was mounted to the top of the force plate, which could be moved in the X-direction (medial-lateral); the platform and the force plate were fully constrained during testing procedures while the horizontal and vertical motors allowed for the shoe to translate in the Y and Z directions and rotate about the X-axis (3 degrees of freedom) (See Figure 3.2 for axes of the testing device). The fluid pressure sensors, each with an inlet diameter of 3.2 mm, were installed in the top of this platform, spaced 25 mm apart. Forces and hydrodynamic pressures were recorded at 500 Hz. The device is conceptually similar to the Portable Slip Simulator device (Aschan et al., 2005; Iraqi, Cham, Redfern, & Beschorner, 2018; Jones et al., 2018) but has 2 horizontal motors that can operate independently to permit active shoe-floor angle control (Figure 3.2).

Shoes were slid across a vinyl composite tile (Armstrong, 51804; R_a = 2.19±0.29 µm, R_z = 16.13±2.74 µm, R_q = 3.13±0.42 µm) which was contaminated with a diluted glycerol solution (90% glycerol, 10% water by volume; 219 cP). Tile roughness was measured in three locations on the tile in four orientations, each 45° apart. Contaminant was spread across the tile prior to each test to ensure that the entire region interacting with the shoe was covered with contaminant. Measurements occurred using a shoe angle of 17°± 1°, a speed of 0.3 m/s, and an average force of 250 N ± 10 N. These conditions were intended to approximate the angle (Albert, Moyer, &

Beschorner, 2017; Iraqi, Cham, Redfern, & Beschorner, 2018), speed (Albert et al., 2017; ASTM, 2011; Iraqi, Cham, Redfern, Vidic, & Beschorner, 2018), and normal force (Iraqi & Beschorner, 2017; Iraqi, Cham, Redfern, Vidic, et al., 2018) at the onset of slipping. These tests were performed at baseline (i.e., prior to any wear cycles) and after each wear cycle as ACOF data using this method has been demonstrated to predict slips (Iraqi, Cham, Redfern, & Beschorner, 2018). Furthermore, as previous research has shown that fluid pressures may vary across the shoe surface (Beschorner et al., 2014; Singh & Beschorner, 2014), the slip tester platform was moved 5 mm in the X-direction four times for a total of five trials and 20 pressure scans per measurement cycle.

3.1.3.4 Heel Tread Mold Protocol

Heel tread at baseline and after each wear cycle was measured by creating a mold of the heel tread using a silicone rubber compound (Smooth-On Inc.; Macungie, PA; Oomoo® 25). To generate the mold, shoes were placed in a frame (92 mm x 76 mm x 28 mm), which was filled with the compound, at a sagittal plane angle of 17° (Figure 3.4). Prior to placement in the mold compound, shoe tread was lightly and uniformly coated with a spray petroleum-based oil (WD-40 Company; San Diego, CA, USA) to allow for easy removal of the shoe from the mold. The molds were used to determine the largest region of the heel that lacked any tread as wear progressed for each iteration. For iterations in which the entire heel had tread, the area of one lug from the tread pattern was measured as the largest continuous area of contact between the shoe and the floor. Once a worn region developed, the size of the region without tread (worn region size) was characterized by the longest length (along the sliding axis) and width (perpendicular to sliding axis) uninterrupted by a tread block (Figure 3.4).

3.1.3.5 Data and Statistical Analysis

The average ACOF for each shoe, wear iteration, and angle was calculated starting 0.1 s before and ending 0.1 s after the shoe crossed the pressure sensors for a total of 0.2 s. ACOF for each frame was determined as the magnitude of the resultant shear force divided by the normal force (Equation 3.1) where F_{x_i} and F_{y_i} are the shear forces and F_{z_i} is the vertical ground reaction force for each frame (*i*). ACOF and fluid pressure data from two wear cycles and select trials were excluded because the normal force was outside of the desired range (240-260 N). Experimental complications also caused data from one shoe for one wear cycle to be excluded.

$$ACOF_i = \frac{\sqrt{{F_{x_i}}^2 + {F_{y_i}}^2}}{F_{z_i}} \quad 3.1$$

The peak fluid pressure was recorded and the force supported by the fluid (fluid force) across the shoe was calculated for each wear cycle. Fluid pressures above five standard deviations from the baseline pressure levels were included in the measurements (Beschorner et al., 2014). The fluid force was determined using numerical integration (Equation 3.2), where p_i is the fluid pressure at the *i*th frame, Δx is the distance between scans in the direction perpendicular to sliding (5 mm), v is the sliding velocity (0.3 m/s), andΔt is the time between each frame (0.002 s) (Singh & Beschorner, 2014). The fluid force was thus summed for all fluid pressure readings across the five trials. Fluid forces were also categorized by percent of normal force during mechanical shoe testing (< 25 N or < 10%; 25-50 N or 10-20%; > 50 N or > 20%). Each shoe was worn until there were five wear cycles for which the fluid force was greater than 50 N – indicated as Fluid Force Threshold (FFT) cycles (Figure 3.1).

$$F_{fluid} = \sum p_i \, \Delta x \, \Delta y = \sum p \, \Delta x \, v \, \Delta t \qquad 3.2$$

Statistical analyses were performed to determine the relationships between ACOF, fluid force (continuous and categorical), the worn region size, tread proportion, and the sliding distance between and within each shoe type. Three generalized linear regression models were used to determine the relationships of each of the dependent variables – ACOF, fluid force, and worn region size – with the independent variables – shoe type (categorical), sliding distance (continuous) as shoes were worn, and their interaction. In the model, a square root transformation was used for fluid force to achieve normally-distributed residuals. Furthermore, a generalized linear regression model was used to determine ACOF differences across fluid force categories and shoe type. Specifically, ACOF was the dependent variable and the independent variables were the fluid force category, shoe type, and their interaction. If an interaction effect was observed between the fluid force category and shoe type, then a Tukey's HSD test was performed to determine significance between the three fluid force categories within each shoe type. Only comparisons across fluid force category within each shoe were analyzed in order to reduce the number of comparisons and maintain sufficient power.

3.1.4 Results

ACOF values ranged from 0.057 to 0.406 with an average ACOF of 0.189. The mean of the standard deviation across a set of ACOF trials within a wear cycle was 0.007 with a maximum standard deviation of 0.025. ACOF increased after the first wear cycle for Shoes A, B, C, and E followed by steady decrease across wear cycles (Figure 3.6). For Shoe D, an initial ACOF decrease

of 0.1 occurred after the first wear cycle followed by a continued steady decrease. ACOF values when a fluid force first exceeded 50 N were 27% to 50% lower than their initial values and 37% to 63% lower than the peak values (Table 3.2). The regression analysis showed that ACOF was affected by the shoe type ($p < 0.001$), the sliding distance ($p < 0.001$), and their interaction ($p < 0.001$).

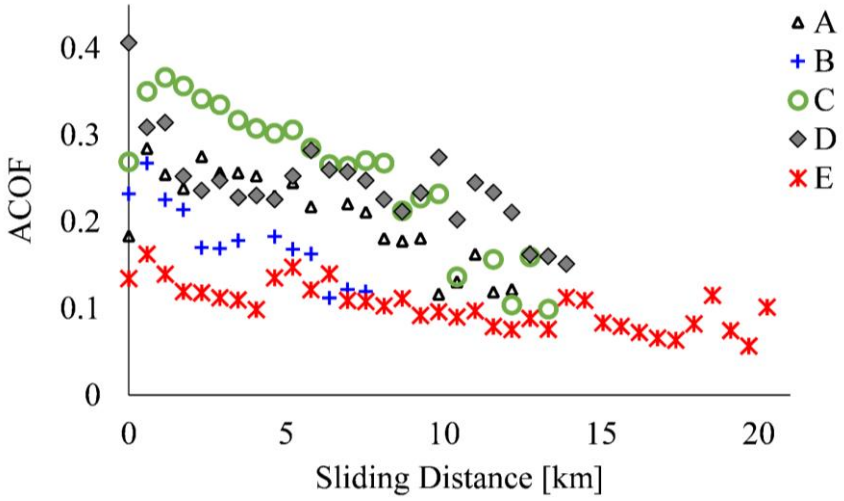

Figure 3.6 ACOF vs. Sliding Distance

ACOF values plotted against the sliding distance that each shoe was worn on the abrasion device. A sliding distance of 0 represents baseline (prior to wear).

Table 3.2 Shoe ACOF and Roughness (R_z)

Baseline (no wear), maximum, and minimum ACOF values across wear cycles, the ACOF values when the fluid force initially reached 50N, and roughness measurements (R_z) of the tread at baseline (no wear) and of the worn region at final wear.

Shoe Code	Total Sliding Distance [km]	Baseline ACOF	Maximum ACOF	Minimum ACOF	ACOF when fluid force first exceeded 50 N	R_z [µm]	
						Baseline	Final
A	12.7	0.183	0.284	0.117	0.117	15.60	13.50
B	7.5	0.232	0.267	0.112	0.168	19.10	14.50
C	13.3	0.269	0.366	0.099	0.136	11.40	14.67
D	13.9	0.406	0.406	0.151	0.202	7.25	12.90
E	20.3	0.134	0.163	0.057	0.066	15.25	12.80

Fluid force values ranged from 0 to 97 N. During the initial wear cycles, when most ACOF values increased relative to baseline, fluid pressures were under 25 N (Figure 3.7). For shoes A, B, and C, there was a distinct increase of fluid force between 4 and 8 km of wear distance accompanied by a steady decrease of ACOF. Shoe D showed an early increase in fluid force (1.2 km of wear), which was also accompanied by a steady decrease of ACOF. Shoe E showed a steady increase in fluid force across all wear cycles. Fluid force was affected by the shoe type ($p < 0.001$), the sliding distance ($p < 0.001$), and the interaction between shoe type and sliding distance ($p < 0.001$).

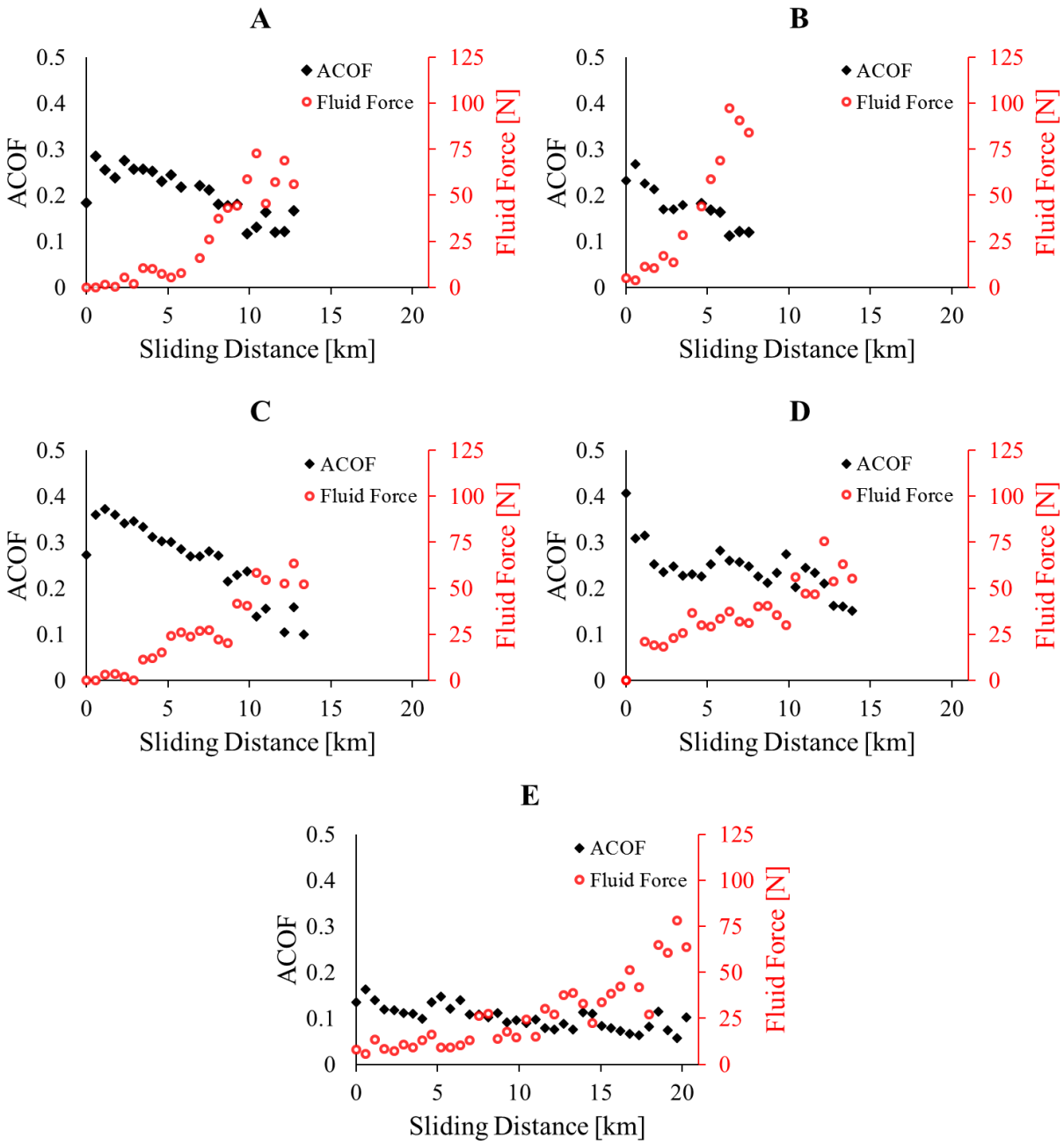

Figure 3.7 ACOF and Fluid Force vs. Sliding Distance

Fluid force and ACOF plotted against the sliding distance that each shoe was worn on the abrasion device. A sliding distance of 0 represents baseline (prior to wear).

Regions of the heel with fully worn tread developed on the lateral side of the heel for shoe A and the medial side of the heel for shoes B, C, D, and E (Figure 3.5). Within the worn region, the length parallel to the sliding axis was greater than the length perpendicular to the sliding axis for shoe A, but smaller for shoes B, C, D, and E. These worn regions ranged from 7 mm^2 to 26 mm^2 at baseline and 1192 mm^2 to 1954 mm^2 after the final wear cycle (Figure 3.8). The worn region size when the fluid force first exceeded 50 N ranged from 840 mm^2 to 1730 mm^2 (mean: 1300 mm^2; standard deviation: 320 mm^2). Subsequently, this region grew at varying rates for each shoe. The worn region size for shoe B and shoe E increased the fastest and slowest, respectively. This region was affected by the shoe type ($p < 0.001$), the sliding distance ($p < 0.001$), and the interaction between shoe type and sliding distance ($p < 0.001$) (Figure 3.8).

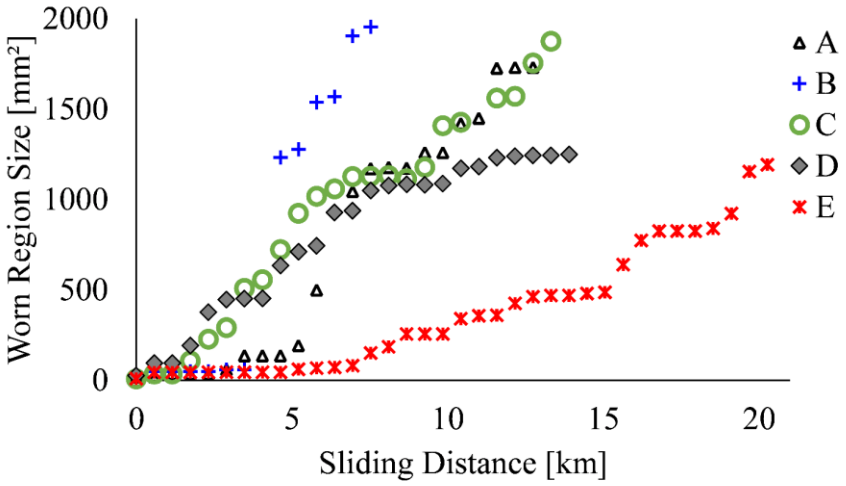

Figure 3.8 Worn Region Size vs. Sliding Distance

The worn region size for each shoe is shown relative to the sliding distance. Each value represents one wear cycle.

Increased fluid loading was associated with a reduction in ACOF which was affected by shoe type ($p < 0.001$), fluid force category ($p < 0.001$), and their interaction ($p < 0.001$) (Figure 3.9). Significant decreases in ACOF between all fluid force categories were seen for two shoes (C

and D) and a significant decrease in ACOF between at least two categories was seen in all shoes. The largest decreases in mean ACOF per category were seen in the shoes with the largest ACOF values at baseline (C and D) (Figure 3.9).

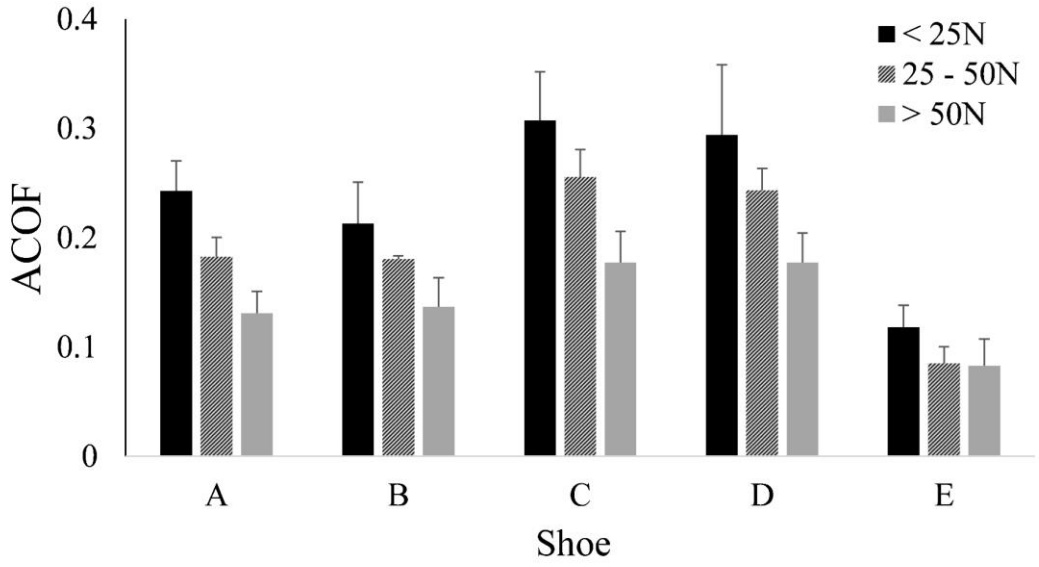

Figure 3.9 Mean ACOF vs. Shoe and Fluid Force Category

The fluid force measured by category (< 25 N, 25-50 N, and > 50 N) for each shoe is shown. Error bars represent standard deviations within fluid force categories. Categories within each shoe connected by a bar are not significantly different.

3.1.5 Discussion

The results confirm that shoe slip-resistance changes as the tread wears. An increase in ACOF and relatively unchanged fluid forces accompanied the initial wear process (< 3 km wear distance) for four of the shoes. After reaching the peak ACOF, fluid forces increased while ACOF values decreased for all shoes. Sudden increases in fluid force occurred at wear distances between 1 and 11 km for four of the shoes indicating that wear thresholds may exist where the shoe performance suddenly changes. The amount of ACOF decrease appeared to scale with the

magnitude of the baseline ACOF: the shoes with the highest baseline ACOF tended to have the largest decrease in ACOF among the fluid force categories.

The results were generally consistent with the literature. Slightly worn shoes tended to have an increase in ACOF consistent with Grönqvist (1995) who suggested this may be due to an optimum combination of surface roughening and sufficient tread depth. In contrast to Grönqvist's suggestions, there was not a clear effect of the change in surface roughness on ACOF for these shoes. An alternative explanation is that slightly worn shoes may lead to higher ACOF due to an increase in contact area as the geometry of the shoe conforms to the floor surface (Moghaddam, 2018; Moghaddam et al., 2019; Moghaddam, Iraqi, & Beschorner, 2014). For all shoes, a decrease in ACOF occurred for severe wear, which aligns with previous research findings that highly worn shoes are associated with a higher risk of slipping (Grönqvist, 1995; Verma et al., 2014). Furthermore, this study supports previous research that related higher fluid forces with increased slip risk and lower ACOF (Beschorner et al., 2014; Beschorner, Lovell, Higgs III, & Redfern, 2009).

Prior to the sudden increase in fluid force, there was gradual decrease in ACOF. This behavior may be due to the shape factor of the tread which is defined by the loaded area of a rubber block divided by its area of lateral surface that is free to expand (Imbimbo & De Luca, 1998). The reduction of tread depth will increase the shape factor of a tread block by decreasing the area of the lateral surface that is free to expand. Consequently, this may result in a higher compression modulus and lower deformability (Imbimbo & De Luca, 1998) of the tread block. In tire traction applications, the geometry of the tire tread block (given the same volumetric properties and contact area) in contact with a rigid surface affects rubber deformation (Sridharan & Sivaramakrishnan, 2012). On the other hand, tread blocks that have too much height (and subsequently tread channels

that are too deep) can reduce the ACOF (Maegawa, Itoigawa, & Nakamura, 2016; Yamaguchi et al., 2017). Specifically, previous research showed that a large tread depth could lead to lower bending stiffness, which could result in an increase in deflection during sliding. This increase in deflection can reduce the contact area and subsequently decrease the friction force in boundary lubrication. Thus, this research suggests there may be an optimal tread depth that minimizes hydrodynamic pressures, reduces the shape factor, and has increased bending stiffness.

Although ACOF decreased as the shoes were worn, increased fluid forces were more dependent on the worn region size (Figure 3.8). Faster growth in the worn region (e.g. Shoe B) was also associated with faster onset of high fluid pressures, whereas a slower growth in worn region (e.g. Shoe E) was associated with slower onset of high fluid pressures. Currently, some footwear providers offer tread gauge meters for tracking the utility of worn shoes (Shoes For Crews, 2019b). However, this metric may not capture the salient features of the worn shoe condition. The minimum tread depth reached 0 mm as soon as the worn region began forming which occurs early in the wear process (Figure 3.10). Furthermore, the reduction of the minimum tread depth to 0 mm occurred prior to substantial increases in the fluid forces. Specifically, this change occurred prior to fluid forces equal to 10% of the normal load during testing (25N) for all shoe types. Thus, the worn region size may be more relevant to the under-shoe tribology dynamics.

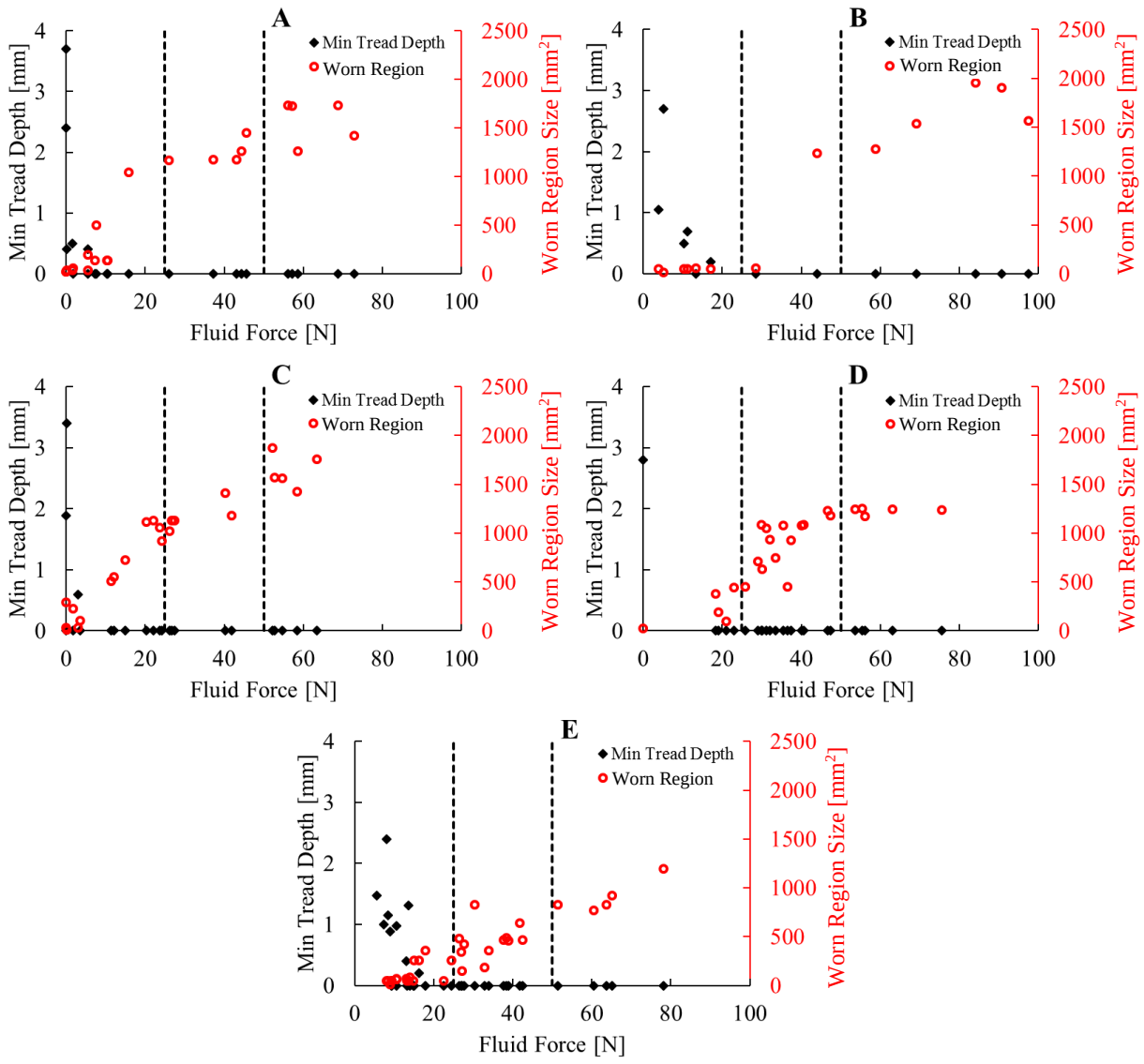

Figure 3.10 Minimum Tread Depth and Worn Region Size vs. Fluid Force

Minimum tread depth on the left y-axis is plotted in black diamonds. Worn region size on the right y-axis is plotted in red circles. Fluid force thresholds of 25N and 50 N are indicated with vertical dashed lines. Minimum tread depth reached 0 when the worn region began forming. Plots are separated by shoe.

Tread may start to be too worn when under-shoe fluid forces rise above 10% of the vertical load (25 N), acting as a first indicator of replacement (Figure 3.9). A fluid force greater than 20% of the vertical load (50 N) may serve as a replacement threshold since our findings suggest that an ACOF decrease of 25% to 50% of the baseline value may be associated with these fluid forces. Fluid forces exceeded this level when the worn region size exceeded between 840 mm^2 and 1720 mm^2. A conservative estimate might be to replace shoes at the lower limit of this range (approximately 800 mm^2). This information has potential to be used to guide footwear replacement thresholds.

While this study was not designed to determine the tread design parameters that influenced wear progression, notable differences were observed across the footwear designs. For example, Shoe B wore out in the shortest sliding distance whereas Shoe E wore out over the longest distance. The statistical modeling in this study using a nominal code for shoe type has limited predictive ability when extrapolating to other tread patterns and materials. However, a post-hoc analysis was performed to further explore the differences across shoes. Interestingly, the difference in the rate of response to wear might be explained by the proportion of the heel's surface covered in tread (Table 3.1). A bivariate correlation analysis was used to determine the relationship between tread proportion and total wear distance. Increased tread proportion was associated with an increased number of wear cycles and thus, increased total sliding distance ($p = 0.026$). As such, Shoe E had the largest proportion of tread coverage over the heel (tread proportion). This effect may be associated with Archard's law which describes how the wear rate is proportional to the contact pressure (Archard, 1953; Moghaddam et al., 2019). Thus, a larger tread proportion produces a larger contact area and reduces the contact pressure on the individual tread blocks. However, a

more robust study with more shoes and systematically varied tread coverage would need to be conducted to confirm this relationship.

As this is the first research study to examine the association between progressive shoe wear and ACOF, fluid force, and worn region size, certain limitations should be acknowledged. First, only a limited number of shoes were examined, chosen as industry-marketed slip-resistant shoes. These shoes have significant tread to provide fluid drainage. Other types of shoes may behave differently. Second, the wear device was effective in producing rapid wear that had profiles on the heel similar in appearance to actual wear from walking. However, there may be unforeseen differences between these methods and naturally worn shoes due to varied gait biomechanics. Furthermore, extending this research to additional flooring (roughness, hardness) and contaminants with varying material properties (e.g., viscosity, surface tension) might lead to different wear thresholds. Improvements for future use of this simulated wear protocol could include employing personal gait characteristics (e.g., supination/pronation, heel strike angle, etc.) to better approximate natural wear.

These results suggest that a worn region on the heel with a size larger than 800 mm^2 leads to increased fluid forces and a reduction in ACOF. Research has shown that these changes are consistent with an increase in slip risk (Beschorner et al., 2014; Hanson et al., 1999). Thus, the amount of wear in specific areas on the shoe may be useful in determining a threshold for shoe replacement to prevent slips. The results are promising and useful for the development of future guidelines for shoe evaluation and for further research taking into account the material properties of shoe wear and flooring and also the gait biomechanics.

3.2 Shoe Wear Geometry Predicts Under-Shoe Hydrodynamics

3.2.1 Abstract

Slips and falls are a leading cause of injuries in the workplace. The risk of slipping increases as shoe tread wears. The mechanics relating shoe wear to slip risk is needed to develop fall-prevention strategies. This research applies a rectangular, tapered-wedge bearing solution to worn shoes and compares the results to experimentally-measured under-shoe fluid pressure results. Changes in the size of the shoe outsole worn region and fluid dispersion capabilities were recorded for four, slip-resistant shoes which were systematically abraded. The applied solution predicted the film thickness between the shoe and flooring during a slipping event based on experimental data. The results provide support that the tapered-wedge solution can be used to assess slip risk in worn shoes.

3.2.2 Background

Slips and falls account for a large portion of non-fatal, occupational injuries. These slips often occur due to a lack of friction at the shoe-floor interface in the presence of a liquid lubricant (Burnfield & Powers, 2006; Hanson et al., 1999). Research has shown that as shoes become worn, the coefficient of friction between the shoe and flooring in the presence of high viscosity fluids decreases (Grönqvist, 1995; Hemler, Charbonneau, et al., 2019) due to a reduced capacity for the tread to disperse fluid (Beschorner, Albert, & Redfern, 2016; Grönqvist, 1995; Hemler, Charbonneau, et al., 2019; Singh & Beschorner, 2014). Therefore, understanding the effects of shoe tread geometry and wear on under-shoe hydrodynamics is important for reducing slip risk.

Shoe performance varies with outsole geometry. Previous studies have analyzed how variations in tread parameters (size, orientation, depth, contact area) affect traction performance (Li & Chen, 2004; Li et al., 2006; Moriyasu, Nishiwaki, Shibata, Yamaguchi, & Hokkirigawa, 2019; Yamaguchi et al., 2017). The effects of material thickness ratios, resultant rubber tread block stiffness, and surface roughness on the friction coefficient have also been explored (Ido et al., 2019; Moriyasu et al., 2019). Shoes marked as 'slip-resistant' (SR) by manufacturers have tread pattern designs that tend to have smaller tread blocks separated by tread channels. These channels allow for fluid dispersion that ameliorate under-shoe hydrodynamic pressures (Beschorner et al., 2014). However, research on predicting changes to under-shoe fluid dispersion based on the tread loss is still emerging.

Mechanics models have emerged as an important tool for understanding shoe-floor friction mechanics and predicting the influence of footwear on shoe-floor friction. These models can be broadly categorized as contact friction models and thin-film fluid models. The contact friction models have used finite element analysis to predict hysteresis friction (Moghaddam et al., 2018; Moghaddam et al., 2019; Moghaddam et al., 2014) and applied beam mechanics to determine the influence of tread bending stiffness on contact area (Moriyasu et al., 2019; Yamaguchi et al., 2017) and slipping (Trkov, Yi, Liu, & Li, 2018). Shoe-floor hydrodynamic models have typically applied Reynolds equation (or derivations based on this equation) to shoe-floor contaminant interactions (Beschorner et al., 2009; Proctor & Coleman, 1988). Of these two hydrodynamic modeling efforts, one modeled the shoe tread as a single rough hemisphere (Beschorner et al., 2009). Proctor and Coleman modeled the entire shoe based on the tapered wedge solution of Reynolds equation (Proctor & Coleman, 1988). This model, however, was not validated against experimental data and was primarily focused on the effects of floor roughness on shoe-floor friction. Thus, further

development of a shoe-floor hydrodynamics solution may yield additional insight into the influence of shoe geometry on shoe-floor-contaminant interactions.

Recently, under-shoe fluid pressures and the friction coefficient have been experimentally measured for progressive shoe wear (Hemler, Charbonneau, et al., 2019). These measurements may offer an opportunity to validate under-shoe hydrodynamics solutions (such as the one suggested by Proctor and Coleman). Past experiments have demonstrated that under-shoe fluid pressures are sensitive to the size of the worn region consistent with the predictions of thrust bearing models (Proctor & Coleman, 1988). However, fluid dynamics models of shoe-floor interactions have not yet been compared to experimental measurements of under-shoe hydrodynamic conditions based on geometrical features of the worn condition.

The purpose of this study is to evaluate the relationship between film thickness prediction based on a rectangular, tapered-wedge bearing solution and experimentally measured fluid dispersion across shoes with simulated wear.

3.2.3 Methods

3.2.3.1 Summary

This study represents a post-hoc analysis of data that has been previously reported (Hemler, Charbonneau, et al., 2019; Moghaddam et al., 2019). Specifically, this study applies the tapered wedge solution of Reynolds equation (modeling) to relate the measured size of the worn region to the measured under-shoe fluid load support (experimental). An iterative procedure was performed that alternated between: 1) abrading of shoe outsoles; and 2) testing coefficient of friction, under-shoe fluid pressures, and tread volume loss (Figure 3.11; adapted from (Hemler, Charbonneau, et al., 2019)). Previously, we have reported changes in friction performance and under-shoe fluid

hydrodynamics during wear progression (Hemler, Charbonneau, et al., 2019). Furthermore, we have reported a finite element model that predicted changes in tread geometry due to wear (Moghaddam et al., 2019). Given these previous reports, the methodological details are only briefly described.

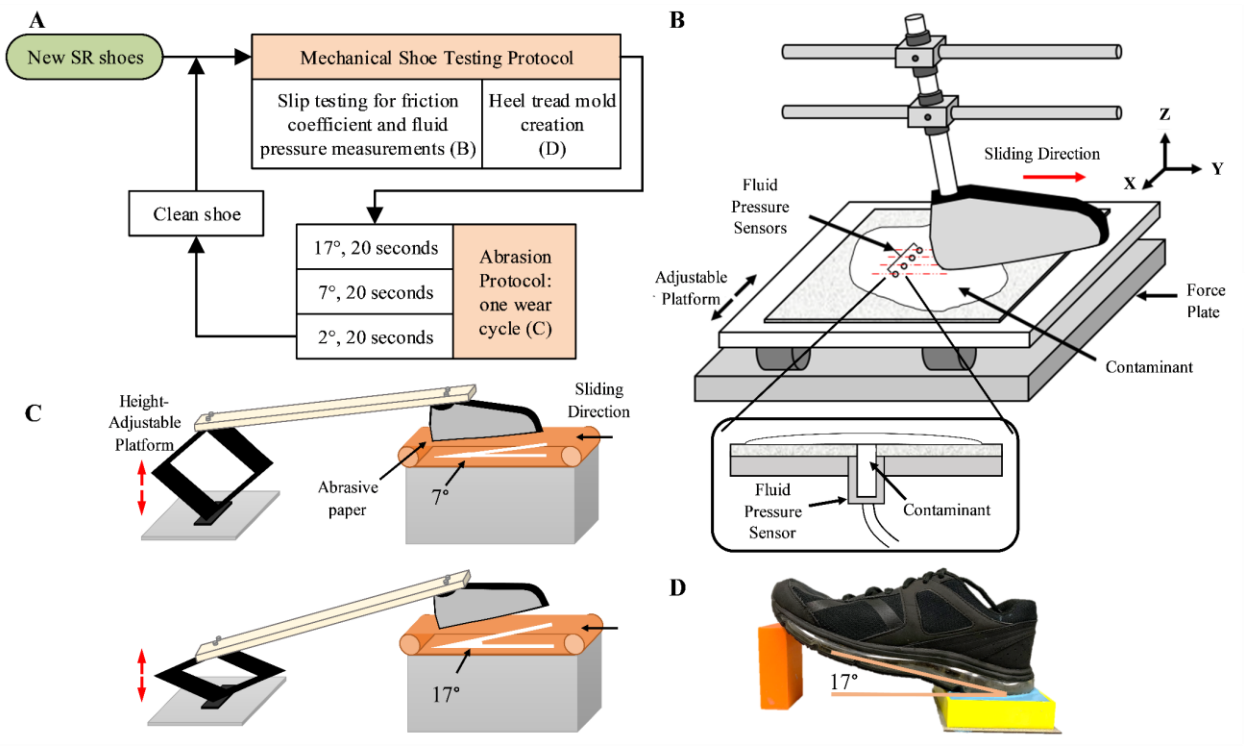

Figure 3.11 Experimental Design & Setup

A) Flow diagram of mechanical shoe testing protocol and abrasion protocol. B) A robotic slip tester was used to slid each shoe across a contaminated surface along the Y-axis with four fluid pressure sensors. The adjustable platform was moved 5 mm in the X-direction after each trial. A cross-sectional view of the fluid pressure sensor is shown. C) The abrasion protocol consisted of wearing down the shoes on abrasive paper at three angles for 20 seconds each. Examples of wear at 7° and 17° are presented. D) Molds of the heel tread were created at baseline and after each wear cycle at a 17° sagittal plane angle.

3.2.3.2 Abrasion Protocol

Five shoes labeled as slip-resistant shoes were used in this study (Figure 3.12). The right shoe of each pair was mechanically abraded at three different shoe orientations (17°, 7°, 2°). The angles were chosen to reflect the orientation of the shoe during walking from heel strike to flat foot (Kadaba et al., 1990). One of the five shoes was excluded from this analysis since two distinct worn regions were observed in the middle of the heel compared to a single worn region at the rear of the heel that was observed for the other shoes. To wear the shoes, abrasive paper (180μm diameter particles) was slid across each shoe at 9.65 m/s for 20 seconds at each of the three angles. The normal force was ~40 N. Abrasive grease was used to reduce heat buildup and was cleaned from the shoes before friction testing. The shoes were progressively worn using this protocol. The number of wear iterations ranged from 13 to 35.

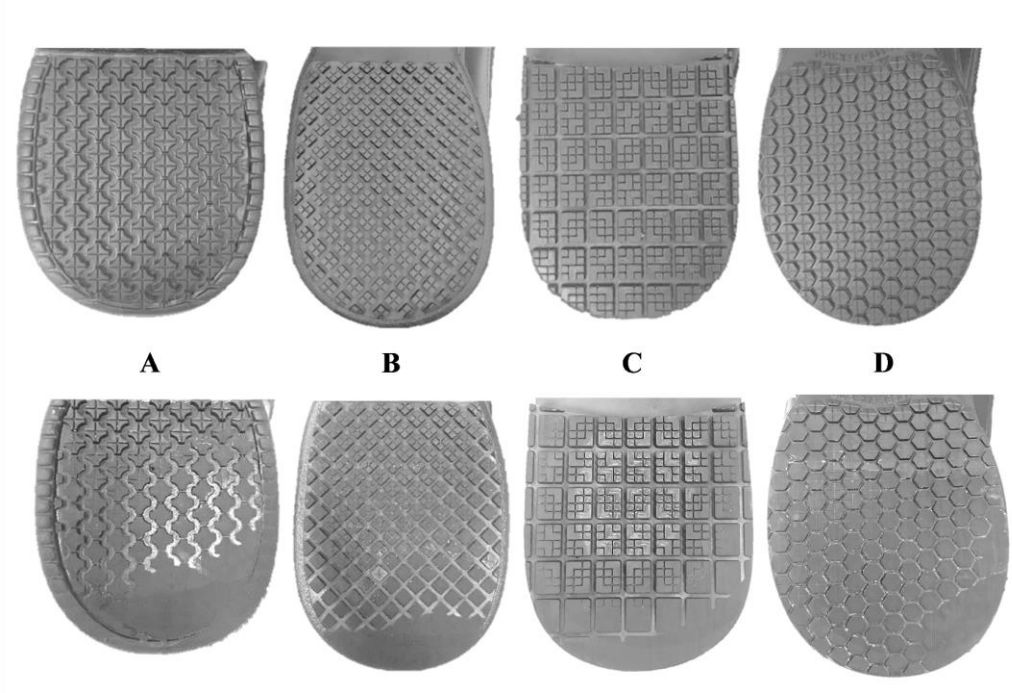

Figure 3.12 Experiment Shoes

The heel of the four shoes mechanically abraded at baseline (top) and after the last wear cycle (bottom) according to shoe type. Figure adapted from (Hemler, Charbonneau, et al., 2019); shoe A from Section 3.1.3 was excluded from this analysis as there were two worn region sizes. Therefore shoe codes were shifted such that shoes B, C, D, and E are labeled as shoes A, B, C, and D in this analysis.

3.2.3.3 Mechanical Shoe Testing Protocol

Prior to wear and after each wear cycle, the shoes were slid across a contaminated floor surface that simulated a slipping action using a robotic device as seen in a previous study (Hemler, Charbonneau, et al., 2019). The robotic slip tester measured ground reaction forces and under-shoe fluid pressures. The fluid pressure sensors each had an inlet diameter of 3.2 mm and were recessed into a platform.

The shoes, attached to a shoe last, were slid across a vinyl composite tile (Armstrong, 51804; R_q = 3.13±0.42 µm) covered with a diluted glycerol solution (90% glycerol, 10% water by volume; 219 cP). Sliding conditions that are valid predictors of slipping and consistent with the

shoe at the onset of slipping were used: shoe angle of 17° (Albert et al., 2017; Iraqi, Cham, Redfern, & Beschorner, 2018), sliding speed of 0.3 m/s (Albert et al., 2017; ASTM, 2011; Iraqi, Cham, Redfern, & Beschorner, 2018), and normal force of 250 N (Iraqi & Beschorner, 2017; Iraqi, Cham, Redfern, Vidic, et al., 2018). Twenty fluid pressure scans were collected at 5 mm intervals to estimate under-shoe fluid pressures.

At baseline and after each wear cycle, the heel tread geometry was recorded by creating a silicone rubber mold of the shoe heel as reported in a previous study (Hemler, Charbonneau, et al., 2019). Using this mold, the size of the worn region was measured for each shoe heel outsole at baseline and after each wear cycle. This metric was defined as the product of the longest and widest continuous area without tread channels. The length (l) was measured along the long axis of the foot (anterior to posterior) and the width (b) was measured perpendicular to the long axis (medial to lateral).

3.2.4 Theory & Calculations

3.2.4.1 Data Analysis

The average friction coefficient across the five trials per wear cycle was calculated from the ground reaction forces. Fluid pressure sensor data that were five standard deviations above the baseline levels were included in the analysis (Beschorner et al., 2014; Hemler, Charbonneau, et al., 2019). Numerical integration was performed to calculate the fluid force (i.e., load supported by the fluid) based on the fluid pressure at the ith frame (p_i), perpendicular distance between scans ($\Delta x = 5$ mm), the sliding velocity (v = 0.3 m/s), and the time between each frame (Δt = 2 ms) (Equation 3.3) (Singh & Beschorner, 2014). Fluid force across the twenty scans (4 scans per trial * 5 trials) was summed.

$$F_{fluid} = \sum p_i \, \Delta x \, \Delta y = \sum p_i \, \Delta x \, v \, \Delta t \qquad 3.3$$

3.2.4.2 Fluid Film Calculations

The tapered-wedge solution by Fuller, which was later applied to shoes by Proctor and Coleman, was used to apply hydrodynamic theory to a shoe-floor contaminant interface (Fuller, 1956; Proctor & Coleman, 1988). In the solution, the minimum film thickness, h_0, occurs at the rear edge of the wedge (Fuller, 1956). As such, the predicted film thickness (PFT) applies to the rear edge of the heel by using the region of the shoe tread that was completely worn was treated as the wedge in the model. The predicted film thickness (PFT) was calculated as a function of dynamic viscosity ($\mu = 214 \; cP$), the sliding speed ($v = 0.3 \frac{m}{s}$), length of the wedge (l), width of the wedge (b), normal force applied to the wedge ($F = 250 \; N$), and K_p, a factor calculated from the incline of the wedge (Fuller, 1956) (Equation 3.4). An average K_p value of 0.025 was used to simplify the calculations (Fuller, 1956).

$$h_0 = \sqrt{\frac{6\mu v l^2 b}{F} * K_p} \qquad 3.4$$

This equation was adapted to allow for side leakage since the shoes contained no border to prevent leakage. Thus, the factor, η, was added as a correction factor related to the ratio of the width over the length of the wedge (Fuller, 1956). The factor, η, is dependent on the geometry of the region of the shoe without tread and was calculated for each shoe and wear cycle. Therefore, η, and thus PFT values were calculated separately for each wear cycle, i (Equation 3.5).

$$h_{0_i} = \sqrt{\frac{6\mu v {l_i}^2 b_i \eta K_p}{F}} \qquad 3.5$$

3.2.4.3 Statistical Analysis

To quantify the relationship between the PFT and the fluid force, ANOVA methods were used. Specifically, the dependent variable was the experimentally-measured fluid force and the independent variables were shoe, PFT, and their interaction. To normalize residuals of the fluid force data and satisfy the assumptions of the statistical model, a square root transformation was used. When the size of the worn region did not change between wear cycles, only the first data point was used until the worn region increased.

3.2.5 Results

In the experiment, the fluid force values ranged from 0 to 97.4 N and the friction coefficient ranged from 0.057 to 0.41. Applying the size of the worn region to the tapered-wedge solution model, the PFT values ranged from 0.6 to 42 μm with an average film thickness of 18.7±11.6 μm. An increase in fluid force was associated with an increase in PFT (Figure 3.13; $F_{1,71} = 462.1$, $p < .001$, $R^2=.89$). Fluid force was influenced by shoe type ($F_{3,71} = 45.7$, $p < .001$). The fluid force was not affected by the interaction of the PFT and the shoe type ($F_{3,71} = 2.2$, $p = .098$).

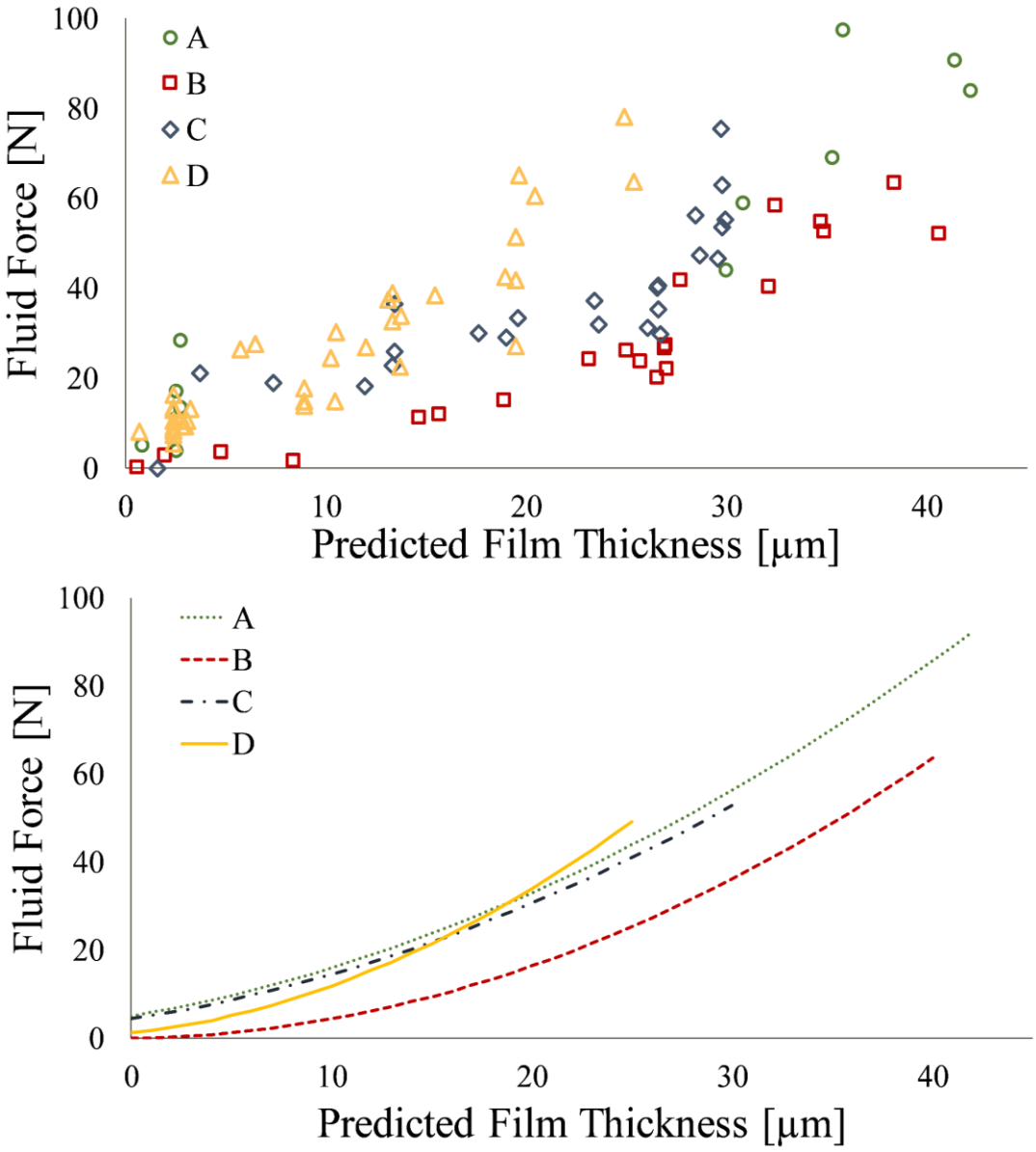

Figure 3.13 Fluid Force vs. Predicted Film Thickness

(Top) Experimentally-measured fluid force with respect to the PFT for the shoes A-D. (Bottom) Regression lines for fluid force and PFT relationship for each shoe based on statistical analysis.

3.2.6 Discussion

In this study, the tapered-wedge model of film thickness was predictive of the experimentally-measured fluid force. An increase in fluid force coincided with an increase in PFT, which was based on size of the worn region and testing parameters. This relationship was seen regardless of shoe tread type for all SR shoes. As such, calculating film thickness based on geometric measures and fluid viscosity may be feasible for predicting the fluid dispersion capabilities of shoe tread.

The PFT values reasonably predicted the lubrication regime of the shoe-floor-liquid system which has been shown in previous studies as a predictor of shoe wear (Hemler, Charbonneau, et al., 2019). The lubrication regime is often described using the lambda ratio (λ) which is the minimum film thickness normalized to the composite RMS surface roughness (R_q) (Equation 3.6) (Stachowiak & Batchelor, 2013). When $\lambda < 1$, the surfaces are acting in the boundary lubrication regime where the dominating asperities are in contact and friction is at a peak. As lambda increases, the interaction operates in the mixed lubrication regime ($1 < \lambda < 5$), and then moves into the hydrodynamic lubrication regime ($\lambda > 5$) or the elasto-hydrodynamic lubrication regime ($3 < \lambda < 10$). In this study, the fluid force started to increase when $\lambda \approx 1$ ($h_{\lambda=1}$=3.5±0.2). Thus, this simple model yields predictors in line with the experimentally observed transition from boundary to mixed lubrication. The friction coefficient decreased as the shoes became more worn. The increase in wear led to an increase in the lambda ratio and PFT values, implying a shift from the boundary lubrication regime to the mixed lubrication. (Figure 3.14).

$$\lambda = \frac{h_0}{\sqrt{{R_q}_{floor}^{\,2} + {R_q}_{shoe}^{\,2}}} \qquad 3.6$$

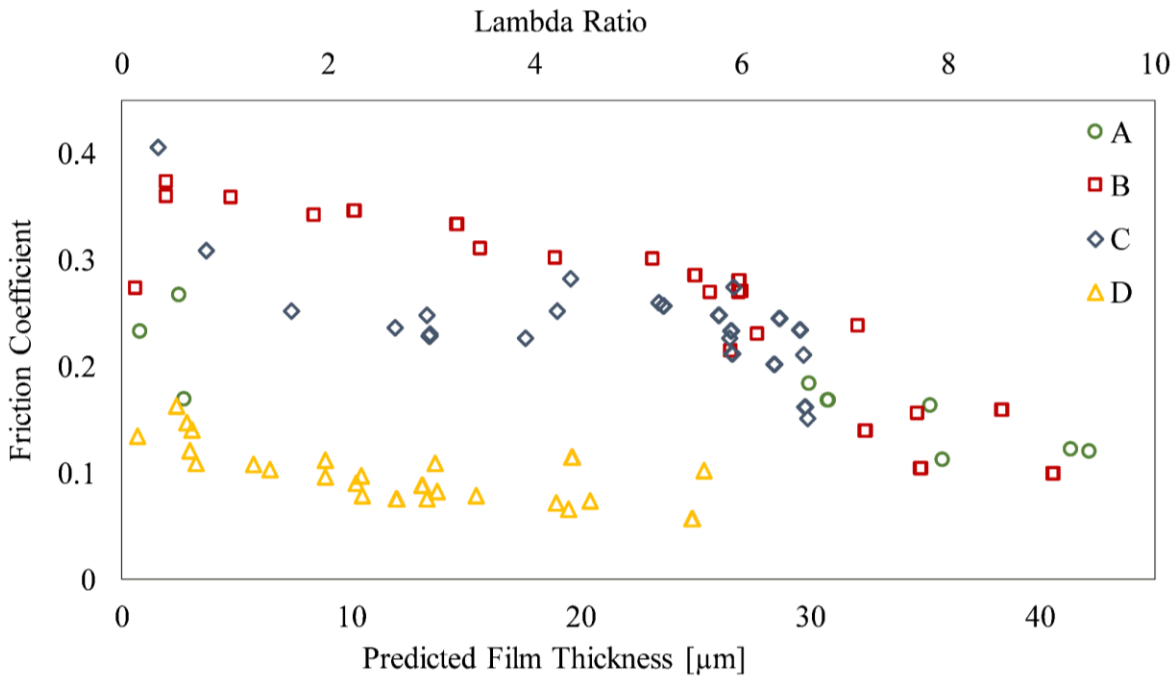

Figure 3.14 Friction Coefficient vs. Lambda Ratio and Predicted Film Thickness

The friction coefficient with respect to the lambda ratio, λ (top axis) and PFT (bottom axis) for each shoe. The average roughness across shoe outsoles was used to determine the lambda ratio.

Simple modeling approaches may be useful for predicting under-shoe hydrodynamics even when more sophisticated approaches are available. Previous models have explored fluid dynamics and wear using sophisticated models. For example, Beschorner, et al. developed a mixed-lubrication model using a pin-on-disk apparatus based on Hertzian contact mechanics and Reynolds equation for understanding how shoe-floor friction changes with varying speed and shoe material changes (Beschorner et al., 2009). Moghaddam et al., demonstrated the use of finite element analysis in modeling shoe wear against a variety of surfaces (Moghaddam et al., 2019). These previous modeling efforts required iterative methods and complex solution techniques (finite difference method and finite element modeling, respectively) that might be inaccessible to non-engineering users. However, the method presented by Proctor and Coleman which is also utilized in the present study uses simpler methods to predict under-shoe hydrodynamic effects

based on a reasonably simple equation (Equation 3.4) and a few simple geometric measurements of the tread's worn region (Proctor & Coleman, 1988). Importantly, this model was valid in its predictions despite its simplicity. The practicality and simplicity of the model presented in this study may enable it to be employed by a wide audience.

This solution can be used as a pragmatic tool for determining slip risk based on shoe geometry. Interestingly, the prediction of fluid force via film thickness (R^2=0.66) in this study was stronger compared to the prediction of fluid force based on wear sliding distance (R^2=0.38) as seen in Figure 3.15 and further explored in a previous study (Hemler, Charbonneau, et al., 2019). Thus, the actual shoe geometry acts as a better predictor of shoe wear and subsequent slip risk compared to the amount of usage. Practically, this is an important consideration for determining slip risk thresholds for shoe wear. Previous studies have focused primarily on time of wear as a metric for replacing shoe wear (Verma et al., 2014). However, the shoe outsole geometry, specifically the size of the worn region, may be a better indicator of under-shoe hydrodynamics and thus, slip risk, as supported by this study and a previous study (Hemler, Charbonneau, et al., 2019).

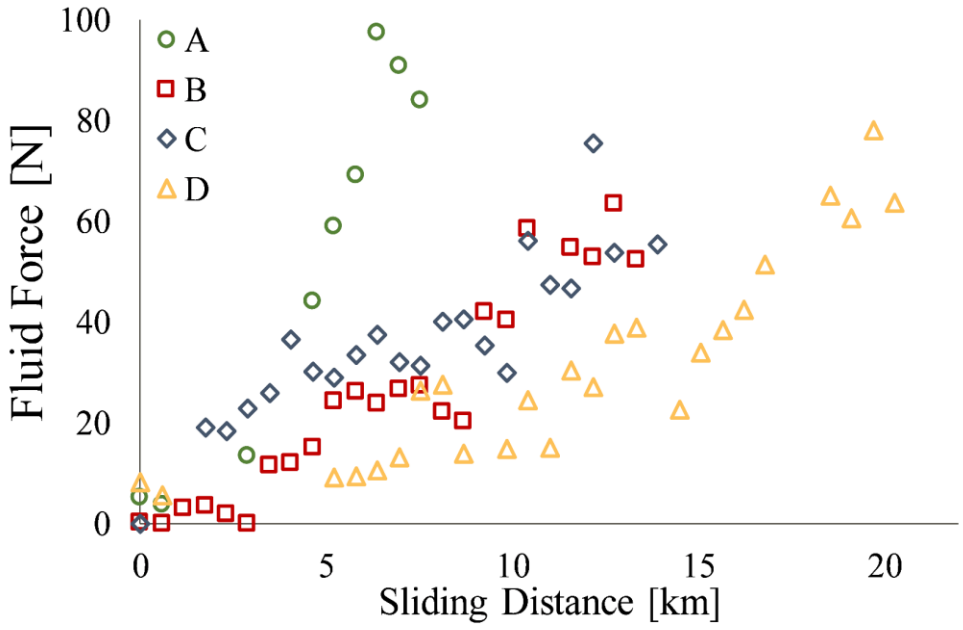

Figure 3.15 Fluid Force vs. Sliding Distance.

Certain study limitations and future directions should be noted. Only one flooring, and contaminant are utilized. Previous research has shown that under-shoe fluid pressures are sensitive to these metrics (Beschorner et al., 2007; Chanda, Jones, & Beschorner, 2018; Chanda, Reuter, & Beschorner, 2019). Thus, futures studies may consider expanding upon the work in this study to contaminants with varying material parameters (viscosity, shoe materials) that encompass an array of materials used in industrial settings. This model excluded one shoe design that contained two worn regions. As such, the model has not been validated with shoes that contain multiple distinct worn regions. The existence of multiple wear patterns and applicability of this model should be considered in future studies. Also, validating this model with naturally-worn shoes and for human slips would increase confidence in its relevance to walking and slipping. Furthermore, comparing the model predictions to experimentally-measured film thickness values (e.g., using ultrasound methods (Dwyer-Joyce, Drinkwater, & Donohoe, 2003) may provide additional detail regarding the ability of this model to assess shoe-floor hydrodynamic conditions. Thus, important

opportunities exist to further our understanding on how to apply the tapered wedge model to worn shoes.

3.2.7 Conclusion

Determining the influence of shoe tread wear on slip risk is a key factor in the design of safe and durable shoe tread for the workplace. The tapered wedge solution is a good start for understanding the relationship between wear and under-shoe hydrodynamics. Furthermore, this model may be useful for determining wear thresholds for particular shoe, floor, and liquid material properties to reduce slipping events.

4.0 Progressive Natural Wear - Changes in and Application of Traction Performance and Geometry

This chapter analyzes changes in traction performance (friction and under-shoe hydrodynamics) and outsole geometry for naturally worn shoes. The structure resembles Section 3.0 with a focus on natural wear. As such, traction performance changes with respect to wear metrics are discussed within Section 4.1. Furthermore, preliminary data of the natural wear study has been published in a peer-reviewed journal (Hemler, Pliner, Redfern, Haight, & Beschorner, 2020) and as conference abstracts (Hemler & Beschorner, 2019a; Hemler, Pliner, Redfern, Haight, & Beschorner, 2021; Hemler, Redfern, Haight, & Beschorner, 2018a, 2018b; Hemler, Sundaram, et al., 2020).

4.1 Natural Shoe Wear

4.1.1 Abstract

Objectives: Adequate footwear is an important tool in efforts to prevent slips and falls. While slip-resistant shoes have been shown to decrease slip risk due to their increased friction and under-shoe fluid drainage (traction performance), their traction performance diminishes with wear. However, these changes have not been extensively studied in in natural settings. This study quantifies slip-resistant shoe traction performance in response to increased usage and the corresponding growth of the tread wear geometry (worn region size).

Methods: Participants wore two pairs of shoes in the workplace for up to 12 months each, while the distance walked was tracked. After each month of wear, traction performance and worn region size were measured for each shoe.

Results: The results showed that increased usage (distance walked, months used, and worn region size) was associated with decreased traction performance. A worn region size of 800 mm^2 was associated with reductions in friction of 16-38% and with increases in the load supported by the fluid (fluid force) by 286-528%. Furthermore, a hydrodynamic model based on the worn region size predicted experimentally-measured under-shoe fluid effects and showed that worn region sizes of roughly 850-1150 mm^2 were associated with a fluid force equal to 10% of the normal force during testing.

Conclusions: Wear metrics, particularly walking distance and worn region size, may be good indicators of loss in traction performance due to wear. Therefore, tracking footwear or monitoring outsole conditions are useful for determining shoe replacement recommendations to reduce occupational slips and falls.

4.1.2 Background

Slips, trips, and falls are a leading cause of injury in the workplace. They account for 28% of nonfatal occupational injuries with over 300,000 injuries annually in the United States (U.S. Department of Labor - Bureau of Labor Statistics, 2021). In addition, workers' compensation costs from falls are over $17 billion annually with falls on the same level responsible for over $11 billion - almost 20% of the financial burden for all occupational injuries (Liberty Mutual Research Institute for Safety, 2016). Research has shown that 40-50% of fall-related injuries have been attributed to slipping (Courtney et al., 2001). As slipping occurs between the shoe-floor interface, there is a need to understand the tribological interactions at this interface.

Proper footwear has been shown to increase health benefits and reduce the occurrence of slips and falls. Bell, et al. showed that a no-cost-to worker slip-resistant (SR) footwear program reduced the number of slip-related worker's compensation claims (Bell, Collins, & Chiou, 2018). Torkki, et al. showed that selecting proper occupational footwear may have increased health benefits and lead to decreased need of health resources (Torkki et al., 2002). Verma, et al. showed that wearing SR shoes rather than non-SR led to a 54% reduction in slipping in the workplace (Verma et al., 2011). Furthermore, shoes that are new or less than 6 months old were more effective at reducing slip risk than older shoes (Verma et al., 2014). However, studying shoes in 6-month increments may not be sufficient for understanding slip risk across the shoe's lifetime (V.H. Sundaram et al., 2020). Therefore, there is a need to understand how traction performance changes with shoe usage and physical wear compared to shoe age.

Slips occur due to decreased friction between the shoe and floor, often in the presence of a contaminant. The available coefficient of friction (ACOF), which is measured as the friction that prevents slipping between two surfaces, has been a useful metric for determining slip risk (Cook

et al., 2021; Hanson et al., 1999; V.H. Sundaram et al., 2020). Various shoe tread factors have been shown to influence ACOF including shoe heel shape (Hemler & Beschorner, 2019a; Iraqi et al., 2020), hardness (Iraqi et al., 2020; Tsai & Powers, 2008), tread surface area (Iraqi et al., 2020), tread depth (Beschorner & Singh, 2012; Blanchette & Powers, 2015; Li et al., 2006), tread width (Blanchette & Powers, 2015; Li & Chen, 2004, 2005), and tread orientation (Blanchette & Powers, 2015; Yamaguchi et al., 2017). Furthermore, SR shoes often have increased ACOF compared to non-SR counterparts (Beschorner et al., 2017) and have been shown to have better fluid drainage properties than non-SR shoes (Hemler, Sundaram, et al., 2019). The improved ACOF and fluid drainage of these shoes is attributed to their tread patterns; they often have small tread blocks that allow for fluid drainage under the shoe during a potential slip. Increased fluid drainage has been shown to lead to increased ACOF which begets lower slip risk (V.H. Sundaram et al., 2020). We define "traction performance" as relating to shoe features that enhance its ability to prevent slips during gait including increased ACOF and increased fluid drainage (Hemler, Pliner, et al., 2020). Reduced fluid pressures are indicative of increased fluid drainage.

As shoes are worn, traction performance decreases (Beschorner et al., 2014; Grönqvist, 1995; Hemler, Charbonneau, et al., 2019). Individual tread blocks wear down to form a worn region on the shoe outsole. The size of the worn region has been shown to be a mechanism by which under-shoe fluid pressures increase which leads to decreased ACOF and increased risk of slipping (V.H. Sundaram et al., 2020). However, this cross-sectional research studied one time point of natural wear. Previous studies have studied progressive wear for simulated protocols (Hemler, Charbonneau, et al., 2019; Walter et al., 2021), and for progressive natural wear across one shoe tread style (Hemler, Pliner, et al., 2020). There is a gap in the literature examining progressive, natural wear across multiple shoe types and tread patterns.

The aims of this study are to track shoe traction performance changes in response to increased usage (months worn and distance walked) and outsole geometry changes (size of the continuous worn region). The secondary goal of this study is to provide quantitative measures guiding the threshold for slip-resistant shoe replacement to reduce the risk of occupational slips and falls.

4.1.3 Methods

4.1.3.1 Summary

Participants wore two pairs of slip-resistant shoes in their workplace alternating shoes every month for up to 24 months. Before and after each month of wear, the traction performance (coefficient of friction and under-shoe fluid pressures between the shoes and flooring) were recorded. A shoe heel mold was created at each of these time points to track the outsole geometry changes. Analyses were performed to assess the impact of shoe usage and wear on traction performance. Pilot data (accounting for ~31% of the full data) from this study was previously published (Hemler, Pliner, et al., 2020).

4.1.3.2 Participants & Shoes

In this study, 23 participants were enrolled to wear two pairs of shoes in their workplace (n_{shoes} = 46). Eight participants were entirely excluded from the analysis (2 pairs of shoes each) and one pair of shoes from six participants were excluded for three primary reasons: three participants (n_{shoes} = 4) discontinued wearing the shoe due to experiencing shoe discomfort, six participants (n_{shoes} = 11) withdrew from the study prior to completing one month of walking in the shoes, five participants (n_{shoes} = 7) walked fewer than 100 km prior to completion of enrollment

due to low activity levels. Furthermore, two boots from two participants were excluded from the analysis because they failed to drain fluid at the baseline level. Therefore, 15 participants (M: 12, F: 3; age: 41.7 ± 12 yrs; mass: 89.8 ± 12.5 kg; height: 176.7 ± 10.3 cm; BMI: 28.8 ± 3.4) and 22 pairs of shoes are included in this analysis (US Men's Shoe Size: 10.1 ±2.3). Participants were provided with two pairs of footwear – shoe A and either: shoe B or shoe C (Figure 4.1). Within each shoe type, boots or shoes with the same tread pattern were provided depending on their occupational requirements. As shoe B was discontinued from manufacturing during the study, four participants received shoe C rather than shoe B. Therefore, the 10 pairs of shoe A (SRMax), 8 pairs of shoe B (safeTstep), and 4 pairs of shoe C (ShoesForCrews) were included in the study.

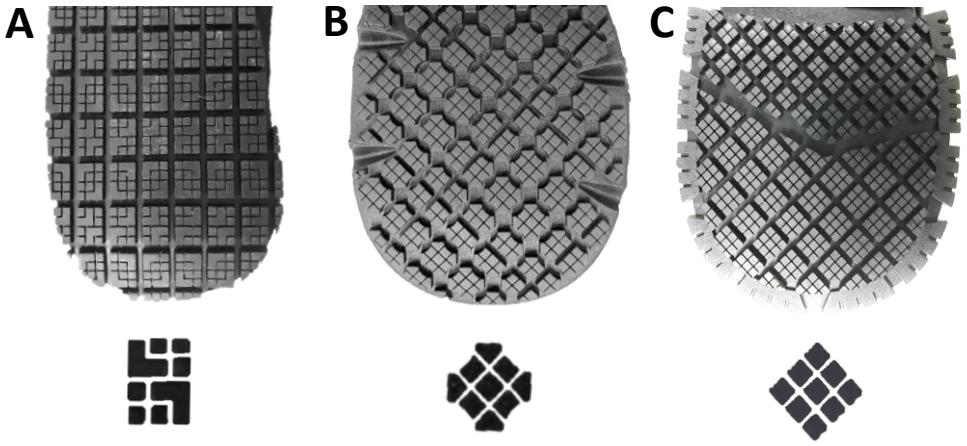

Figure 4.1 Shoe Tread Patterns

Examples of the shoe tread designs included in the study for shoes A, B, and C as labeled.

Participants wore the shoes in the workplace for one month at a time per shoe. Participant workplaces included the following industry sectors: education, health services, hospitality, manufacturing, professional and business services, trade, transportation, and utilities. A pedometer was fixed to the right shoe of each pair to track the distance walked in the shoes during each month (MilestonePod, Milestone Sports, Columbia, MD) (Hunter, Miller, & Suydam, 2017). Shoes were

retired from the study when the fluid force exceeded 25N and ACOF decreased at least 25% from baseline, or when the shoe upper or outsole became too worn at the discretion of the participant.

4.1.3.3 Mechanical Testing of Shoes

Traction performance was assessed before and after each month of wear using a robotic slip tester with identical methods as described in previous studies (Hemler, Charbonneau, et al., 2019; Hemler, Pliner, et al., 2020). The robotic slip tester apparatus consists of a force plate (BP400600-1K-Q2046, AMTI, Watertown, MA, 02472), an adjustable platform instrumented with four fluid pressure sensors, and three electromagnetic motors to control antero-posterior sliding, vertical load, and sagittal plane angle (Figure 4.2). The pressure sensors were aligned 25 mm apart in the direction perpendicular to sliding (along the X-axis, Figure 4.2). Shoes were slid in the forward direction (along the Y-axis, Figure 4.2) across a contaminated (90% glycerol, 10% water by volume; 214 cP) vinyl composite tile (Armstrong, 51804; surface roughness characteristics: R_a = 2.19 ± 0.29 mm, R_z = 16.13 ± 2.74 mm, R_q = 3.13 ± 0.42 mm; where R_a is the average asperity deviation from the mean line, R_z is the maximum asperity peak to valley distance, and R_q is the root mean square height of the profile) at a normal force of 250 ± 10 N, sliding speed of 0.3 m/s and sagittal plane angle of 17°. These sliding parameters were chosen to most closely align with the normal force (Iraqi & Beschorner, 2017; Iraqi, Cham, Redfern, Vidic, et al., 2018), speed (Albert et al., 2017; ASTM, 2011; Iraqi, Cham, Redfern, & Beschorner, 2018), and angle (Albert et al., 2017; Iraqi, Cham, Redfern, & Beschorner, 2018) during natural slipping.

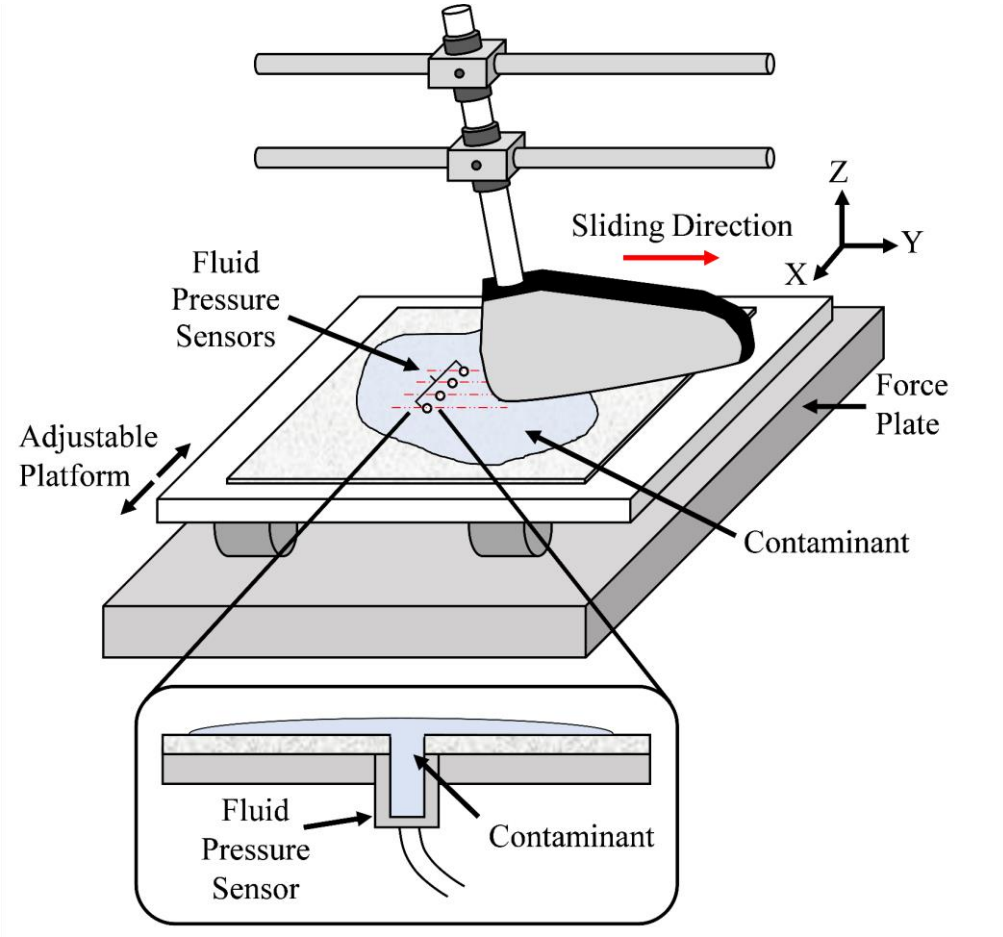

Figure 4.2 Robotic Slip Tester

Figure adapted from (Hemler, Charbonneau, et al., 2019)

Five sliding trials were conducted for each shoe at each month timepoint. The contaminant was spread to achieve uniform coverage prior to every trial. The adjustable platform was moved 5 mm laterally between each of the five trials. In each trial, fluid pressures were collected from four sensors (spaced 25 mm apart) resulting in 20 fluid pressure scans (4 sensors x 5 trials) each spaced 5 mm apart. The ACOF was calculated as the resultant shear force divided by the normal force during the first 200 ms of sliding after the normal force reached 250 N. The ACOF was averaged across the five trials. The fluid force was calculated using a numerical integration technique from the 20 fluid pressure scans and represents the load supported by the fluid during sliding (Hemler, Charbonneau, et al., 2019; Singh & Beschorner, 2014).

4.1.3.4 Worn Region Measurement

To track the outsole geometry changes, shoe heel molds were created using a silicone rubber compound (Smooth-On Inc.; Macungie, PA; Oomoo® 25). Shoes were set in the apparatus at an angle of 17°. The largest wear region (worn region size) was evaluated for each time point using the shoe molds. The worn region size was measured as the longest continuous region without tread along the long axis of the shoe (length) multiplied by the widest continuous region without tread along the short axis of the shoe (width). For the baseline condition or when there was no worn region, measurements from the largest continuous tread block were used to determine the worn region size (Hemler, Charbonneau, et al., 2019).

4.1.3.5 Predicted Film Thickness

A tapered-wedge bearing solution was adapted as in previous methods to relate hydrodynamic theory to the shoe-floor behavior (Hemler, Charbonneau, et al., 2020). Within the solution, the geometry of the tapered-wedge bearing was modeled as the shoe worn region; the

lack of tread definition offers a continuous surface simulating a bearing under which fluid would become pressurized. Therefore, the shoe worn region measurements were used to determine the bearing size within the solution at each shoe wear time point. The predicted film thickness (PFT) of the contaminant between the shoe and the floor was calculated using techniques from previous research (4.1):

$$PFT_i = \sqrt{\frac{6\mu v {l_i}^2 b_i \eta K_p}{F}} \quad 4.1$$

where the iterative (i) calculation of PFT for each shoe wear time point was a function of the contaminant's dynamic viscosity ($\mu = 214\ cP$), the sliding speed ($v = 0.3\frac{m}{s}$), the worn region length (l), the worn region width (b), the geometry-dependent fluid leakage correction factor, η, the wedge incline correction factor $K_p = 0.025$, and the normal force applied during slip testing ($F = 250\ N$) (Fuller, 1956; Hemler, Charbonneau, et al., 2020).

4.1.3.6 Statistical Analysis

Statistical analyses were performed to test the effects of wear (distance walked, months worn, and WRS) on changes in traction performance (ACOF and fluid force). Specifically, six repeated-measures ANOVA models were performed to assess the impact of the distance walked, months worn, and WRS (predictor variables, one investigated per model) on the ACOF and fluid force (dependent variables in each model). In each model, shoe type (A, B, C) and side (left, right) were covariates. Finally, all first-order interaction effects were included. A repeated-measures ANOVA was used to assess the relationship between PFT and fluid force with subject as a random variable. Specifically, the dependent variable was fluid force and the independent variables were PFT, shoe type, and their interaction. For all models, a square root transformation was applied to

the distance walked to correct for a positive skew, and the ACOF and fluid force were cube root-transformed to normalize residuals. All statistical models were determined *a priori* (JMP, SAS Corp., NC).

4.1.4 Results

Participants walked 103-2053 km in the shoes across 1-11 months for a total of 113 subject-months of data. Across the shoes, participants walked an average (standard deviation) of 497.8 (467.6) km across 5.0 (3.1) months with 100.8 (85.2) km per month (Table 4.1). The ACOF was highest for shoe A and smallest for shoe B at baseline and at the final month. Fluid force was highest at baseline and final month for shoe A, lowest for shoe B at baseline, and lowest for shoe C at the final month. Decrease in ACOF from baseline to final month was the largest for Shoe A and smallest for shoe C. ACOF increased from baseline for 50 of the 226 shoe months with the majority of months above baseline ACOF occurring in shoe B.

Table 4.1 Anthropometric and Shoe Data

Data organized by shoe type and then across all shoes. Data is the average (standard deviation) unless otherwise stated in the column description.

	A	B	C	All Shoes
Sex (M/F)	(8/3)	(8/1)	(3/1)	(12/3)
Age (yrs)	41 (11)	40 (12)	45 (14)	41.7 (12)
Mass [kg]	90.0 (12.6)	95.0 (12.5)	81.4 (11.1)	89.8 (12.5)
Height [cm]	1.78 (0.10)	1.86 (0.09)	1.74 (0.06)	176.7 (10.3)
BMI	29.1 (3.2)	28.4 (3.2)	27.6 (2.7)	28.8 (3.4)
Shoe Size [US Men's]	8.9 (1.7)	11.7 (2.0)	8.4 (1.9)	10.0 (2.3)
Number of months worn	3.9 (3.3)	6.8 (2.1)	5.0 (4.2)	5.0 (3.1)
Total distance walked [km]	519 (614)	437 (345)	588 (431)	498 (468)
Distance walked per month [km]	133 (104)	65 (71)	98 (64)	101 (85)
Baseline ACOF (prior to wear)	0.330 (0.045)	0.172 (0.024)	0.205 (0.047)	0.234 (0.083)
Final month ACOF	0.201 (0.053)	0.136 (0.027)	0.166 (0.039)	0.168 (0.050)
Final month %ACOF from baseline	62% (20%)	81% (23%)	87% (35%)	75% (26%)
Number of shoe months with ACOF (above/below) baseline	0/94	45/89	5/43	50/226
Baseline peak fluid pressure [kPa]	33 (18)	31 (20)	25 (10)	30 (18)
Final month peak fluid pressure [kPa]	56 (52)	48 (36)	26 (7)	47 (41)
Baseline fluid force [N]	3.8 (2.9)	2.1 (2.1)	2.2 (0.7)	2.8 (2.4)
Final month fluid force [N]	13.2 (12.5)	10.7 (14.4)	7.5 (7.0)	11.1 (12.5)
Baseline Worn Region Size [mm^2]	25.2 (0.7)	1.0 (0.6)	8.4 (0.0)	17.2 (7.0)
Average Worn Region Size [mm^2]	248.0 (313.2)	296.0 (299.3)	271.7 (339.3)	277.0 (310.2)
Final month Worn Region Size [mm^2]	320.7 (429.6)	534.5 (373.1)	412.0 (525.2)	430.6 (420.7)
Baseline Predicted Film Thickness [um]	1.5 (0)	1.0 (0.1)	0.7 (0.0)	1.6 (1.6)
Average Predicted Film Thickness [um]	6.2 (6.0)	8.1 (6.5)	8.0 (7.7)	7.5 (6.6)

4.1.4.1 ACOF

As distance walked, months worn, and the worn region size increased, the ACOF decreased (Figure 4.3, Table 4.1). In all three models, shoe type had a main and an interaction effect with the wear parameter (walking distance, month, or worn region size) (Table 4.2). This suggests that the wear response was dependent on the shoe; this effect is shown more prominently when analyzing the ACOF change relative to baseline (Table 4.1). Six months of wear was associated with decreases in ACOF (%ACOF from baseline) of 0.108 (41%), 0.021 (12%), and 0.062 (32%) for shoes A, B, and C, respectively. A distance walked of 600km (average distance walked at 6 months of wear) was associated with decreases in ACOF (%ACOF from baseline) of 0.041 (17%), 0.033 (20%), and 0.055 (28%) for shoes A, B, and C, respectively. A WRS of 200 mm^2 (the size in which the end of an AA battery would fit) was associated with decreases in ACOF (%ACOF from baseline) of 0.025 (11%), 0.007 (4%), and 0.016 (9%) for shoes A, B, and C, respectively. Furthermore, a WRS of 800 mm^2 (threshold identified in previous work (Hemler, Charbonneau, et al., 2019)) was associated with decreases in ACOF (%ACOF from baseline) of 0.090 (38%), 0.026 (16%), and 0.058 (32%) for shoes A, B, and C, respectively.

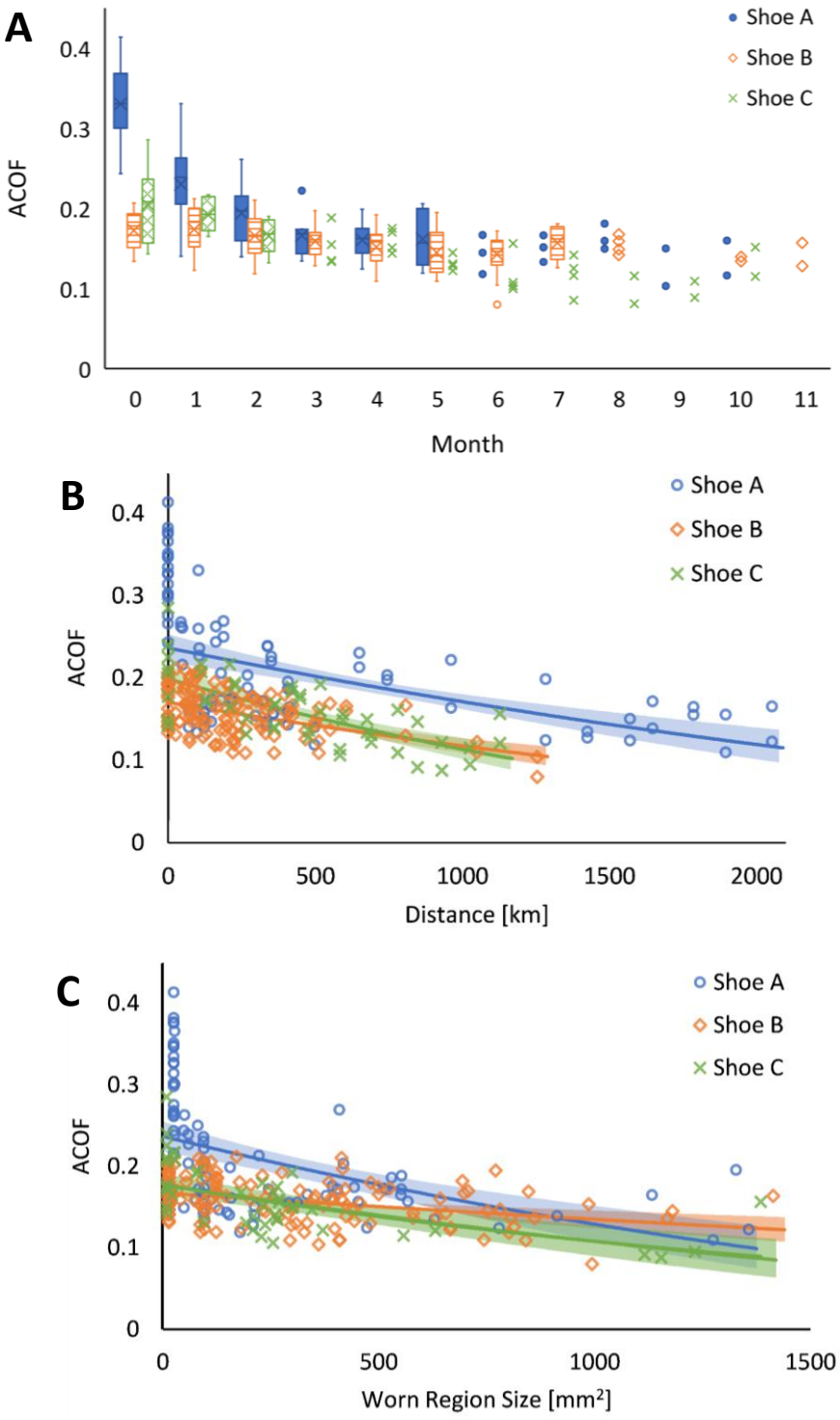

Figure 4.3 ACOF vs. Month, Distance, and Worn Region Size

ACOF with respect to A) months of shoe wear; B) distance walked in the shoes; and C) worn region size. In plot A, box plots are shown for months in which there were more than 4 data points per shoe. Regression lines with a 95% confidence interval are shown for in plots B and C.

Table 4.2 Statistical Analyses

The effects of wear on traction performance and fluid modeling analysis. Significant p-values are bolded.

Dependent Variable	R^2	Independent Variable(s)	F-ratio	p-value
ACOF	0.633	Month	$F_{(1,260)}$=150.9	**<.001**
		Shoe	$F_{(2,150)}$=41.6	**<.001**
		Side	$F_{(1,245)}$=0.5	0.485
		Month*shoe	$F_{(2,257)}$=19.8	**<.001**
		Month*side	$F_{(1,245)}$=0.9	0.341
		Shoe*side	$F_{(2,245)}$=1.0	0.376
ACOF	0.690	Distance	$F_{(1,260)}$=184.5	**<.001**
		Shoe	$F_{(2,183)}$=64.9	**<.001**
		Side	$F_{(1,246)}$=0.3	0.563
		Distance *shoe	$F_{(2,259)}$=9.0	**<.001**
		Distance *side	$F_{(1,246)}$=5.3	**0.022**
		Shoe*side	$F_{(2,246)}$=0.5	0.610
ACOF	0.526	Worn Region Size	$F_{(1,248)}$=61.9	**<.001**
		Shoe	$F_{(2,148)}$=36.6	**<.001**
		Side	$F_{(1,233)}$=1.6	0.203
		Worn Region Size*shoe	$F_{(2,243)}$=7.9	**<.001**
		Worn Region Size*side	$F_{(1,241)}$=0.2	0.631
		Shoe*side	$F_{(2,232)}$=0.1	0.949
Fluid Force	0.553	Month	$F_{(1,257)}$=85.6	**<.001**
		Shoe	$F_{(2,230)}$=8.6	**<.001**
		Side	$F_{(1,246)}$=2.0	0.157
		Month*shoe	$F_{(2,253)}$=1.0	0.382
		Month*side	$F_{(1,246)}$=3.3	0.072
		Shoe*side	$F_{(2,246)}$=2.0	0.137
Fluid Force	0.640	Distance	$F_{(1,260)}$=158.7	**<.001**
		Shoe	$F_{(2,196)}$=7.7	**<.001**
		Side	$F_{(1,245)}$=1.8	0.176
		Distance *shoe	$F_{(2,257)}$=2.3	0.098
		Distance *side	$F_{(1,245)}$=8.7	**0.004**
		Shoe*side	$F_{(2,245)}$=1.4	0.243
Fluid Force	0.589	Worn Region Size	$F_{(1,248)}$=103.2	**<.001**
		Shoe	$F_{(2,156)}$=8.9	**<.001**
		Side	$F_{(1,235)}$=0.3	0.600
		Worn Region Size*shoe	$F_{(2,244)}$=0.3	0.778
		Worn Region Size*side	$F_{(1,242)}$=2.2	0.141
		Shoe*side	$F_{(2,234)}$=1.1	0.339
Fluid Force	0.604	Predicted Film Thickness	$F_{(1,251)}$=134.4	**<.001**
		Shoe	$F_{(2,150)}$=14.8	**<.001**
		Predicted Film Thickness*shoe	$F_{(2,251)}$=0.9	0.402

4.1.4.2 Fluid Force

Fluid force was positively correlated with the distance walked, months used, and worn region size (Figure 4.4). The rate of fluid force change did not vary across shoe types for any of the independent variables (Table 4.2). Six months of wear was associated with fluid forces of 14 N, 6 N, 11 N for shoes A, B, and C, respectively. A distance walked of 600 km was associated with fluid forces of 10 N, 11 N, 10 N for shoes A, B, and C, respectively. A WRS of 200 mm^2 was associated with an increase in fluid force from baseline of 2 N (49%), 2 N (78%), and 2 N (49%) for shoes A, B, and C, respectively. Additionally, a WRS of 800 mm^2 was associated with an increase in fluid force from baseline of 14 N (286%), 11 N (528%), and 12 N (287%) for shoes A, B, and C, respectively.

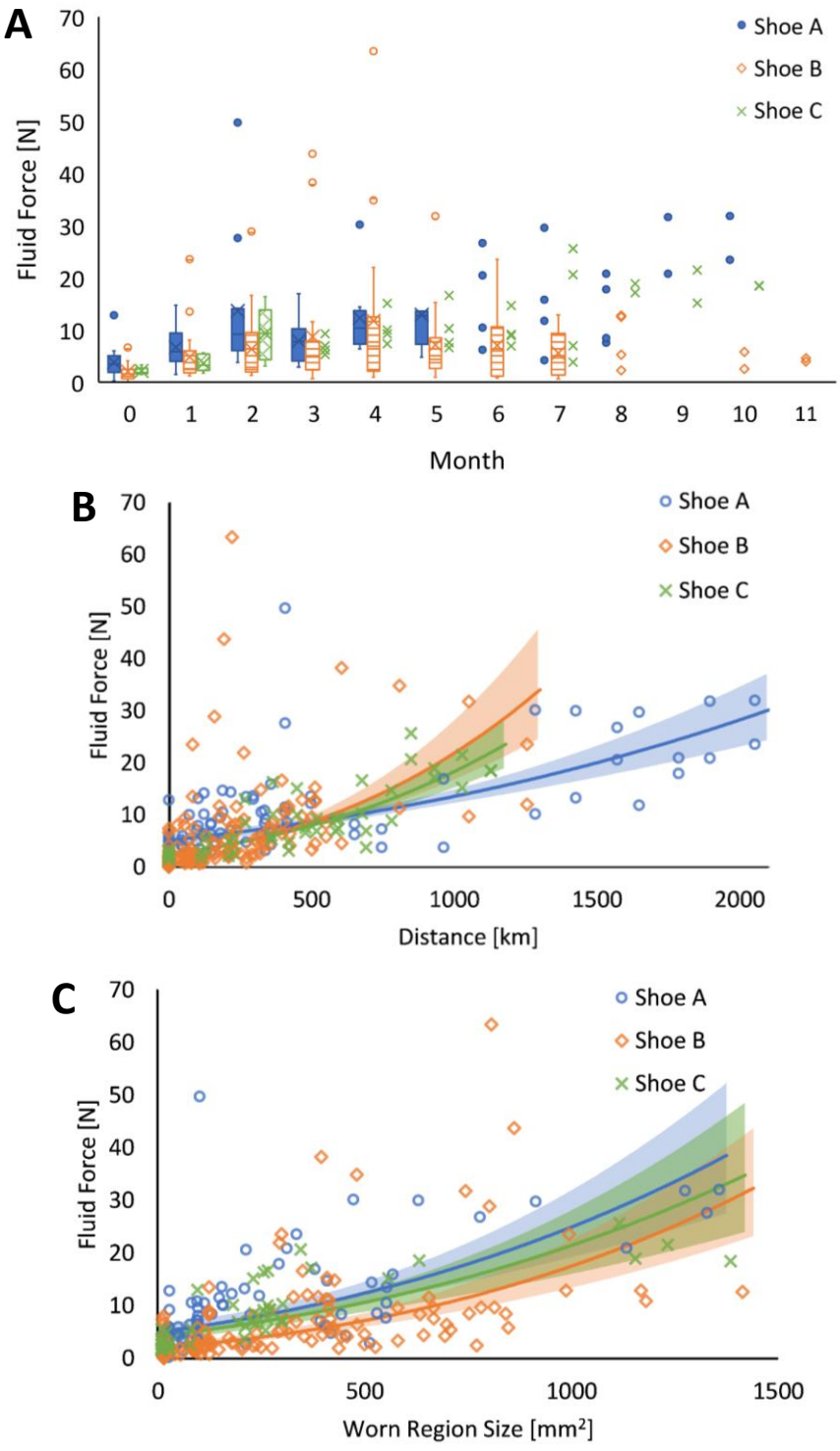

Figure 4.4 Fluid Force vs. Distance, Month, and Worn Region Size

Fluid force with respect to A) month of shoe wear; B) distance walked in the shoes; and C) worn region size. In plot A, box plots are shown for months in which there were more than 4 data points per shoe. Regression lines with a 95% confidence interval are shown for in plots B and C.

Fluid force increased as PFT based on the worn region size increased (Figure 4.5, Table 4.2). The shoe type influenced the fluid force, but not the rate at which fluid force increased per PFT. A fluid force of 25 N (shown to be a level associated with a meaningful drop in friction performance, (Hemler, Charbonneau, et al., 2019) was associated with a PFT of 20.5 µm, 25.8 µm, and 25.0 µm for shoes A, B, and C, respectively. These PFT values correspond to worn region size measurements of 850 mm^2, 1155 mm^2, and 1108 mm^2, respectively, assuming the worn region has equal lengths and widths.

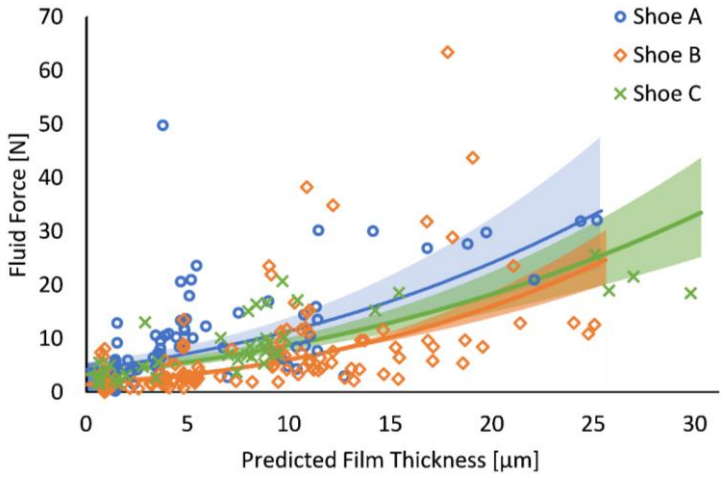

Figure 4.5 Fluid Force vs. Predicted Film Thickness

Regression lines with a 95% confidence interval is shown for each shoe type.

4.1.5 Discussion

Increases in shoe usage and wear led to decreases in ACOF and increases in fluid force. Decreases in traction performance (decreased friction and poorer under-shoe fluid drainage) varied across the three shoe types and the rate of decrease in friction varied per shoe type. The fluid model applied to this study showed that PFT which employed the shoe outsole worn region size was associated with the under-shoe fluid force during sliding.

These findings are consistent with and build upon previous research addressing traction performance and wear. The results of decreased traction performance with wear are consistent with simulated and natural wear experiments (Beschorner et al., 2014; Grönqvist, 1995; Hemler, Charbonneau, et al., 2019; Hemler, Pliner, et al., 2020; V.H. Sundaram et al., 2020). The results of this study are also consistent with previous work that demonstrated that PFT predicts fluid drainage of shoes that experience simulated wear (Hemler, Charbonneau, et al., 2020). Importantly, this study extends that previous study by demonstrating that this model predicts tread drainage in naturally worn shoes. Furthermore, this study found that WRS is a good indicator of traction performance. This finding is supported by previous work which determined that measuring the outsole worn region using a common household items of a particular size (AA and AAA batteries) was indicative of slip risk (Beschorner et al., 2020). Previous work suggests that the first replacement indicator may exist when under-shoe fluid forces rise above 25 N or 10% of the vertical load and a WRS of 800 mm^2 (Hemler, Charbonneau, et al., 2019). Eight out of 22 shoes in this study exceeded a WRS of 800 mm^2 at a range of 2-7 months, indicating that shoe replacement may be needed near 6 months of use as supported by previous research (Verma et al., 2014).

Because all metrics for tracking wear (months used, distance walked, and WRS) were similarly able to predict traction loss, the metric used for an application can be selected based on practical considerations. Using time as a wear metric is consistent with existing recommendations for footwear companies who commonly recommend replacement every 6 to 12 months of wear (Shoes For Crews, 2013; Skechers, 2013; SR Max Slip Resistant Shoe Company, 2017). Time that shoes are worn offers consistency and ease of management for scheduling replacement purchases. However, in settings where shoes are not worn consistently or for individuals with varying wear

rate (Hemler, Sider, Redfern, & Beschorner, 2021), using time as an indicator for wear may not be adequate. Walking distance can be easily tracked using wearable technology that is becoming increasingly available and utilized. However, certain individuals have higher wear rates based on their gait kinetics (Hemler, Sider, et al., 2021). Walking distance as a wear metric may result in too infrequent replacement for high wear rate individuals and too frequent replacement for low wear rate individuals. The WRS may detect real life variability better than other wear metrics and can be measured without any foreknowledge of how long or far the shoe has been worn, unlike the metrics of months used and distance walked. A disadvantage of monitoring shoes based on the WRS is the need to train users to make accurate measurements. One potential easy solution is to compare the WRS to a common object like a battery which has been promoted as a feasible safety monitoring device for healthcare and food service industries (Beschorner et al., 2020; National Occupational Research Agenda (NORA) Traumatic Injury Prevention Cross-Sector Council, 2021). These wear metrics have varied benefits, though the WRS may be the most accurate assessment given emerging ergonomic tools to indicate size.

There are a few limitations of this study that should be addressed. As the steel-toe boot option for Shoe B was discontinued from production during the study, Shoe C was introduced. This study design change did not allow for an ideal repeated measures design. However, the addition of this shoe tread pattern provided more robust evidence that these results are generalizable across more shoe designs. Therefore, these results indicate the real variability in gait biomechanics and shoe wear, providing support for utilizing wear metrics. Furthermore, shoes were removed from the study when they were deemed unsafe, which limited our ability to understand severely worn shoes. As the sizes of the shoes varied to fit the participants, the placement of the tread blocks on the outsoles also changed within the same shoe type to

accommodate the outsole size. Therefore, the traction performance of shoes in the same shoe type of different sizes may have varied due to this variation of tread placement. Lastly, the high viscosity fluid used in this study may not relate to all potentially slippery conditions (water or detergent contaminants). However, this study did consider one of the worst-case scenarios, which is likely to cause the greatest slipping risk.

In summary, this study quantified wear metrics that are associated with traction performance changes which has important implications for public safety. As the distance and time shoes were worn and the worn region size on the shoe outsole increased, the shoe-floor friction and fluid drainage decreased. Distance walked and time worn may be more difficult to track than worn region size as wear metrics in certain work environments. Therefore, measurements involving worn region geometry may be more feasible in many environments as it does not require tracking of shoe use and is feasible with simple tools (Beschorner et al., 2020). Furthermore, this study showed that the worn region size aligns with lubrication theory and under-shoe fluid hydrodynamics which links the gap between practical safety and scientific theory. This study suggests that any of the wear metrics of distance, time, and outsole geometry, are valuable for monitoring traction performance changes; workplaces with different needs may adopt their preferred monitoring method.

5.0 Impact of Gait Kinetics and Shoe Outsole Hardness on Wear

In this chapter, the contributions of individual gait kinetics and shoe outsole hardness on wear will be discussed. Section 5.1 primarily discusses the effect and implications of gait kinetics on shoe tread wear. In Section 5.2, the contribution of shoe outsole material hardness to wear across multiple modes of wear is analyzed. The data presented in this chapter incorporates data originally presented in Sections 3.1 and 4.1 but with new analyses. An ancillary study will also be presented. Section 5.1 has been published in a peer-reviewed journal (Hemler, Sider, et al., 2021) from which permission has been granted to adapt the text to this dissertation (Appendix B). Preliminary results from this research were presented at several conferences (Hemler & Beschorner, 2020; Hemler, Sider, & Beschorner, 2019) and were accepted to a conference which was cancelled due to the COVID-19 pandemic (Hemler, Tushak, Walter, & Beschorner, 2020).

5.1 Gait Kinetics

5.1.1 Abstract

Background: Adequate footwear is an important factor for reducing the risk of slipping; as shoe outsoles wear down, friction decreases and thus, slip and fall risk increases. Wear theory suggests that gait kinetics may influence rate of tread wear.

Research question: Do the kinetics of walking (i.e., the shoe-floor force interactions) affect wear rate?

Methods: Fourteen participants completed dry walking trials during which ground reaction forces were recorded for different types of shoes. The peak normal force, shear force, and required coefficient of friction (RCOF) were calculated. Participants then wore each pair of shoes in the workplace every other month for up to 24 months. A pedometer was used to track the distance each pair of shoes was worn and tread loss was measured. The wear rate was calculated as the volumetric tread loss divided by the distance walked in the shoes. Three, mixed linear regression models were used to assess the impact of peak normal force, shear force, and RCOF on wear rate.

Results: Wear rate was positively associated with peak RCOF and with peak shear force but was not significantly related to peak normal forces.

Significance: The finding that shear forces and particularly the peak RCOF are related to wear suggests that a person's gait characteristics can influence wear. Therefore, individual gait kinetics may be used to predict wear rate based on the fatigue failure shoe wear mechanism.

5.1.2 Background

Slips and falls are a major cause of injury that can cause severe health loss (James et al., 2020). In the United States, 18% of non-fatal occupational injuries occur every year due to same-level falls with a Worker's Compensation financial burden of $10.6 billion (Liberty Mutual Research Institute for Safety, 2017). Additionally, over 5 million hospitalizations occur annually as a result of falling in the non-elderly population (National Center for Injury Prevention and Control, 2018). Slipping has been found to contribute to 40-50% of occupational fall-related injuries (Courtney et al., 2001). Thus, there is a need to improve slip and fall prevention strategies.

Slips resulting in falls are caused by a lack of friction between the flooring and footwear. Previous research has shown that increased required coefficient of friction (RCOF) and/or decreased available coefficient of friction (ACOF) are associated with a higher risk of slipping (Beschorner et al., 2016; Burnfield & Powers, 2006; Hanson et al., 1999). The RCOF is the ratio of shear to normal forces during walking and varies depending upon walking speed and other characteristics of gait (S. Kim, Lockhart, & Yoon, 2005). The ACOF is the measured friction capability of a shoe-floor-contaminant interface. Footwear outsole design has been shown to be a modifiable factor that influences the ACOF and slipping (Bell et al., 2018; Iraqi et al., 2020; Jones et al., 2018; Verma et al., 2011; Verma et al., 2014).

Slip-resistant shoes, which are designed for enhanced friction, typically have small tread blocks separated by tread channels. When the shoe contacts a fluid-covered floor surface, these tread blocks disperse the fluid out of the shoe-floor interface to reduce under-shoe fluid pressures (Hemler, Charbonneau, et al., 2019), therefore decreasing the risk of slipping (Beschorner et al., 2014; V.H. Sundaram et al., 2020). However, as shoe tread wears down, under-shoe fluid dispersion capability decreases and slip risk increases (Beschorner et al., 2014; Hemler,

Charbonneau, et al., 2019; Vani H Sundaram et al., 2020). Furthermore, research has shown that in the workplace, shoes worn for more than six months present a higher risk of slipping than those worn less than six months (Verma et al., 2014). While tread wear has emerged as an important feature influencing ACOF and slip risk, the factors influencing the rate at which shoes become worn remains largely unknown. As such, there is a paucity of research examining factors influencing the mechanisms and rate of shoe tread wear.

Multiple potential mechanisms may explain the impact of kinetics on shoe wear (Sato et al., 2020). Given that the shoe outsole is typically manufactured from elastomeric material, elastomeric wear theory is relevant to shoes. Elastomeric wear has been analyzed in a plethora of applications including bearing seals and tires (Békési, 2012; Békési & Váradi, 2010; Békési, Váradi, & Felhős, 2011; Lupker, Cheli, Braghin, Gelosa, & Keckman, 2004); two common theories to explain elastomeric wear include fatigue failure (Mars & Fatemi, 2002, 2004) and Archard's wear, which is an empirical relationship that is intended to capture multiple modes of wear (e.g., abrasive, fretting) (Archard, 1953). Fatigue failure can occur when elastomers experience cyclic loading (Mars & Fatemi, 2004). Under uniaxial compressive loads, cracks in the material are unlikely to form as no tensile stress is present (Mars & Fatemi, 2002) (Figure 5.1, stage 1). As the compressive load is accompanied by a shear load (Figure 5.1 – stage 2), the material encounters principal tensile stresses leading to crack nucleation and growth (Mars & Fatemi, 2002). Further increasing shear forces leads to increased tensile forces and potential crack propagation. Normal compressive forces and shear forces interact to form directions of principal tensile stress, which are likely to cause more crack nucleation and growth, (Figure 5.1 – stage 3) eventually leading to fatigue failure that causes the material to dislodge from the shoe. Thus, shear

and normal forces applied to an elastomeric material are potentially relevant in determining fracture lines and therefore wear profiles.

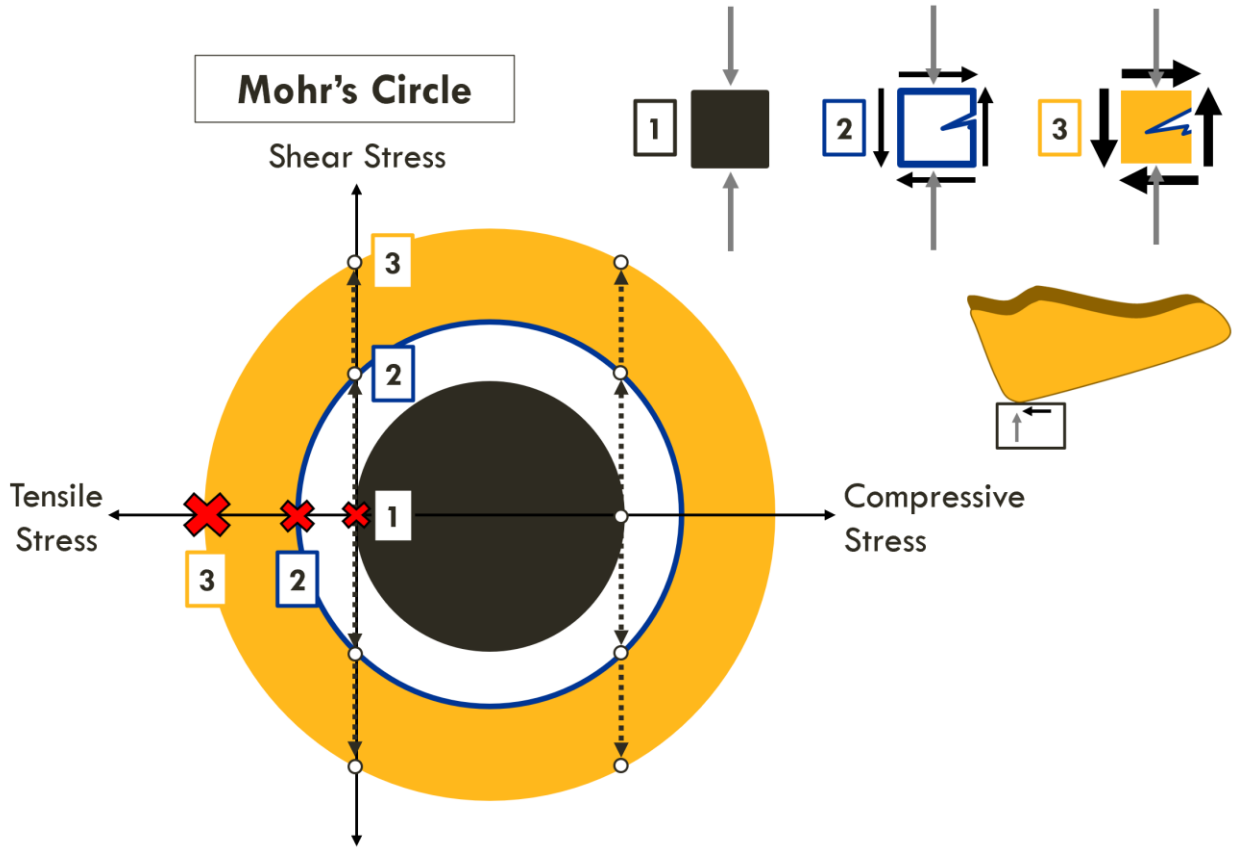

Figure 5.1 Fatigue Failure for Elastomeric Wear Diagram

At stage 1 (black block and small black circle on the shear stress diagram), the block experiences uniaxial compressive (normal) loading. There is zero tensile stress in this scenario. At stage 2 (hollow, thick blue-outlined block and circle), shear stresses are added to the block with the same normal stress. The shear stress causes an increase in the principal tensile stress (shown by the small red 'x' above indicator '2'). At stage 3 (yellow block and large yellow circle), shear stress magnitudes are increased with the same normal load; shear stress increases on the diagram and likewise, the tensile stress on the horizontal axis also increases. The kinetics during gait heel strike are represented with the shear force in black and normal force in gray (middle right side of figure).

In gait analysis, shear and normal forces, along with the ratio of the shear to normal forces (RCOF) are commonly used to describe the interaction at the shoe-floor interface (Beschorner et al., 2016; Chang et al., 2011). As shear forces increase, especially relative to the normal force (increases in RCOF), the principal tensile stress of the shoe outsole elastomer concurrently increases, leading to the potential for material failure and the formation of wear particles (Mars & Fatemi, 2004). As such, fatigue failure applied to gait indicates that increased shear forces and subsequent RCOF may lead to increased elastomeric tread wear. Archard's wear has also been used to understand elastomer wear; this theory states that the volumetric wear of a material is proportional to the sliding distance and the applied normal force while inversely proportional to the material hardness (Archard, 1953). Archard's wear suggests that increased normal force during gait leads to increased volumetric tread wear. Thus, ground reaction force parameters that are commonly measured in gait analysis are potentially relevant to shoe tread wear.

In summary, shoe wear is an important risk factor relevant to slipping; wear theory suggests that gait kinetics (in particular, normal forces, shear forces, and RCOF) may contribute to shoe wear, yet there is a lack of empirical evidence linking gait kinetics to wear rate. Thus, the purpose of this study is to understand the effects of gait kinetics on the rate of shoe tread wear.

5.1.3 Methods

5.1.3.1 Summary

This research consisted of a longitudinal study comprised of a gait assessment and wearing shoes in the workplace (Figure 5.2). Two pairs of SR shoes were fitted to each participant. Gait kinetics and kinematics were collected during dry, over-ground walking in each pair of shoes. Participants then wore the shoes in the workplace alternating between pairs each month. At

baseline and during the off-month of wear, tread geometry was captured using negative molds of the shoe heels to determine the volumetric tread loss and subsequent wear rate based on the distance walked by the participants. The change in ACOF and under-shoe fluid pressures was also tracked and reported (Beschorner et al., 2020; Hemler, Pliner, et al., 2020).

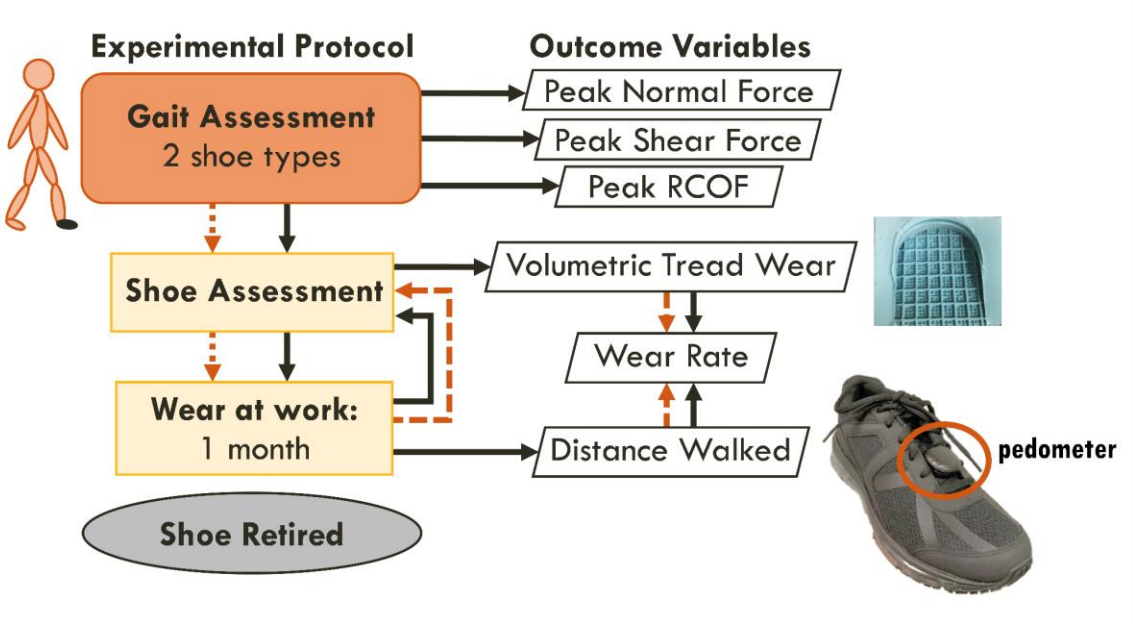

Figure 5.2 Experimental Protocol Flowchart

Participants wore 2 types of shoes in a gait assessment during which peak normal force, peak shear force, and peak RCOF were measured. Heel tread molds were created at baseline and after each month of wear to calculate the volumetric tread wear. The wear rate was calculated as the volumetric tread wear normalized by the distance walked as measured from the shoe pedometers. After 12 months of wear or substantial wear of the shoe upper or outsole at which the shoes were deemed unsafe, the shoes were retired.

5.1.3.2 Participants

Fourteen healthy participants (11 male and 3 female; age: 42 ± 13 yr; height: 177 ± 11 cm; mass: 91 ± 13 kg; shoe size 9.6 ± 2.3 US Men's Sizing) from a recruited cohort of 23 recruited participants were analyzed. Inclusion criteria included participants who regularly wore treaded shoes, spent more than 75% of walking time on manmade surfaces, and were on their feet for at

least 4 h in a typical day. Exclusion criteria included any neurological problems, musculoskeletal history in the previous 2 years, musculoskeletal disorders, neurological problems, osteoporosis, or arthritis. Included participants worked in the following industries on primarily indoor flooring surfaces: trade, transportation & utilities, manufacturing, leisure and hospitality, and education and health services. Only right shoes that were worn for 100 km were included in this analysis (excluding 23 pairs of shoes leading to 23 pairs of shoes included in the study) since preliminary observations revealed that this was the minimum amount of use where a reliably measurable amount of wear could be observed. There were three reasons that shoes were excluded from analysis: the participant discontinued wearing the shoe because they reported discomfort while wearing the shoes at work ($n_{shoes} = 4$), the participant withdrew from the study prior to completing one month of walking in the shoes ($n_{shoes} = 11$), and the participant walked fewer than 100 km total in the enrollment period due to low activity levels ($n_{shoes} = 8$).Written informed consent was obtained at the start of the study according to the University of Pittsburgh Institutional Review Board and the research has been conducted in accordance with the principles of the Declaration of Helsinki.

5.1.3.3 Kinetics Analysis

Participants were provided with two pairs of footwear – shoe A and: shoe B or shoe C (Figure 5.3). Within each shoe type, boots or shoes with the same tread pattern were provided depending on their occupational requirements (Table 5.1). As shoe B was discontinued from manufacturing during the study, four participants received shoe C rather than shoe B. All participants were asked to complete a series of dry, over-ground walking trials in a biomechanics lab at a pace resembling their gait while in their workplace. While wearing each pair of the given shoes and reflective markers to track motion, participants walked over two force plates (Bertec

4060A, Columbus, OH) which collected normal and shear forces at 1080 Hz. The gait assessment concluded when ten good force plate hits were recorded for the right foot for each shoe type. Peak normal forces and shear forces prior to flat foot during stance phase were recorded (Figure 5.4). The peak RCOF was calculated based on a 100 N normal force threshold, positive longitudinal shear component, and during the first 200 ms of stance phase (Chang et al., 2011). This corresponded to the maximum between the 3rd and 4th peak characterized by Perkins (Perkins, 1978). The right shoe of each pair was fitted with a pedometer to track the distance walked (MilestonePod, Milestone Sports, Columbia, MD), (Hunter et al., 2017). Shoes were then shipped to participants to wear in their workplace for one month at a time.

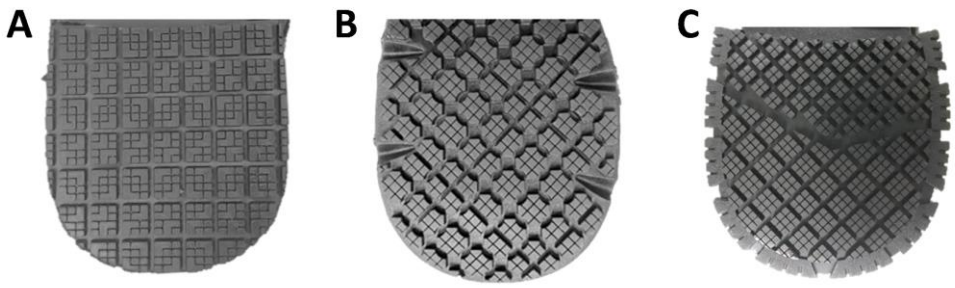

Figure 5.3 Shoe Types and Code

A) shoe A, B) shoe B, and C) shoe C.

Table 5.1 Footwear Description

List of shoe code, brand, model, and short-term hardness for each men's and women's footwear option.

Shoe Code	Shoe/Boot Option	Footwear Brand	Men's Model	Women's Model	Short Term Hardness (Shore A)
A	Shoe	SRMax	SRB1977	SRB972	48.3
	Boot	SRMax	SRM4750/SRM225	SRM2550	50.5/48.5
B	Shoe	safeTstep	Blast Bouffee 159961	Blast Bouffee 159961	65.4
	Boot	safeTstep	Dawson 160004	–	74.1
C	Boot	ShoesForCrews	Rowan 77280	August 77319	49.9

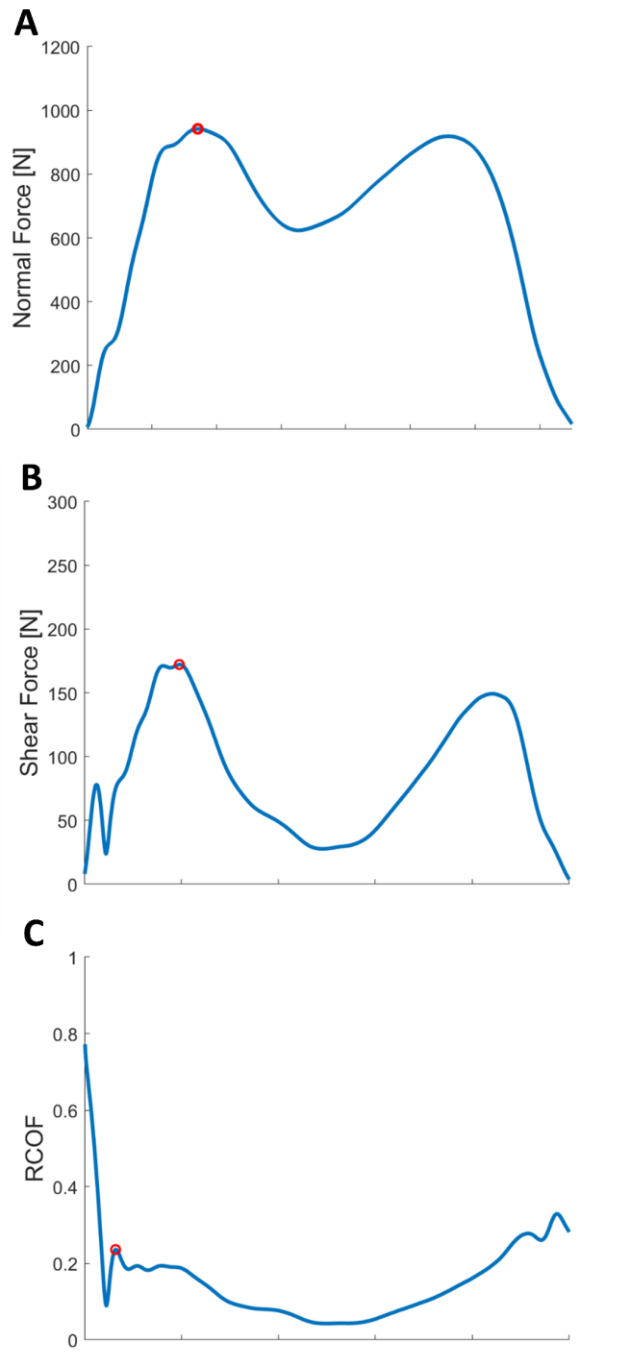

Figure 5.4 Representative Kinetic Data

Representative data is shown for the A) normal force, B) shear force, and C) RCOF during stance phase of gait. Peak measurements for each plot are signified with a red circle. X-axis is non-descript.

5.1.3.4 Wear Measurements

At baseline and after each month of wear, the tread wear of the shoes was measured. A rectangular mold (92 mm x 76 mm x 28 mm) of each shoe heel was made using a silicone rubber compound (Smooth-On Inc.; Macungie, PA; Oomoo® 25) at an angle of 17° as in previous experiments (Hemler, Charbonneau, et al., 2019; Hemler, Pliner, et al., 2020). The right foot molds for the baseline level and the first month of wear that surpassed the 100 km threshold were used to determine the volumetric tread loss during wear in the workplace. Each mold was measured three times. The mold was placed on a scale (MicroMall™ 300g/0.001g B3003T) and the inverse tread blocks were filled with water using a pipette. The mass of the water required to fill the molds was measured three times. The molds were allowed to dry between measurements. The change in the water mass between the baseline level and threshold-passing mold was calculated, converted to volume, and normalized to the cumulative distance that the shoes were worn. This metric was termed the wear rate [mm^3/km].

5.1.3.5 Statistical Analysis

Four mixed linear regression models were used in this study to assess the impact of gait kinetics and shoe design on wear rate. Specifically, the first model consisted of testing the effect of peak normal force (between subject) and shoe type (within subject) on wear rate (dependent variable). The second model assessed the effect of peak shear force (between subject) and shoe type (within subject) on wear rate (dependent variable). The third model tested the effect of peak RCOF (between group) and shoe type (within group) on wear rate (dependent variable). Lastly, the fourth model assessed the impact of outsole Shore A hardness (independent) on wear rate (dependent) across subjects. For all models, wear rate was logarithmic-transformed to normalize residuals and satisfy the linearity assumption.

5.1.4 Results

Participants walked a cumulative distance of 167 ± 69 km (range: 101-351 km) in 1.9 ± 1.4 months (range: 1-7 months) (i.e., before the end of the first month when shoe usage exceeded the 100 km threshold). Within those months, participants walked 100 ± 80 km per month. The standard deviation between the three volume measurements of each mold was 54 mm^3, on average (the standard deviation ranged from 6-125 mm^3). The cumulative volumetric tread wear ranged from 324-3450 mm^3 (baseline to the 100 km threshold month) across the shoes.

Across all shoes and participants, peak normal force ranged from 816 to 1270 N, peak shear force ranged from 87-235 N, and peak RCOF ranged from 0.090-0.23 (Table 5.2). The geometric mean of the wear rate was 6.7 mm^3/km with a range from 1.7-20.0 mm^3/km, and a mean 95% confidence interval of 5.1-8.9 mm^3/km. Overall, Shoe A had the largest range for the wear rate, peak normal force, peak shear force, and peak RCOF. Shoe C had the smallest range for the wear rate, peak normal force, and peak shear force, and lowest average values across all four variables, while Shoe B had the highest average values across the four variables.

Table 5.2 Participant Information, Kinetic Results, & Wear Rate

Participant information (n, Age, Mass, Height, BMI) and kinetic results (normal force, shear force, RCOF), and wear rate grouped by shoe type. Mean (standard deviation) is listed with the range in italics. Geometric mean is listed for wear rate.

Shoe Type	No. Shoes	Age [yrs]	Mass [kg]	Height	BMI	Peak Normal Force [N]	Peak Shear Force [N]	Peak RCOF	Wear Rate [mm^3/km]	Wear Rate 95% CI [mm^3/km]
A	11	41 (11) *25-55*	89.5 (12.3) *71.1-106*	174.5 (9.8) *162.5-192*	29.3 (3.2) *25.0-34.9*	1009 (150) *816-1252*	153 (46) *87-230*	0.18 (0.05) *0.09-0.24*	6.8 (5.0) *2.0-18.4*	*4.76-11.5*
B	8	41 (14) *24-58*	95.1 (12.7) *76.8-110.2*	182.1 (10.3) *169.5-198*	28.7 (3.2) *24.0-34.0*	1079 (135) *850-1270*	180 (37) *121-235*	0.20 (0.02) *0.18-0.22*	9.7 (4.3) *5.6-19.6*	*6.8-14.0*
C	4	45 (14) *25-55*	83.7 (13.3) *71.1-95.6*	170.1 (5.4) *164.5-177.5*	28.9 (4.7) *25.0-34.9*	968 (141) *833-1115*	114 (33) *94-164*	0.13 (0.06) *0.09-0.22*	3.1 (1.5) *1.7-4.9*	*1.0-5.7*

In the first model (Akaike Information Criterion corrected: AICc = 63.2), peak normal force ($F_{1,12}$=0.01, p=0.924) and shoe type ($F_{2,9}$=3.8, p=0.063) were not associated with wear rate (Figure 5.5). In the second model, (AICc = 56.4), the peak shear force was positively associated with wear rate ($F_{1,14}$=5.4, p=0.037), but there was no association between wear rate and the shoe type ($F_{2,9}$=2.7, p=0.118). In the third model (AICc = 42.6), peak RCOF ($F_{1,14}$=6.6, p=0.023) was positively associated with wear rate, and shoe type ($F_{2,11}$=2.9 p=0.100) was not. Furthermore, in the third model, increases in RCOF of 0.01 and 0.1 were associated with 6.8% and 93.0% increased wear rate, respectively. The fourth model showed that wear rate was not affected by the shoe outsole hardness ($F_{1,11}$=0.6, p = 0.472).

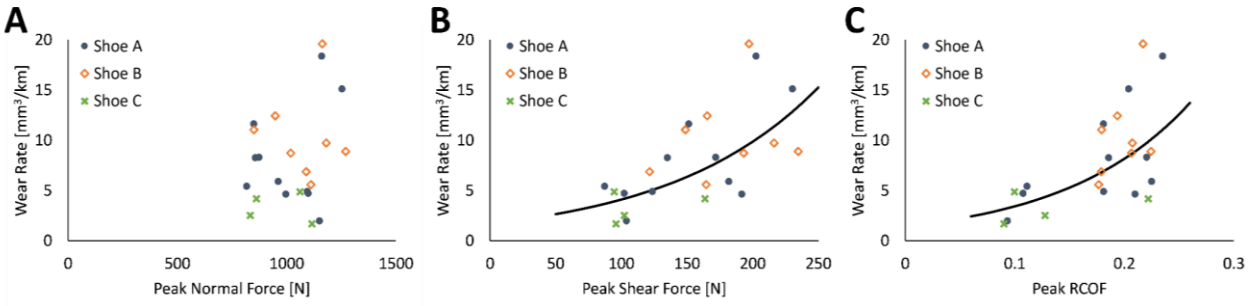

Figure 5.5 Wear Rate vs. Kinetics

Wear rate is shown with respect to A) peak normal force, B) peak shear force, and C) peak RCOF for the three shoe types. The regression line is shown in black for the peak shear force ($wear\ rate = 2.2 * e^{\frac{0.0066}{N} * Shear\ Force}$) and peak RCOF ($wear\ rate = 1.92 * e^{6.58 * RCOF}$) (these fit lines are non-linear due to te log transformations).

5.1.5 Discussion

In this study, the peak shear forces and peak RCOF, but not the peak normal force nor shoe outsole hardness, were associated with the wear rate. The peak RCOF model showed increases of

0.1 in the RCOF were associated with nearly doubling of the predicted wear rate. As such, the service life of shoes (use before requiring replacement) is highly dependent on that individual's gait kinetics, specifically the shear force and its ratio to the normal force (RCOF).

This research builds on previous literature which has shown that gait parameters are related to slip risk (Beschorner et al., 2016; Hanson et al., 1999; Iraqi, Cham, Redfern, Vidic, et al., 2018). Previous research has shown that RCOF during dry locomotion is predictive of slip risk (Beschorner et al., 2016), and thus a reasonable gait metric to study for assessing slip risk. The present study identifies a second pathway in which RCOF could increase slip risk: higher RCOF will lead to increased volumetric tread loss which may indicate faster growth of a worn region. The amount of shoe outsole wear, measured by the size of the worn region, is associated with decreased ACOF, increased under-shoe fluid pressures, and increased slip risk (Hemler, Charbonneau, et al., 2019; Hemler, Sundaram, et al., 2019; V.H. Sundaram et al., 2020).

These results are consistent with the fatigue failure wear theory as a mechanism for shoe outsole elastomeric wear. Tearing energy, also known as the strain energy release rate, has been shown to contribute to elastomer fatigue and subsequent failure (De & White, 2001; Mars & Fatemi, 2002). Furthermore, an advantage of applying this fatigue failure wear theory is that it uses a geometry-independent method for determining fatigue life (De & White, 2001). These findings on fatigue failure are applicable for shoe outsole wear regardless of tread design. However, designs to reinforce material properties in the directions of principle shear for a given tread design could potentially influence wear rate. These principal shear directions are determined by the characteristics of locomotion. Archard's wear equation, however, relies on normal force and shoe outsole hardness for predicting wear. This study shows that neither normal force nor

hardness influenced shoe wear rate, supporting the use of fatigue failure wear theory as a relevant basis for predicting shoe outsole elastomeric wear.

There are a few limitations from the study that should be acknowledged. The participants wore shoes on primarily indoor surfaces. As surface roughness has a strong influence on wear, these results may not generalize to outdoor wear (Sato et al., 2020). Furthermore, the specific material composition may affect the wear rate of the shoes which could lead to the slight changes in wear rates between shoe brands (Sato et al., 2020). Participants worked in a variety of fields possibly introducing gait variability among participants to perform different movements across work environments. Further studies with a greater degree of control over the workplace conditions may be helpful for confirming the results of this study. However, the clear trend in the data is seen even with this variability, supporting the robustness of the results to assess natural wear in the general workplace.

Gait kinetics impact shoe wear rate. The results are consistent with an elastomer fatigue failure model of shoe wear. Although this work focused on slip-resistant shoes, the theoretical approach and conclusions are expected to apply to both slip-resistant and non-slip-resistant shoes. Furthermore, this research suggests that a person's gait has an impact on wear which influences shoe traction performance. By measuring and analyzing simple gait kinetics (peak shear force or peak RCOF), individual shoe replacement recommendations could be made to improve shoe safety.

5.1.6 Conclusion

Overall, this research identifies individual peak shear forces and peak RCOF as predictors of shoe wear rate, which may also provide insight into a fatigue failure as the mechanism

dominating the wear of shoe outsoles. In this study, peak shear forces and peak RCOF, a measure of peak shear forces relative to normal forces during dry walking, were found to be associated with tread wear rate. This work supports fatigue failure as a mechanism of shoe tread wear for normal gait. Therefore, this understanding of gait kinetics and the wear mechanism may inform the need for individualized shoe replacement recommendations to prevent injury caused by the decline in traction performance of worn shoes.

5.2 Shoe Outsole Hardness

5.2.1 Background

As shoes wear down, traction performance decreases and slip risk increases (Hemler, Charbonneau, et al., 2019; Hemler, Pliner, et al., 2020; V.H. Sundaram et al., 2020). Furthermore, Section 5.1 primarily showed that shoes wear down at varying rates which may be influenced by gait kinetics. However, there is a gap in the literature understanding the impact of shoe outsole hardness on wear rate for a variety of shoe outsole types. The purpose of this analysis is to understand the relationship between shoe outsole material hardness and wear rate across multiple modes of wear and shoe outsole patterns. This work specifically explores the hypothesis first discussed in Section 2.2.2, that decreased hardness leads to increased wear rate for shoes worn via natural and simulated protocols.

5.2.2 Methods

5.2.2.1 Summary

In this analysis, shoes of varying hardness and varying tread design were worn down via simulated or natural wear. Volumetric tread loss was recorded for each shoe after routine abrasive wear (accelerated wear) or specific time points (natural wear). The rate of tread loss was calculated as the amount of tread loss per distance worn.

5.2.2.2 Accelerated Wear Experiment #1 (AW1)

The five shoes that were worn down via an accelerated wear protocol as first described in Section 3.1 were included in this analysis (Figure 5.6). As such, wear methodology can be accessed in the previously described accelerated wear experiment (Section 3.1.3.2). Shoe designs were recoded (see Figure 5.6 caption description) since this study merged data from multiple studies.

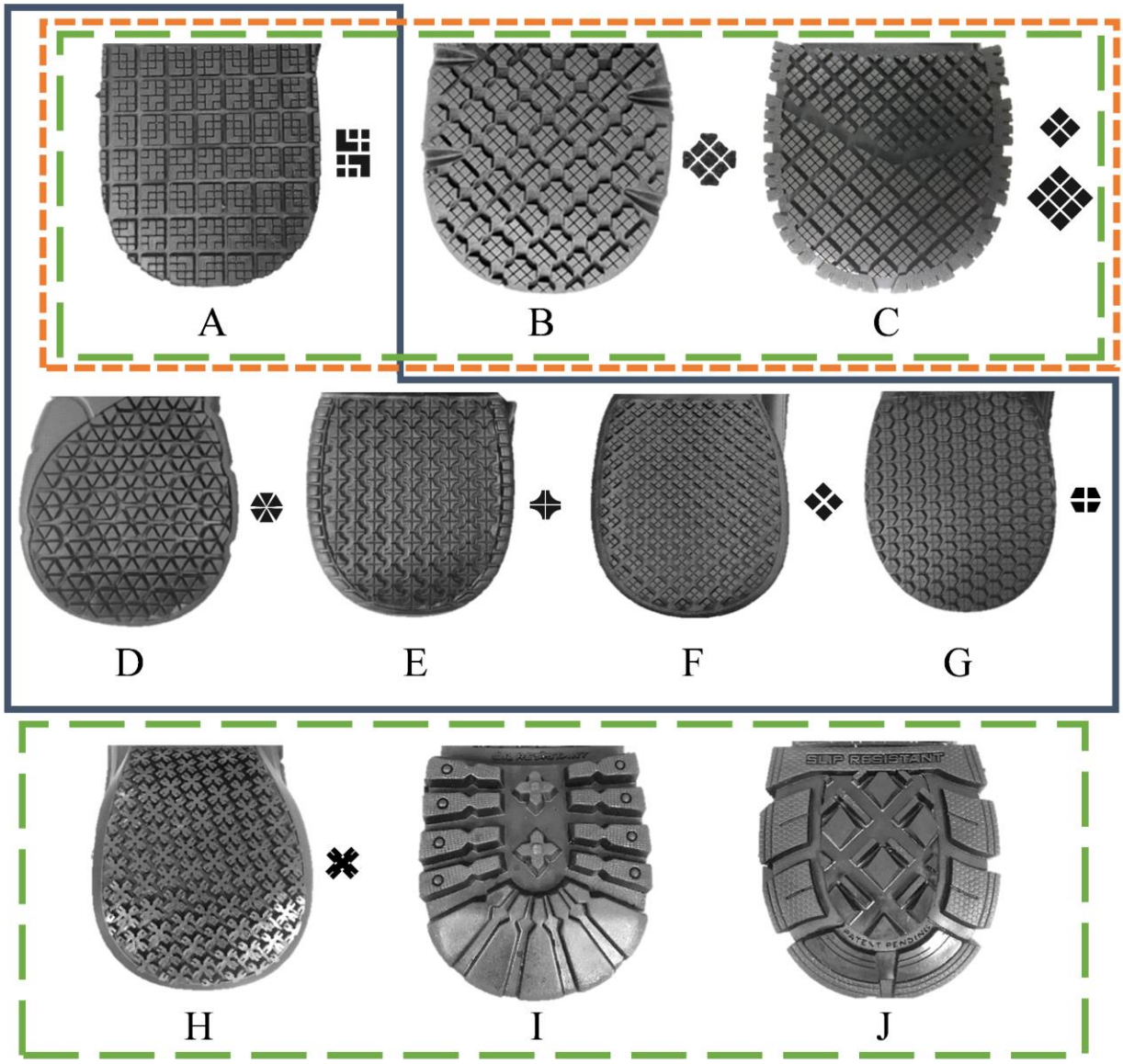

Figure 5.6 Tread Patterns

Accelerated Wear #1 shoes A, D-F enclosed in solid blue line, Accelerated Wear #2 shoes enclosed in long, green dashes, and Natural Wear shoes enclosed in short, orange dashes. Representative tread blocks are shown to the right of the shoes. Shoes D, E, F, A, and G were recoded from the original shoe codes in Section 3.1.3.2 which were A, B, C, D, and E, respectively.

5.2.2.3 Accelerated Wear Experiment #2 (AW2)

Twelve pairs of shoes with varying tread designs and hardness levels were used in this experiment. Shoes A, B, and C had the same tread design as those used in the natural wear experiment (Section 4.1). Shoes with three tread patterns (labeled H, I, and J) accounted for nine shoes in this analysis: (three tread patterns) × (three Shore A hardness values) (Figure 5.6).

The shoes were worn down using a wear protocol modified from Section 3.1.3.2. (Walter et al., 2021). The wear apparatus consisted of a last to attach a shoe to a mechanism that controlled shoe-floor angle. The shoes were slid on abrasive paper (165 µm particles of aluminum oxide - POWERTEC #110530) at a speed of 9.65 m/s (Rikon Power Tools 50-122). One wear cycle consisted of wearing the shoes at three sagittal plane angles (17°±1°, 7°±1°, and 2°±1°) for 10 seconds each (total of 289.5 m in 30 seconds). These angles were used to simulate the stance phases of gait consistent with previous research (Kadaba et al., 1990). Additionally, an inversion angle of 6° along the frontal plane was applied using a 3D printed bracket (fused deposition modeled polylactic acid, HATCHBOX 3D PLA-1KG 1.75-BLK) between the shoe last and the apparatus arm. A preliminary analysis showed that this inversion angle corresponded with the lateral contact region observed during natural wear (Section 4.1) and human slipping (Iraqi, Cham, Redfern, Vidic, et al., 2018). After each wear cycle, the shoes were cleaned of the abraded particles and grease residue (Formax, No. F26). The grease was used to reduce heat accumulation. The abrasive paper was also replaced after the twelve shoes had each undergone a wear cycle to reduce the impact of worn abrasive paper on the wear protocol.

5.2.2.4 Natural Wear Experiment (NW)

Twenty-four shoes ($n_{shoe\ A} = 12$; $n_{shoe\ B} = 8$; $n_{shoe\ C} = 4$) that were naturally worn by 15 participants as first described in Section 4.1 were included in this analysis (Figure 5.6). As such,

that wear methodology was presented in Section 4.1.3. The required coefficient of friction during normal walking was quantified for each participant as described in Section 5.1.3.3.

5.2.2.5 Hardness & Wear Measurements

For each shoe in the three experiments, the Shore A hardness was measured according to the ASTM standard for durometer hardness of rubber material (ASTM, 2015). After each wear cycle (AW1 and AW2) or month of wear (NW), heel molds of the shoe tread were created consistent with methodology described in Section 3.1.3.4. The volumetric tread loss was measured from each mold using pipetting techniques addressed in Section 5.1.3.4. The volumetric tread loss was measured after a sliding distance of 1.12 km for AW1 and AW2 (AW1 - wear cycle #2, AW2 - wear cycle #4) and after the first month of wear once the 100 km threshold was reached for NW. The wear rate was quantified as the volumetric tread wear per sliding distance for the AW1 and AW2 and per distance walked for NW.

5.2.2.6 Data & Statistical Analysis

Two analyses were used to determine the relationship between hardness and wear rate. Specifically, in model 1, a mixed linear regression was used to assess the effect of hardness and wear experiment (independent variables) on wear rate (dependent variable) for the combination of the AW1 and AW2 data (n_{shoes}=17). In model 2, a repeated-measures ANOVA was used to assess the effect of hardness and RCOF (independent variables) on wear rate (dependent variable) for the NW data (n_{shoes}=23). RCOF was included in the model as previous research has shown that RCOF influences wear rate (Hemler, Sider, et al., 2021).

5.2.3 Results

5.2.3.1 Accelerated Wear

Among the 17 shoes in the accelerated wear experiments, the Shore A hardness values ranged from 48.3-71.0 (Figure 5.7). The volumetric tread loss varied from 641.9-3940.4 mm^3 with a mean (standard deviation) of 2248.1 (995.4) mm^3 at a sliding distance of 1.12 km. The corresponding wear rate ranged from 0.6-3.5 mm^3/m with a mean (standard deviation) of 2.0 (0.9) mm^3/m. Hardness ($t_{2,14}$=-0.8, p=0.441) and experiment type ($t_{2,14}$=1.9, p=0.077) did not affect wear rate.

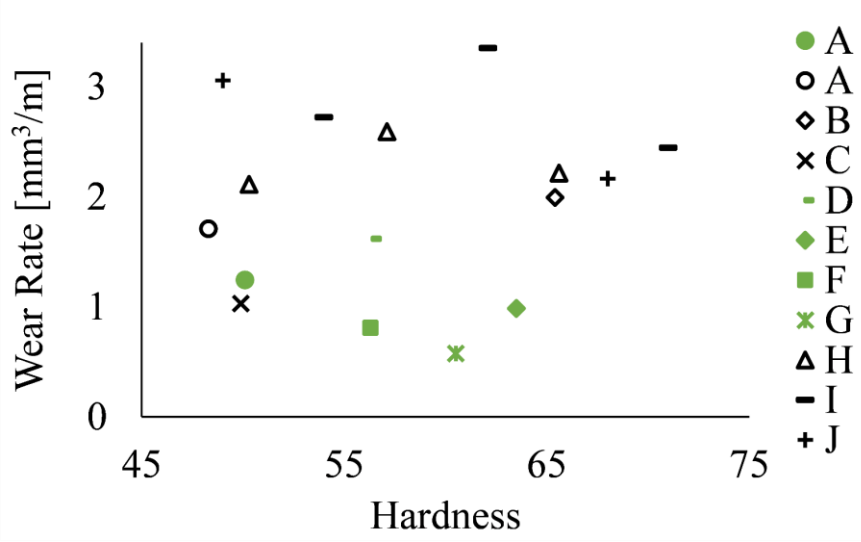

Figure 5.7 Wear Rate vs. Hardness – Accelerated Wear

The tread wear rate for shoes from AW1 are shown in solid green shapes and shoes from AW2 are shown in hollow black shapes. All shoes are shown with respect to the outsole Shore A hardness. Shoes with the same tread block arrangement but different hardness values have the same marker label shape (A, H, I, & J). Shoe A was represented in both AW1 and AW2 and as such, is shown with a solid green and hollow black circle.

5.2.3.2 Natural Wear

Shore A hardness ranged from 48.3-74.1 across the 23 shoes of three shoe types (Figure 5.8). The range and mean (standard deviation) of the volumetric tread loss was 324.6-3469.6 mm^3 and 1218.9 (751.8) mm^3, respectively. Distance walked ranged from 101.4-350.8 km with a mean (standard deviation) of 171.5 (68.4) km. RCOF ranged from 0.09-0.23. The wear rate ranged from 1.7-19.6 mm^3/km with a mean wear rate of 7.6 (4.8) mm^3/km. Wear rate was not associated with hardness ($F_{1,10}$=4.3, p=0.066), nor RCOF ($F_{1,15}$=3.3, p=0.088) in the model.

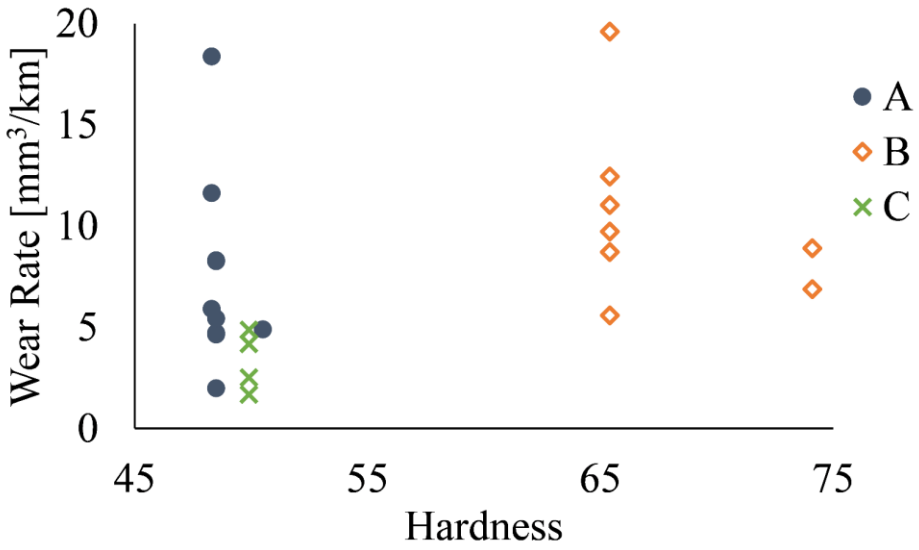

Figure 5.8 Wear Rate vs Hardness – Natural Wear

The tread wear rate for the three shoe types from the natural wear experiment are shown with respect to the outsole Shore A hardness.

5.2.4 Discussion

This analysis showed that within accelerated and natural wear experiments, shoe tread wear rate was not associated with outsole material hardness, contrary to the hypothesis. The wear rates for the AW2 were higher than those of AW1 though this difference was not significant.

The findings are consistent with previous findings that there may be other factors that better determine shoe wear factors. Gait kinetics as discussed in Section 5.1 and published work have shown that the shear forces during walking are indicative of tread wear rate (Hemler, Sider, et al., 2021). The proportion of tread that covers the heel may also be a good indicator for shoe wear rates as shown in previous work (Section 3.1.4) which analyzed the tread from shoes A, D, E, F, and G in this analysis (Hemler, Charbonneau, et al., 2019).

This analysis showed that hardness may not be a determining factor for predicting wear rate. Wear of elastomers, of which shoe outsoles are often comprised, is influenced by multiple mechanisms: abrasion (Southern & Thomas, 1979), adhesion and tearing (Gent & Pulford, 1983; Thomas, Gupta, & De, 1987), and fatigue (Mars & Fatemi, 2004; Razzaghi-Kashani & Padovan, 1998). In this study, the shoes worn via accelerated wear protocols experienced primarily abrasive wear from the wear apparatus. Previous work has theorized that natural wear on indoor surfaces is associated with fatigue wear (Hemler, Sider, et al., 2021) and may also be associated with adhesive wear (Myshkin et al., 2006). Therefore, this study shows that hardness may not be an indicative factor for abrasive, adhesive or fatigue wear of shoes within the studied range of hardness. Other tests such as abrasion resistance may be useful for shoes as this metric is related to material properties such as the strength of the elastomer matrix, and crack growth resistance under dynamic conditions, in addition to external factors such as frictional force applied and the nature of the abrasion (Thomas et al., 1987). Furthermore, this work supports other metrics such as gait kinetics as useful for understanding wear rate (Hemler, Sider, et al., 2021).

A few limitations of the study should be acknowledged. Across all the experiments, only one time point of wear was measured. During initial wear, the wear rate is expected to be constant. However, with increased wear, this relationship may not hold. Furthermore, multiple modes of

wear were used in this analysis. Shoes in the accelerated wear experiments were worn down via abrasive wear whereas shoes worn in the workplace may have experienced multiple modes of wear including abrasion, adhesion, and fatigue wear. Additionally, the material properties (fatigue resistant, material composition) of the outsoles were not tested or given, and as such were not considered in the analysis. This study however shows that regardless of wear type, shoe hardness is not associated with tread wear rate.

5.2.5 Conclusion

Although hardness is a descriptive material property for rubber, this analysis showed that there was no strong relationship between shoe outsole hardness and wear rate. These findings support that other factors such as gait kinetics and tread proportion may be better indicators for wear resistance.

6.0 Development of a Tool to Assess Outsole Worn Region Size and Determine Slip Risk

Previous chapters demonstrated that the worn condition of footwear influences traction performance changes and can be used to guide replacement. Chapters 3.0 and 4.0, in addition to previous research (Beschorner et al., 2020; V.H. Sundaram et al., 2020), show that the size of the continuous worn region is a good indicator for shoe replacement to prevent slips and falls. Currently, there are no tools which efficiently and simply determine when shoes should be replaced. This chapter will discuss the process, objectives, and hypotheses for developing a low-cost tool to assess shoe outsole wear. Aspects of this work have been published in conference proceedings (Bharthi, Sukinik, Hemler, & Beschorner, 2020; Sukinik, Bharthi, Hemler, & Beschorner, 2020). Further explanation of experiment protocols for this chapter can be found in Appendix C.

The purpose of this chapter is to describe the development of a low-cost tool designed to give shoe replacement recommendations (Figure 6.1). There is a lack of a tool that provides a clear recommendation of when shoes should be replaced in the workplace. Food service employees were interviewed to assess their understanding of footwear safety and gain feedback on several potential tools that could be employed. Interview feedback favored development of a shoe scanner concept which employed current optics technology and was translated into a proof-of-concept prototype. A functional prototype was then created based on the proof-of-concept prototype. The functional prototype was assessed according to two objectives (verification and user feedback assessment) and two hypotheses (validation). Once the objectives and hypotheses could be appropriately tested and achieved, Aim 3 was accomplished.

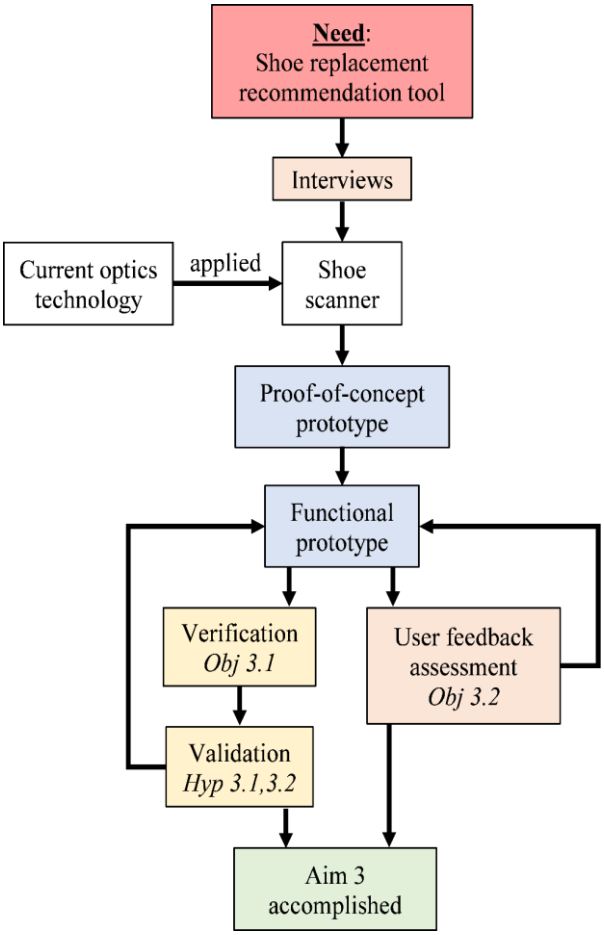

Figure 6.1 Aim 3 Flowchart

6.1 Interviews

6.1.1 Methods

User-centered design principles addressed in Section 2.4 were used to determine the feasibility for using FTIR technology as a potential tool for determining shoe replacement. Primarily semi-structured interviews were used (Jordan, 1998). Seven participants who worked in the food service industry (e.g., restaurants, grocery stores) were interviewed as subject matter experts (SMEs). Six of the seven SMEs were full-time employees and one was employed as a part-time employee. At least three of the SMEs had worked in the service industry with at least two employers. Three of the SMEs were managers at their respective locations. All the SMEs were employed in the food-service industry with companies that served a regional, national or international market (Manager of Fast Food Restaurant A - SME #3, 2020; Manager of Fast Food Restaurant A - SME #7, 2020; Manager of Fast Food Restaurant B & C - SME #2, 2020; Team Member of Fast Food Restaurant A & B - SME #5, 2020; Team Member of Fast Food Restaurant B - SME #1, 2020; Team Member of Full Service Restaurant A and Grocery Store A - SME #4, 2020; Team Member of Grocery Store B - SME #6, 2020).

The first three sections of the interview assessed the SMEs perception of slip and fall risk and prevention techniques in their workplaces. Section 1 included open-ended questions on slip risk and prevention and one structured question to assess the frequency of slips and falls in the workplace (for full interview, see Appendix C.1). For the structured question, SMEs were asked to indicate on a scale from 1-10 with 1 being not a problem and 10 being a serious issue, the extent to which slips and falls were a problem at their site. Section 2 asked semi-structured questions on workplace apparel requirements and maintenance checks. Section 3 assessed the SMEs perception

of the importance of footwear in the workplace. Questions included ‘when do you decide to buy new shoes?’ and ‘if your shoes would be replaced because of wear on the bottom of your shoes, when do you think you would replace them and why?’. The questions in this section were organized to ask broader questions about slip and fall prevention programs prior to the questions about footwear and worn condition. This ordering was intended so that the detailed questions about footwear did not bias the broader answers about slip and fall prevention programs. The last question in Section 3 assessed the SME’s perception of shoe tread wear by having the SME choose ‘the size of the worn region at which a shoe may no longer protect you from slipping’. For this question, two shoe tread patterns that were used in the natural wear experiment (described in Section 4.1) were shown at six wear points (Figure 6.2).

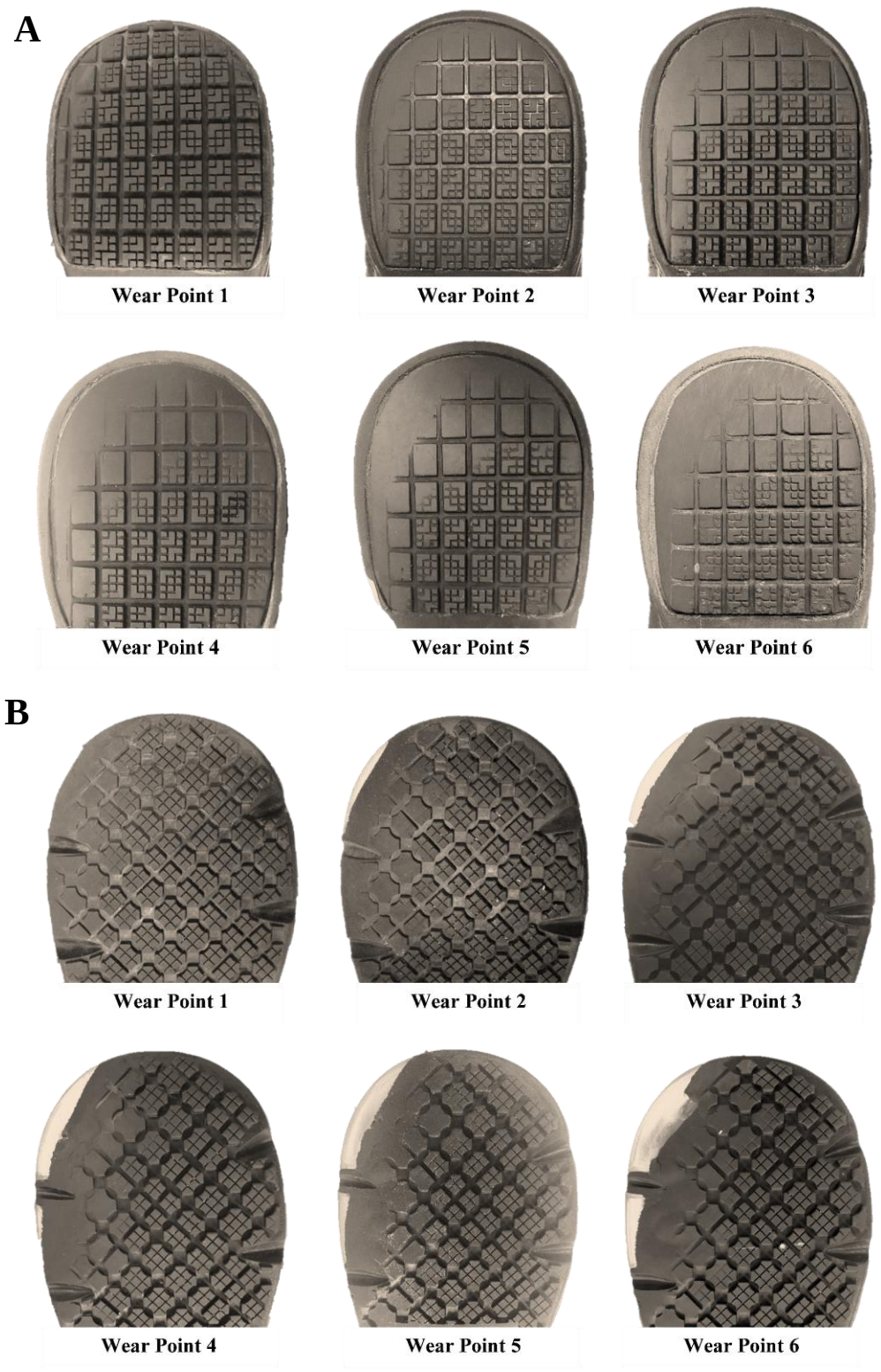

Figure 6.2 Interview Wear Point Images

Wear point images from naturally worn shoes for A) Shoe A and B) Shoe B.

Section 4 of the interview was semi-structured and consisted of presenting and gathering qualitative and quantitative feedback for potential shoe replacement recommendation tools. The three tool options were shown in randomized order and represented tools that could be used in the workplace to assess whether shoes should be replaced. Option 1 represented a lower-technology option – a handheld tool: a simple handheld tool would be held against the shoe tread to indicate a replacement recommendation (Figure 6.3). Option 2 represented a higher-technology option – a phone app: a phone or other device would be used to take a picture of the shoe tread and then it would give a replacement recommendation (Figure 6.4). Option 3 represented a higher-technology option – portable shoe scanner; the user would stand on the scanner to have the shoe tread scanned and then the scanner would present a replacement recommendation (Figure 6.5). Option 3 represents an existing technology as the scanning concept has been developed (see Section 6.2), but not applied to this need. After the first tool was presented and the SME expressed an understanding of how the tool worked, the SME was asked to share what they liked about the tool, what they thought might make the tool challenging to use, and if they would recommend any changes to the tool. This process of presenting the tool and asking for feedback was repeated for each tool.

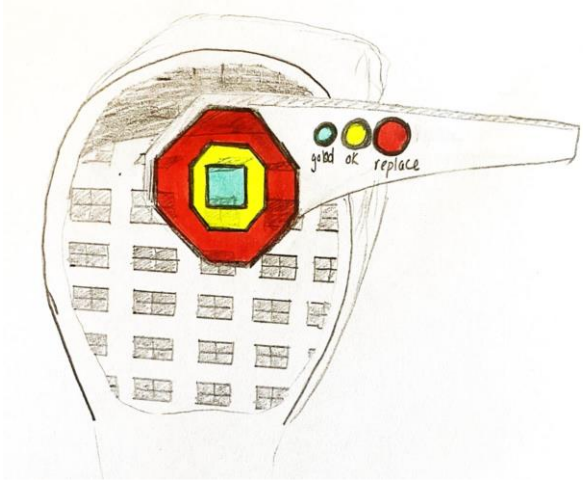

Figure 6.3 Interview Tool – Option 1: Handheld tool

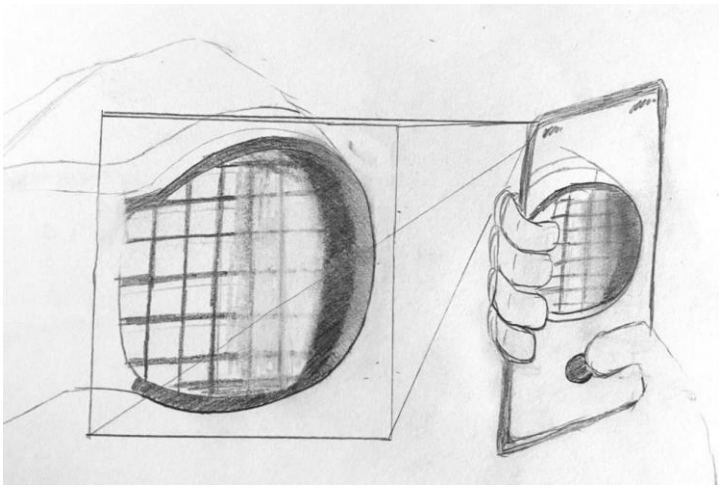

Figure 6.4 Interview Tool – Option 2: Phone app

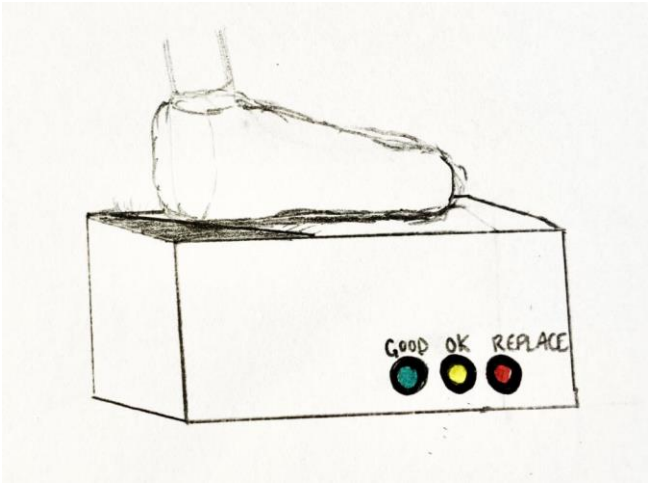

Figure 6.5 Interview Tool – Option 3: Portable Shoe Scanner

The final sections of the interview consisted of semi-structured and structured components. In Section 5, qualitative and quantitative answers from the SMEs were used to assess the usefulness, usability, and desirability of each of the tool options in the workplace. For the quantitative (structured) assessment, SMEs were asked to rate each of the tool options as to how well they might integrate into the SME's work environment on a scale from 1-10, with 1 being integrate poorly and 10 being integrate very well. The question was asked of the three tool options in the same order that the options were presented to the SME. The SMEs were also asked to describe, qualitatively, how they thought the tools might be best integrated into their workplace

and how often they would be willing to use them at work. Section 6 consisted of asking the SMEs if there was anything else that might be helpful to know when creating a shoe replacement indicator tool.

6.1.2 Results

Several sections of the interviews yielded quantitative results. From Section 1, SMEs indicated that the extent to which slips and falls were a problem at their site ranged from 1-6. In Section 3, an average wear point of 3 (5 SMEs) was chosen for shoe A, and for shoe B, an average wear point of 2.5 (6 SMEs) was chosen (Figure 6.2). Wear point 3 for shoe A corresponds to a measured worn region size (length and width measurements of the continuous worn region as described in Sections 3.1.3.4, 3.2.3.3, and 4.1.3.4) of 629 mm^2 (Section 4.1, right, month 5, distance of 1425 km). For shoe B, wear points 2 and 3 correspond to a measured worn region size of 481 mm^2 and 499 mm^2 (Section 4.1, left, months 2 and 3, distances of 396 and 605 km). In Section 5, the handheld tool scored the lowest (worst), the phone app tool scored in the middle, and the portable shoe scanner scored the highest with average (standard deviation) scores of 5.5 (2.2), 6.4 (2.1), and 6.4 (2.3) on the 10-point scale.

Based on the responses of the SMEs, the concept of tread wear as a good indicator of shoe replacement was not broadly known at the start of the interview. One SME noted that shoes are more likely to be replaced at work if there are holes or tears on the top; managers are less likely to notice wear on the heel to inform team members to replace shoes (Manager of Fast Food Restaurant A - SME #3, 2020). One team member stated that “no worker replaces their shoes when they start to feel slipping” (Team Member of Full Service Restaurant A and Grocery Store A - SME #4, 2020). Furthermore, the SMEs expressed advantages and disadvantages for each tool.

For the handheld tool, the advantages included that it might be easy to simply hold this indicator to the shoe and tell if the shoe needed to be replaced. One SME stated that this tool "gives people a sense of measurement" of an acceptable worn region size (Team Member of Full Service Restaurant A and Grocery Store A - SME #4, 2020). However, overall, there was the most confusion of how the handheld tool worked compared to the other tools. Also, there seemed to be the least excitement for this tool compared to the intrigue of the other two tools. One SME stated that the handheld tool seemed a bit subjective because it could not take into account the wear on the entire shoe outsole (Team Member of Fast Food Restaurant A & B - SME #5, 2020).

For the phone app, most SMEs liked the tool with one SME stating that it would be easier to hold people accountable with this option given that checking the worn region on the shoe would be recorded digitally. The concern for learning to use the technology and having access to a device that could scan the shoes was mentioned in several interviews. It was also stated that for team members that were older and less familiar with technology, the phone app may be harder to use. Furthermore, it may be harder to implement this tool into the work schedule if employees were to use devices (e.g., iPad) that were already being used in other parts of the store (e.g., purchases at storefront in restaurant).

For the portable shoe scanner, the most common advantages stated were that it would be easy to use as a part of the daily, weekly, or monthly routine since it is separate from other devices used in the store, and that since it looks like an interesting piece of equipment, employees might use it on their break time. The main disadvantages expressed for the scanner included space and cost constraints.

Overall, the SMEs expressed that they would be willing to use any of the tools from once every 2 weeks to 6 months. One manager stated that it might be easier to implement the tools if

they could check shoes as some sort of game among the employees, making it into a fun, morale-building competition to stay safe (Manager of Fast Food Restaurant A - SME #3, 2020). Along those lines, several SMEs also expressed that an active incentive would work best to encourage people to check their shoes. Other common remarks from the interviews that may influence future directions for this work are discussed in Sections 7.1.1.

The quantitative and qualitative feedback were used to determine which potential tool option would be chosen for prototyping. The portable shoe scanner received the highest quantitative score. Furthermore, there were no explicit qualitative remarks that would rule out the portable shoe scanner as a feasible tool for the workplace. Therefore, this option was chosen for development and is discussed further in the following sections.

6.2 Frustrated Total Internal Reflection (FTIR)

Frustrated Total Internal Reflection (FTIR) technology has been used by scientists for centuries dating back to Newton and Fresnel in the 18th century (Newton, 1952; Zhu, Yu, Hawley, & Roy, 1986). Over the last several decades, the technology has been used for a variety of imaging applications ranging from measuring multi-touch sensing to capturing fingerprint scans (Han, 2005; Harrick, 1962). Furthermore, FTIR has been used to study foot contact area in clinical settings and to analyze prints from footwear for forensics analysis (Betts, Franks, Duckworth, & Burke, 1980; Needham & Sharp, 2016). FTIR describes the process of shining light into a transparent plate (waveguide) at an incident angle larger than the critical angle which ensures the light is internally reflected when contacted by air (Figure 6.6). The boundary condition changes when materials with a larger refractive index than air, such as shoe outsoles or skin, encounter the

waveguide. The change enables light to be transmitted out of the waveguide, into the shoe outsole or skin, and scattered. The scattered light illuminates the contact region which can then be detected by a camera.

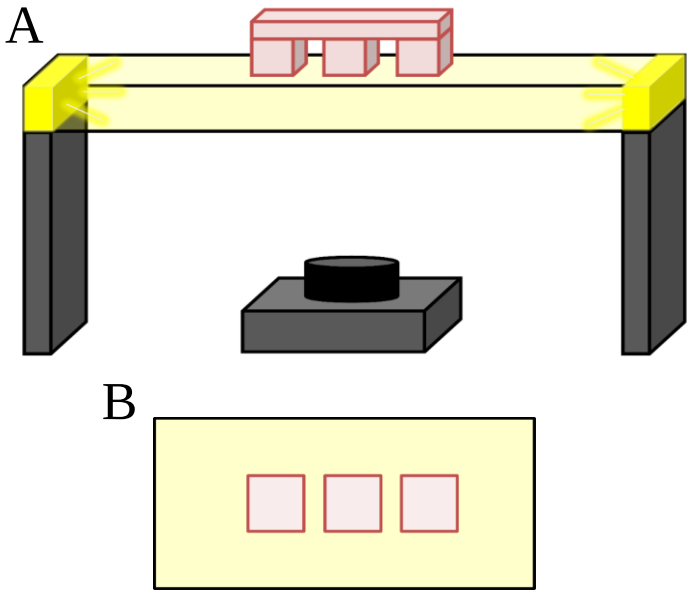

Figure 6.6 FTIR Concept Diagram

A) 3D Diagram of FTIR. Light illuminates the waveguide on which the object rests. The camera captures the view from underneath B) which shows only the parts of the object in contact with the waveguide.

6.3 Tool Design & Prototyping

6.3.1 Proof-Of-Concept Prototype

A proof-of-concept prototype was created to verify the concept of the portable shoe scanner which was presented to the SMEs. Materials consisted of a light source (HitLights, 36in, 5050 LED), a waveguide (Americanflat Acrylic Picture Frame – 6in x 8in), and scrap wood, nails, and tape for construction (Figure 6.7). The camera (GoPro Hero 3+, GoPro, Inc., San Mateo, CA,

USA) sat on the base of the prototype under the platform. Images from two footwear types were collected to verify that the contact area of tread of multiple colors could be detected from the prototype (Figure 6.8). The prototype showed that a simple lighting device around an inexpensive waveguide (acrylic sheet) could sufficiently light up the contact area for colored (Figure 6.8A) and black (Figure 6.8B) tread. Future iterations may use colored lighting as shown in Figure 6.8. This prototype found that white light could detect multiple colored tread well.

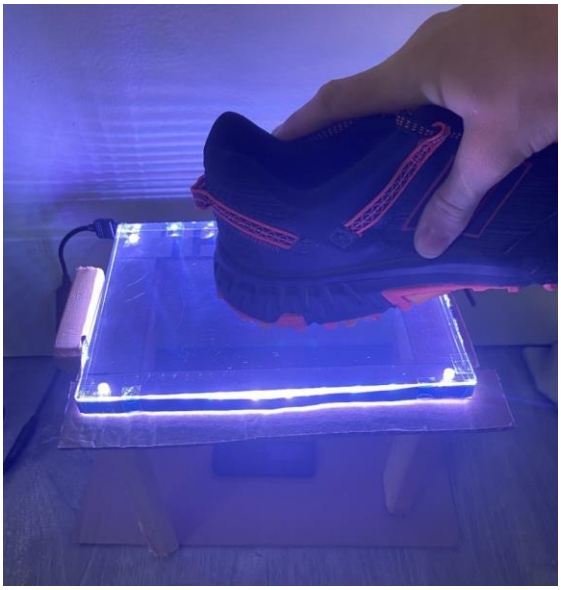

Figure 6.7 Proof-of-Concept Prototype

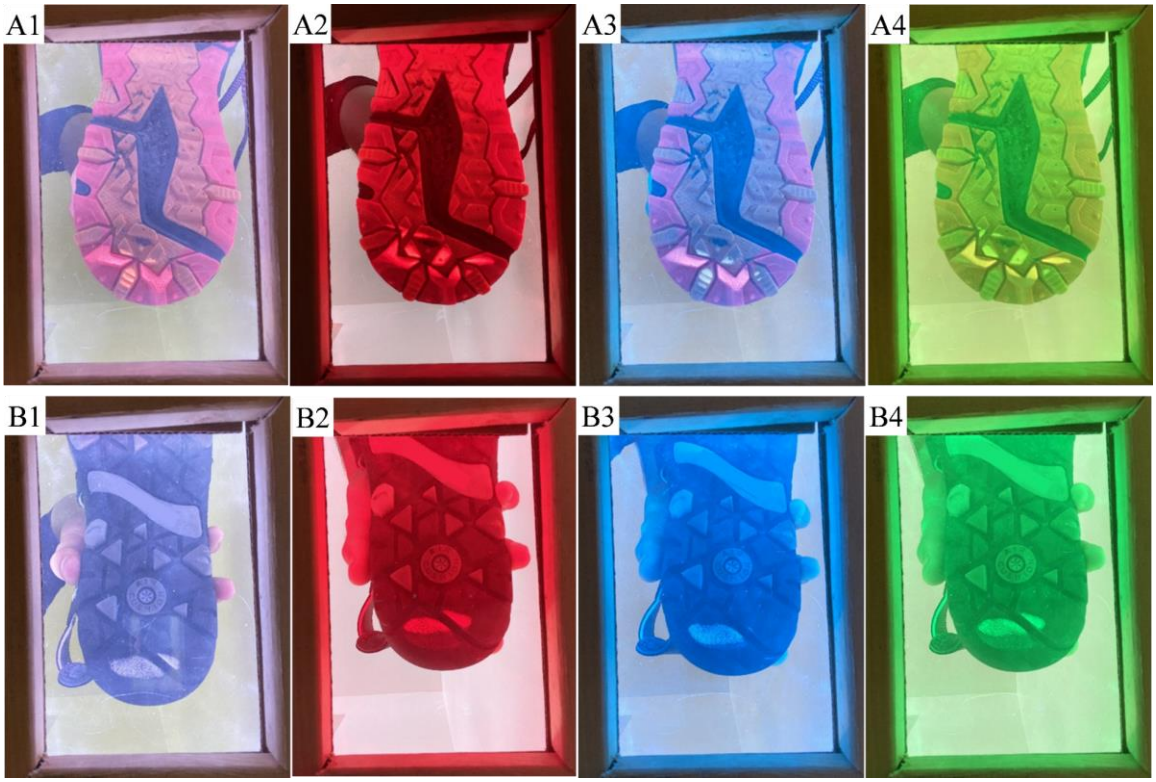

Figure 6.8 Proof-of-Concept Prototype Representative Images

Images of two shoes types (A and B) with four colors (1-4) illuminating the waveguide in the prototype. White light is shown in A1 and B1. The shoe heel section in contact with the acrylic sheet (seen in the bottom half of the images) is consistently a different color than the rest of the heel.

6.3.2 Functional Prototype

The functional prototype was created with adaptation from the proof-of-concept prototype (Figure 6.9). The materials included the same light source, waveguide, and camera as in the proof-of-concept prototype, and extruded t-slot aluminum (80/20, Inc., Columbia City, IN). The framing allowed for the waveguide to sit at angles between 7° and 17° (Figure 6.10). This framing also is strong enough to hold the full weight of an average individual. Prototype 2 functioned as a working prototype which was used to test the objectives and hypothesis of Aim 3 of this dissertation.

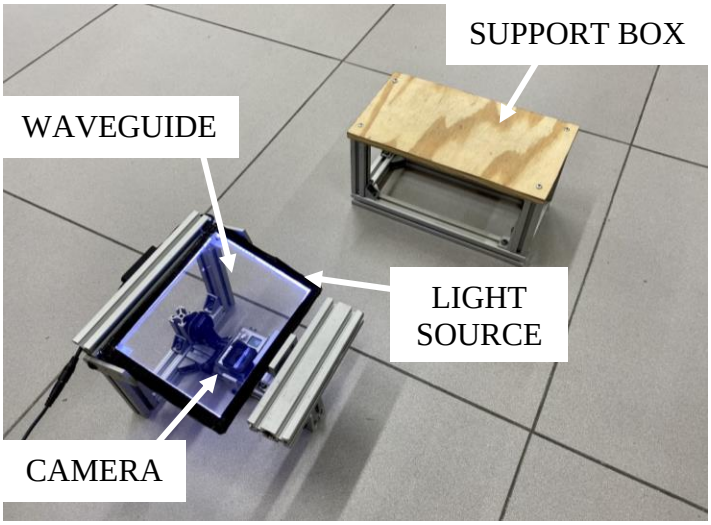

Figure 6.9 Functional Prototype

The frame, waveguide, camera (below the waveguide) and light source can be seen on the left. The support for the other foot is seen on the right.

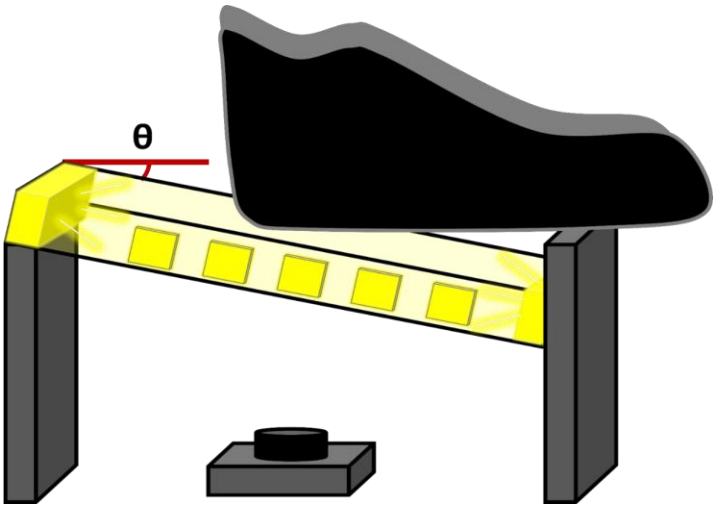

Figure 6.10 Functional Prototype Schematic

The angle, θ, was adjustable to accommodate angles of 7° and 17°.

6.4 Image Processing

The raw images from the scanner camera were processed in a series of steps to obtain the area of the largest continuous worn region on shoes (Figure 6.11). Raw images of the shoe-waveguide contact were captured on the same camera as in the proof-of-concept prototype (GoPro Hero 3+, GoPro, Inc., San Mateo, CA, USA) with the camera in 7MP Medium mode for the still images (Figure 6.11, step 0). MATLAB® (R2020a, Natick, Massachusetts: The MathWorks Inc.) was used to process the images using a series of steps. After the raw image was imported, a calibration function was used to flatten the wide-angle image using a checkerboard with 9x10 blocks each with 11.4 mm lengths (Figure 6.11, step 1). A cropping function was used to allow the user to select the portion of the image containing the tread in contact with the waveguide (Figure 6.11, step 2). The contact regions were determined by the user selecting two of the brightest and dullest features of the contact regions. Within those four points, the minimum and maximum

hue, saturation, and value measured were used to create a range of acceptable contact pixels. A buffer of 0.05 was added to the maximum value and subtracted from the minimum value to slightly increase the range which was used to determine the contact regions on the image (Figure 6.11, step 3). Connected pixel components were identified so that the largest continuous regions were identified and quantified (Figure 6.11, step 4). The calibration board from step 1 was used to determine the size of the pixels closest to the largest contact regions (Figure 6.11, step 5). This pixel-to-area conversion was then used to determine the size of the largest contact regions in sq. mm. (Figure 6.11, step 6).

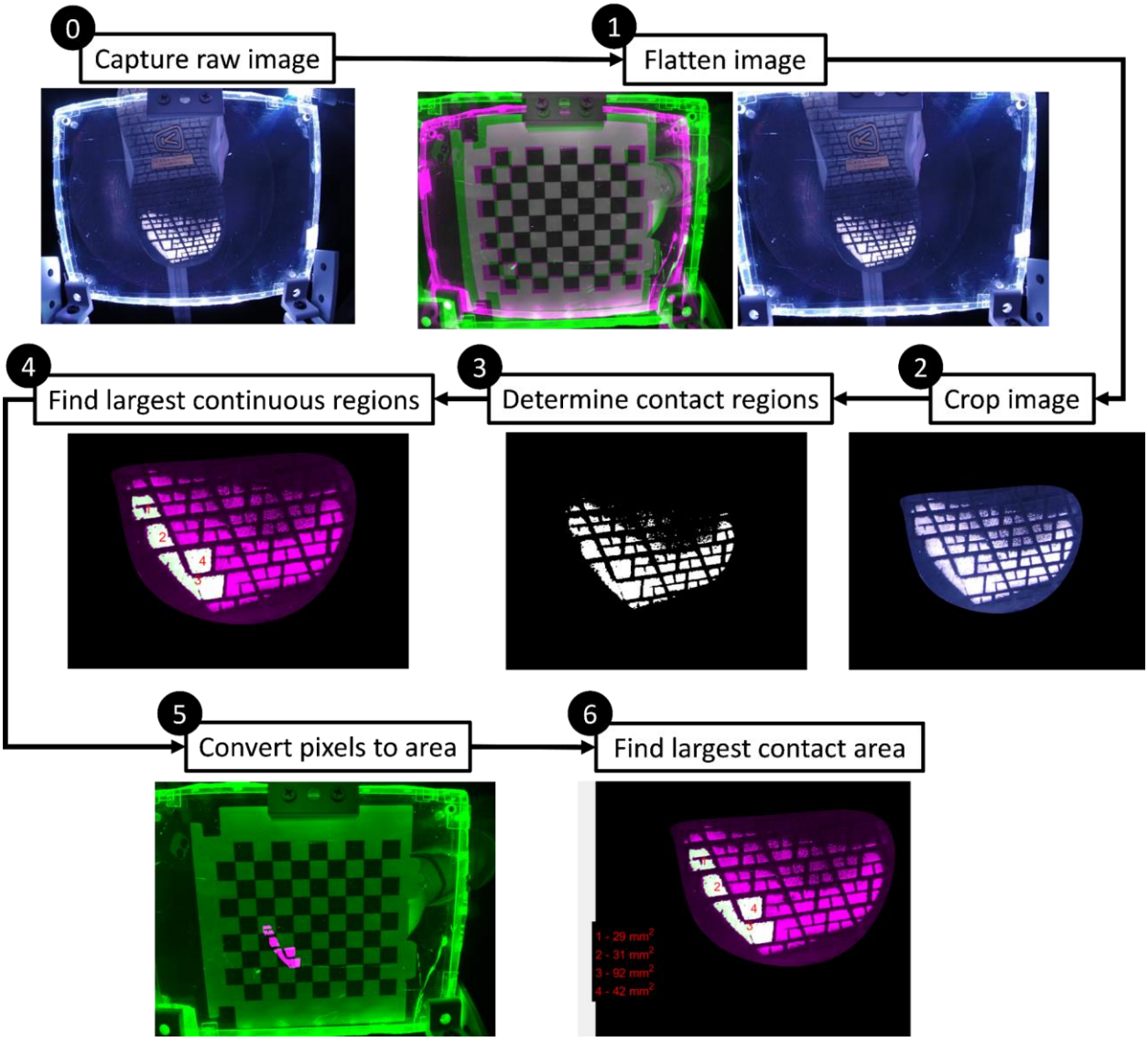

Figure 6.11 Image Processing Flowchart

The raw image (0) was flattened (1) via a calibration technique involving a 9x10 checkerboard. The image was cropped (2) to select only the regions of the shoe in contact. These regions were then isolated to determine the contact regions (3) and the largest continuous regions were identified (4). The location of the largest continuous regions were used to determine the pixel-size conversion (5). This conversion was then applied to the largest continuous regions to obtain the largest contact area (6).

6.5 Tool Verification (Objective 3.1)

The tool underwent a verification process to assess accuracy; shoes were scanned on the tool and the scanned small tread block areas were compared to the true block areas. The verification objective was that the root mean square error of the tool's measurement for the tread block size would be less than 10% of the true block size.

6.5.1 Methods

Three types of slip-resistant shoes with consistently sized small tread blocks were used in the analysis to assess the precision and accuracy of the tool (Figure 6.12). Ink imprints of the shoe outsoles were measured to determine the true area of the small tread blocks.

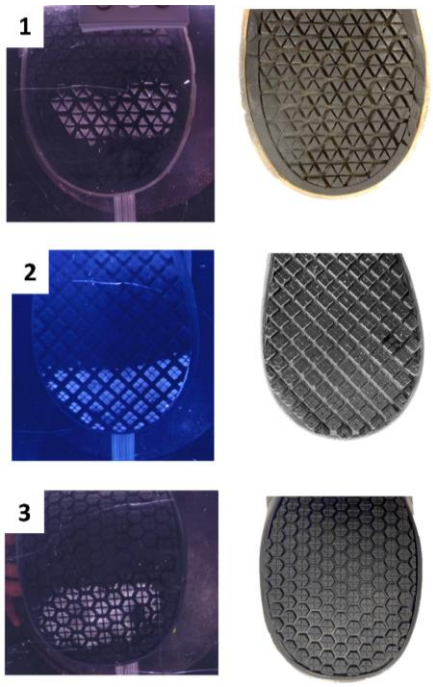

Figure 6.12 Verification Shoe Types

Individual blocks for verification: a single triangle tread for shoe 1, a whole square block grouping (4 small treads in a square) for shoe 2, and 1 of the 4 smaller treads on the individual tread blocks for shoe 3.

The shoe setup on the scanner consisted of placing each shoe at an angle of 0º on the waveguide which was set up at angles (θ) of 7º and 17º (Figure 6.13). These angles were chosen to capture the range of angles between slip onset and peak slipping speed (Albert et al., 2017; Iraqi, Cham, Redfern, Vidic, et al., 2018). A normal force of 75 lbs (334N) was applied to simulate just less than half of average bodyweight of an individual (Fryar, Carroll, & Ogden, 2018). Images were collected in the dark to optimize image quality (Figure 6.14). Image processing was used to identify the area of the 20 largest tread blocks detected.

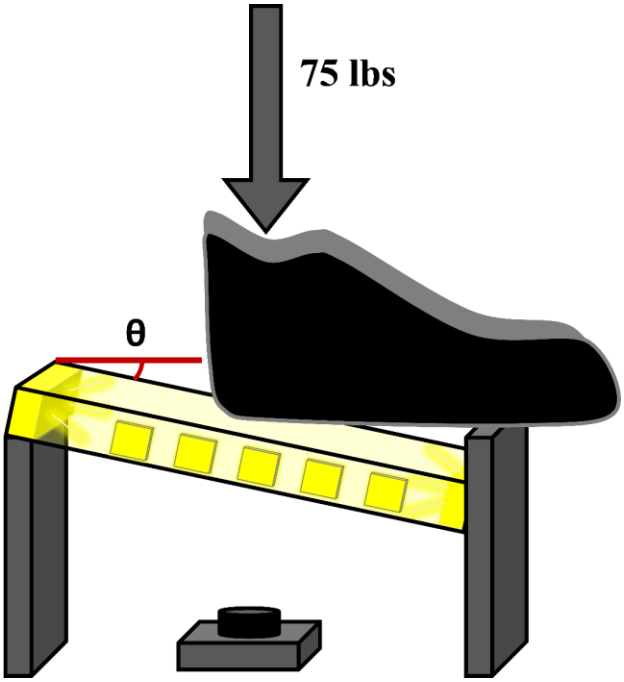

Figure 6.13 Scanner Verification and Validation Setup Schematic

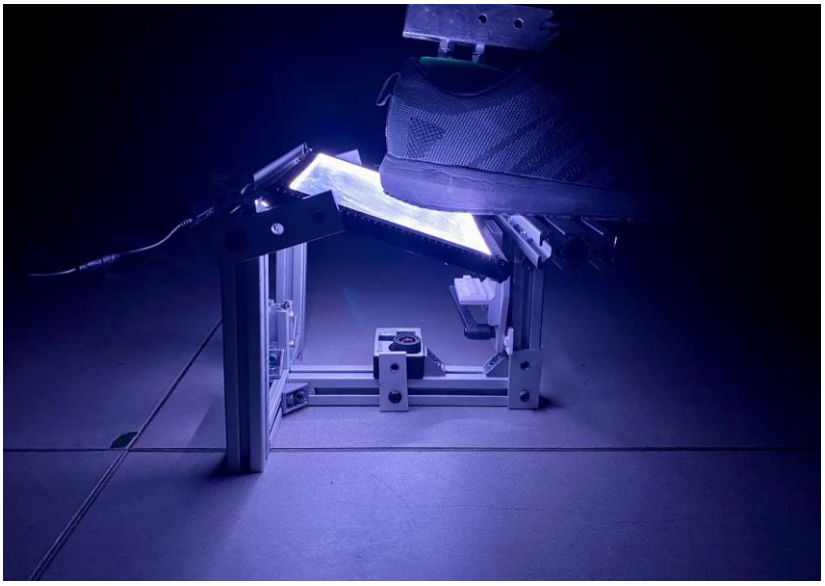

Figure 6.14 Scanner Verification and Validation Setup

Illuminated waveguide angled at 17º shown in the dark with shoe on waveguide and camera underneath.

6.5.2 Results

The true sizes of the small tread blocks were 10 mm^2, 23 mm^2, and 5 mm^2 for shoes 1, 2, and 3, respectively as shown in Figure 6.12. The average (standard deviation) of the measured block sizes from the scanner and image processing were 11.2 (1.3) mm^2, 23.9 (2.8) mm^2, and 5.5 (1.0) mm^2 for shoes 1, 2, and 3, respectively. Therefore, the mean deviation of the measured block sizes compared to the true sizes was 12.1%, 4.1%, and 9.1%, respectively. The root mean square of the percent difference between true and measured block sizes were 17.6%, 12.5%, and 8.2%, respectively. Therefore, the objective of maintaining a root mean square error below 10% was not achieved. However, the scanner was able to achieve a root mean square error below 20% which was deemed acceptable for this analysis. Limitations of the scanner and future improvements can be seen in Sections 6.7.4, 6.8, and 7.2.

6.5.3 Discussion

A functioning prototype was developed consistent with recommendations of the subject matter experts. The image processing technique was able to identify and quantify the tread block size on the shoe outsole. The objective of the verification was not met since the measured error was just above the *a priori* threshold, although the accuracy of the device could still yield potentially useful measurements.

The methods used for verification of the tool are consistent with how the tool would be used in the workplace and provides a stable, useful framework on which to build. The weight added to the shoe during testing (75 lbs) is consistent with the half of the weight of an average individual that would stand on the device (Fryar et al., 2018). The design of the framing allowed for the camera to sit in the exact same location every time ensuring that calibration was consistent throughout all trials. The use of ink imprints to determine the true size of the tread is consistent with previous research that has utilized this technique to measure shoe tread contact area (Iraqi et al., 2020; Jones et al., 2018). Lastly, the materials used to construct the tool cost less than $200, and there was minimal labor assembly and no custom machining. The ease of design of this prototype is a good start such that future iterations can reduce cost with improved design.

The verification analysis varied from the expected results for several proposed reasons. SR shoes were used for this analysis because these shoe outsoles have small, identically sized rubber tread blocks. The small size of the tread (smallest true tread block size of was 5 mm^2) may have allowed small errors in an absolute sense to appear larger from a percentage perspective. Second, as rubber is a viscoelastic material, the shoe tread deformed with time as it was pressed on the waveguide; the deformed tread block with the full load was used to calculate the tread block size. The ink imprint does not capture this change in contact with deformation. For the ink imprint, the

ink is translated to the paper once any contact has been made. Therefore, the size of the tread block from zero-load to full load (deformed state) is detected. Therefore, the ink imprint technique has potential to give a slightly larger true size than can be detected by the tool. Future verification may improve the experimental design to determine the true size under similar conditions to the tool's measurements.

There are a few limitations in the development of the tool and in this analysis. At this stage, the tool requires an external power source; the tool could be adapted to contain an independent power source in future iterations. This verification process was only conducted with black tread. Future work should conduct a verification process with not only larger tread as mentioned above, but also with tread of varied color. Lastly, additional experiments that better controlled for deformation during verification testing (e.g., using a deformable sphere and applying Hertzian contact mechanics) might provide more precise data on its verified accuracy.

6.6 Tool Validation (Hypothesis 3.1 and 3.2)

A validation process was completed to assess the tool's ability to predict the likelihood of a slip based on the size of the worn region on the shoe outsole. The premise of this validation is based on findings from a previous human slipping study which showed that as shoe worn region size (WRS) increases, the under-shoe fluid pressures and risk of slipping increase (V.H. Sundaram et al., 2020). Hypothesis 3.1 is that the tool will be able to significantly predict the likelihood of a slip. Hypothesis 3.2 is that the tool will be able to significantly predict fluid pressures based on the shoe scans.

6.6.1 Human Slipping Study

Fifty-seven participants took part in this experiment while wearing their own naturally worn shoes (SR: 36; non-SR: 21). Participants were outfitted in tight-fitting clothing and a set of 79 reflective markers (Moyer, 2006) while they walked over dry ground. During the dry walking trials, participants walked over two force plates (Bertec 4060A, Columbus, Ohio) from which each participant's RCOF was calculated. After a series of dry walking trials, the participant unexpectedly walked over a contaminated surface (100 mL of a 90% glycerol-10% water by volume solution). The contaminant was applied on top of a 5 x 6 array of fluid pressure sensors which were embedded in the floor. The peak fluid pressure during the step was recorded as the maximum value across the 30 fluid pressure sensors. The anterior-posterior and medial-lateral positioning components of the inferior heel marker were used to calculate the slip speed using numerical differentiation (Cham & Redfern, 2002). The peak slip speed (PSS) was calculated as the local maximum speed at least 50 ms after heel contact. A step was identified as a slip if the PSS exceeded 0.2 m/s. This classification was based on previous research that found a bimodal distribution for slips with low-severity slips of fully treaded shoes below this cutoff and high-severity slips with untreaded shoes above this cutoff (Beschorner et al., 2014). Therefore, a PSS exceeding 0.2 m/s was designated as the cutoff variable for a slip. A detailed description of the study can be found in the full manuscript (V.H. Sundaram et al., 2020).

6.6.2 Experimental Protocol

The SR shoes from the human slipping study were used in this analysis as previous work in this dissertation has found the WRS of SR shoes to be associated with slipping. Two of the 36

pairs could not be located and shoes from three individuals were excluded from the analyses including peak fluid pressure because the individuals did not fully step over the fluid pressure sensors. Thus, 31 shoes are included for the analyses involving peak fluid pressure and 34 shoes are included for all other analyses. The contact region and WRS of the shoes was measured on the shoe scanner using the same methods as described for tool verification in Section 6.5.1. Additionally, the shoes were rotated along the frontal plane (i.e., inversion or eversion) to capture the largest worn region on the shoe. The only difference within this validation protocol was that the shoes were positioned on the waveguide such that the most worn region was in contact with the waveguide. This technique was employed to simulate as if a person was standing on the scanner and was asked to shift body weight back and forth so that the most worn region could be identified by the scanner.

The tool validation was applied to two image processing methods: automated selection and manual selection (Section 6.4, step 3). The manual method allowed the operator to correct errors from the first selection; the automated procedure did not involve researcher review of the images. Of the 68 total shoe scans (34 shoes x 2 angles), there were 11 images that were corrected via manual selection; 57 of the shoe scans were identical between the manual and automated selections. Eight of these 11 images that were corrected did not have sufficient contrast between the contact regions and non-contact tread for the image processing technique to easily distinguish the contact region. These images required multiple manual selections to identify the correct regions of tread in contact.

6.6.3 Statistical Analysis

Multiple models were used to assess the ability of the scanner to predict peak fluid pressures and slip outcome. In the models, there were two separate dependent variables used in the models: peak fluid pressure or slip outcome. There were two independent variables in the analyses: WRS and RCOF from the human slipping study. WRS was broken into four datasets based on the selection type (manual/automated) and angle (7°/17°) (Table 6.1). Therefore, four linear regression models were used to test the effect of WRS on peak fluid pressure. Four univariate logistic regression models were used to test the effect of WRS on the slip outcome. Furthermore, four multivariate logistic regression models were used to assess the impact of WRS and RCOF on the slip outcome. Therefore, a total of 12 models were used to test the effectiveness of the scanner (Table 6.1). The WRS and peak fluid pressure were square-root transformed to normalize residuals. Sundaram, et al, showed that peak fluid pressure and slip risk increase with increased WRS (2020). Therefore, one-tailed analyses were used for all models such that increasing WRS would be associated with increasing peak fluid pressures and increasing slip risk. All statistical analyses were determined prior to performing the tests. Two statistical software packages were used to perform the analyses; models including peak fluid pressure utilized JMP (JMP, SAS Corp., NC) and models including slip outcome utilized Stata/SE (Stata/SE 15, StataCorp, College Station, TX).

Table 6.1 Statistical Models

A total of 12 models (each cell is a different model) were used with two dependent variables: peak fluid pressure and slip outcome, and two independent variables: WRS (separated by selection type (automated/manual) and angle (7°/17°)) and RCOF. The models involving peak fluid pressure used a linear regression approach. The models involving slip outcome without RCOF used a univariate logistic regression approach. The models involving slip outcome with RCOF used a multivariate logistic regression approach.

	Dependent Variable	
Independent Variable(s)	**Peak Fluid Pressure**	**Slip Outcome**
	WRS (*Automated, 7º*)	WRS (*Automated, 7º*)
	WRS (*Automated, 17º*)	WRS (*Automated, 17º*)
	WRS (*Manual, 7º*)	WRS (*Manual, 7º*)
	WRS (*Manual, 17º*)	WRS (*Manual, 17º*)
		WRS (*Automated, 7º*) x RCOF
		WRS (*Automated, 17º*) x RCOF
		WRS (*Manual, 7º*) x RCOF
		WRS (*Manual, 17º*) x RCOF

6.6.4 Results

The WRS across all shoes ranged from 1-2762 mm^2 (Table 6.2). The automated values ranged from 1-2762 mm^2 and 2-866 mm^2 for 7° and 17°, respectively. The manual values ranged from 1-1006 mm^2 and 2-535 mm^2 for 7° and 17°, respectively. Nineteen individuals slipped according to the cutoff variable of slip outcome. Of these shoes, the measured WRS ranged from 7-2762 mm^2 across both angles and selection types (Table 6.2). The measured WRS across shoes that did not slip ranged from 1-866 mm^2 across both angles and selection types.

Table 6.2 Measured Worn Region Size

The mean (standard deviation) and range (in italics) are shown for the WRS according to the peak fluid pressure analysis and slip outcome analyses (all data). WRS is also shown segregated by slip outcome.

	7°		17°	
Independent Variable	***Automated***	***Manual***	***Automated***	***Manual***
Worn Region Size [mm^2] (peak fluid pressure analysis, n=31)	326 (647) *1-2762*	140 (233) *1-1006*	12 (222) *2-866*	166 (145) *2-535*
Worn Region Size [mm^2] (slip outcome analyses, n=34)	325 (624) *1-2762*	133 (224) *1-1006*	150 (213) *2-866*	117 (140) *2-535*
Slip	423 (636) *7-2762*	215 (275) *7-1006*	187 (205) *11-780*	154 (145) *11-535*
No Slip	200 (606) *1-2372*	30 (34) *1-99*	103 (222) *2-866*	71 (122) *2-456*

Peak fluid pressures ranged from 3-696 kPa with a mean (standard deviation) of 102 (154) kPa. All four of the linear regression models showed a positive correlation between WRS and peak fluid pressure (Table 6.3) (Figure 6.15). The rate of increase of peak fluid pressure with WRS was higher for the models utilizing manual selections.

Table 6.3 Model Statistics

Outcome statistics from the 12 models are shown. One-tailed p-values are shown. Significant values are bolded.

		7°				17°			
		Automated		***Manual***		***Automated***		***Manual***	
Dependent Variable	**Independent Variable(s)**	*statistic*	*p-value*	*statistic*	*p-value*	*statistic*	*p-value*	*statistic*	*p-value*
Peak Fluid Pressure	WRS	$t_{31} = 3.9$	**<.05**	$t_{31} = 6.6$	**<.05**	$t_{31} = 2.6$	**<.05**	$t_{31} = 3.2$	**<.05**
Slip Outcome	WRS	$\chi^2_{(1, n=34)} = 4.5$	**0.038**	$\chi^2_{(1, n=34)} = 10.9$	**0.010**	$\chi^2_{(1, n=34)} = 3.6$	**0.045**	$\chi^2_{(1, n=34)} = 4.9$	0.233
Slip Outcome	WRS	$\chi^2_{(1, n=33)} = 14.0$	0.221	$\chi^2_{(1, n=33)} = 17.3$	**0.032**	$\chi^2_{(1, n=33)} = 14.7$	0.146	$\chi^2_{(1, n=33)} = 14.4$	0.159
	RCOF		**0.005**		**0.019**		**0.017**		**0.019**

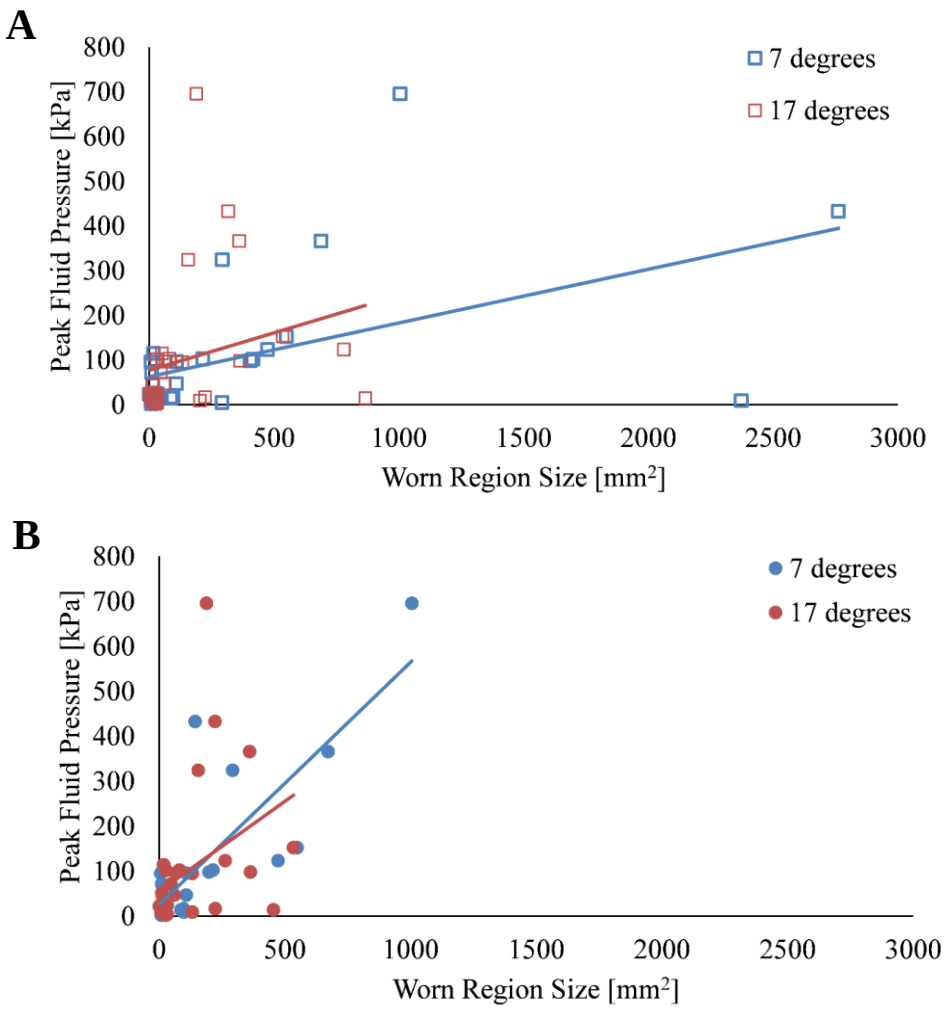

Figure 6.15 Peak Fluid Pressure vs. Worn Region Size

Under-shoe peak fluid pressures during the human slipping study with respect to the A) automated (squares) and B) manual (circles) selections of WRS on the tool

Of the models that included manual selection, the univariate and multivariate logistic regressions at 7° showed that the WRS was able to significantly predict slip outcome ($\chi^2_{(1, n=34)}$ = 10.9, p = 0.010; $\chi^2_{(1, n=33)}$= 17.3, p = 0.032, respectively) (Figure 6.16). Furthermore, the univariate models for automated selection showed that the WRS was able to predict slip outcome for 7° ($\chi^2_{(1, n=34)}$ = 4.5, p = 0.038) and 17° ($\chi^2_{(1, n=34)}$= 3.6, p = 0.045) (Figure 6.17).

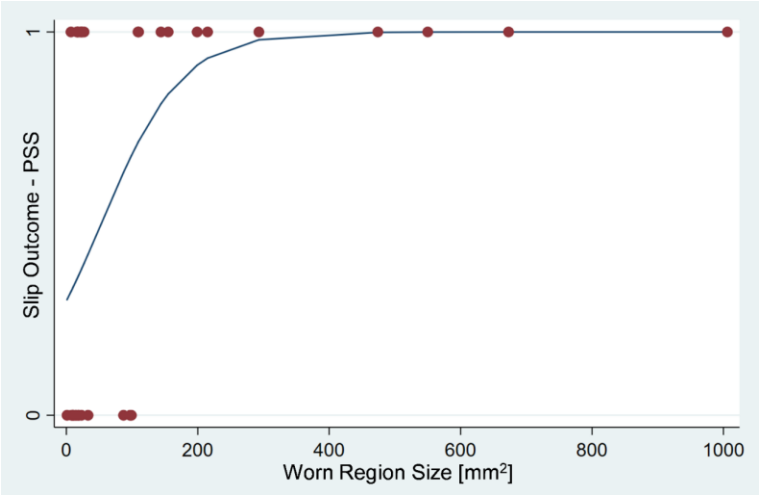

Figure 6.16 Slip Outcome vs. WRS (Manual, 7°)

The manual selection at 7° is shown for the univariate logistic regression.

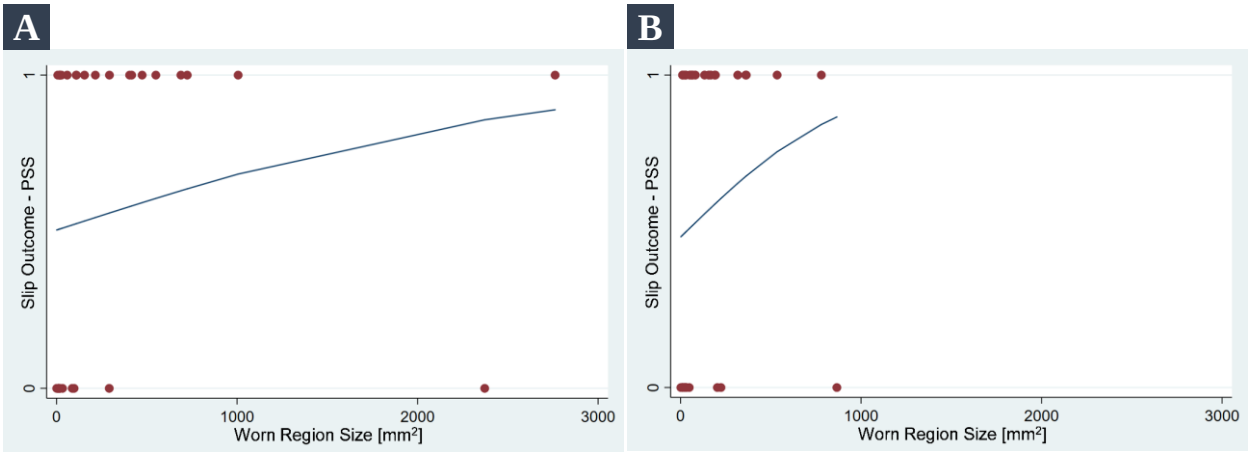

Figure 6.17 Slip Outcome vs. WRS (Automated, 7° and 17°)

The automated selections at A) 7° and B) 17° are shown for the univariate logistic regressions.

6.6.5 Discussion

The validation assessment confirmed that the tool predicted slipping given the measured WRS of the shoe outsole. The tool was most successful with predicting the peak fluid pressures and slip risk at a 7° waveguide tilt.

The development of this tool aligns with previous methods and expands upon previous findings. Previous work found that the size of the worn region is associated with under-shoe fluid pressures and slip severity (Beschorner et al., 2020; Hemler, Charbonneau, et al., 2019; Hemler, Pliner, et al., 2020). This study confirmed these relationships using a tool to objectively measure the worn region. Also, the previously observed trends were confirmed using a different data set from those presented in the preceding chapters. Previous methods that studied the use of a common household item, AA and AAA battery (Beschorner et al., 2020), to assess slip risk were also consistent with the results in this analysis that the continuous worn region could predict under-shoe traction performance. The results showed that a larger WRS is consistent with increased under-shoe fluid pressures, decreased friction, and increased slip severity as shown by the battery test.

Based on these initial findings, this scanner would be a practical tool for reducing slip and fall risk. This tool was tested on SR shoes. However, the variety in tread shape and color tested in this analysis gives a good indication that the tool may work well for non-SR as well. For example, one shoe had multi-colored, marbled tread. The manual image processing technique was able to accurately identify the tread regions in contact for this shoe (Figure 6.18). Furthermore, many of the shoes did not have the typical SR tread patterns of uniform, small tread blocks, but rather some large and long tread blocks. The effective scanning of these shoes provides evidence that shoes with designs atypical to traditional SR shoes may work well on the tool. The slip risk and

associated WRS for the human slipping study (measured using calipers as described in Sections 3.1.3.4 and 3.2.3.3) were compared to the slip risk and associated WRS determined by this aim's analysis. For SR shoes within the human slipping study, slip risks of 50%, 80%, and 95% were associated with worn region sizes of 365 mm^2, 1089 mm^2, and 2342 mm^2, respectively. Within the tool measurement at 7° with manual selection, slip risks of 50%, 80%, and 95% were associated with worn region sizes of 39 mm^2, 136 mm^2, and 331 mm^2, respectively. A slip risk of 80% associated with the tool is just slightly less than the size of an AA battery (165 mm^2) which has been shown to be a good indicator for when to replace shoes to reduce slip risk (Beschorner et al., 2020). Therefore, the threshold for when shoes should be replaced may be set to a slip risk of 80% and corresponding size of 136 mm^2 for the tool.

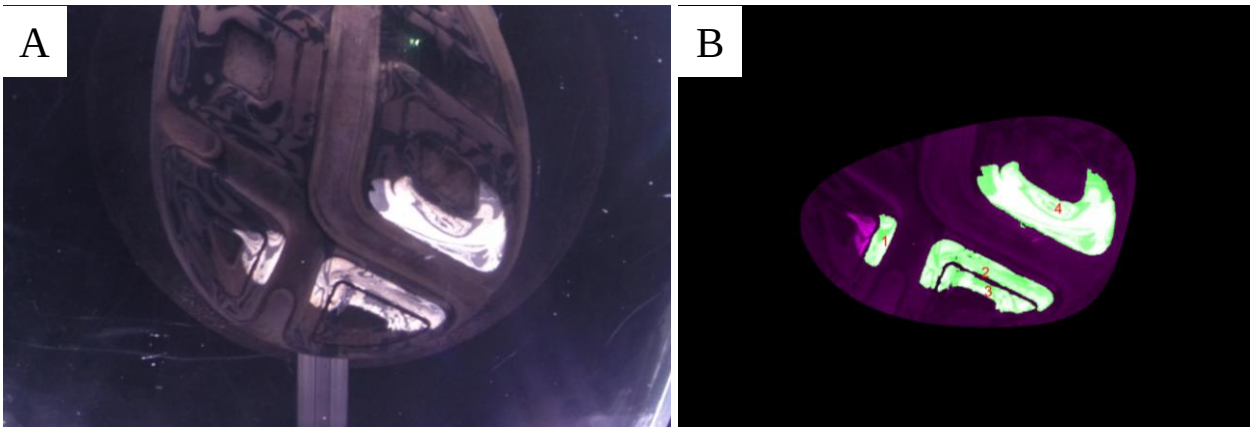

Figure 6.18 Shoe Scan – Multi-Colored Tread

A) Raw scan on tool of shoe with white and black, marbled tread at 17°. B) Image processing of contact region detection using automated selection. Bright white and green tread indicate four largest contact regions detected within image processing.

Thresholds for wear may be dependent on the tool used to define the WRS. The tool in this study generally identified worn region sizes that were smaller than the entire continuous worn region on the shoe as identified in the human slipping study. For example, the manual selection measurements at 7° were an average (standard deviation) of 21.5% (20.6%) of the WRS measured

on the shoe outsole in the human slipping study (range = 0.8-89% of the measured size). However, both the tool and human slipping study accurately predicted slip risk based on their measured WRS. Therefore, it is important to note that these two methods of measuring the WRS – the tool or from calipers as in the human slipping study – may provide different slip risk thresholds that are accurate within each respective method.

Certain limitations of the tool should be considered. The camera used in the prototypes had a color-correcting function that resulted in the scans appearing to have one of three filter shades – black, blue, or purple. The filter associated with the blue color did not contrast well with black tread. Therefore, five of the eight images that were reprocessed using manual selection due to a lack of contrast in the automated selection showed the blue filter. A camera with consistent image coloring would eliminate this limitation. Furthermore, four shoes had fine surface texturing that may have inhibited detection of the worn region as one continuous area. However, these shoes were not outliers within the models which suggests the texturing does not affect the accuracy of the model. Lastly, as the shoes were loaded on the scanner, angles along the frontal plane of the shoe (inversion/eversion) were applied to best capture the largest region of wear at the specified sagittal plane angle of 7° or 17°. Due to the constraints of the apparatus, however, the largest worn region could not always be fully captured. As such, future work may develop a method to capture the worn regions across the heel portion or entire outsole of the shoe.

6.7 User Feedback Assessment – Experimental Questionnaire (Objective 3.2)

6.7.1 Assessment Approach

A user feedback assessment was developed to evaluate the user-centered design (UCD) principles of the scanner. Specifically, the objective of this assessment was to achieve a user approval score equal to or greater than 80% based on tool usability, usefulness, and desirability (UUD). The assessment consisted of an eligibility screening, scanner demonstration video, and questionnaire. Participants were eligible if they were 18 years old or older, had worked in the service industry (e.g., restaurant) since January 2020, and were available for a 20-minute online session (full eligibility screening within Appendix C.2.1). If the participant was eligible, they were presented with a short video (< 3 minutes) which was used to describe the purpose of the study and give participants a demonstration of how to use the scanner. The video demonstration was available during the questionnaire so participants could refer to the demonstration at any time. The assessment was approved as an exempt study by the University of Pittsburgh Institutional Review Board.

6.7.2 Questionnaire

After confirming eligibility and watching the demonstration video, participants were asked to complete a questionnaire that assessed the usefulness, usability, and desirability of the scanner. The questionnaire was separated into three parts: Usability, Usefulness, and Desirability (full questionnaire in Appendix C.2.2). Within the usability section, questions focused on how the scanner would be used and how well it would integrate into the work schedule (e.g., ‘the

instructions were clear and I know how to use the scanner'). The usefulness section asked questions to gauge how valuable the scanner and output were to the participant (e.g., 'I feel it is important to know when to replace my shoes'). The desirability section addressed the aesthetics of the scanner (e.g., 'the overall size of the scanner is good'). A section was then available for free-form responses followed by participant information including age, sex, type of service facility, length of employment, position worked, and if they regularly wear SR shoes. The questions followed a 5-point response scale with the following descriptions and corresponding number of points for each response: (1) Strongly disagree, (2) Somewhat disagree, (3) Neither agree nor disagree, (4) Somewhat agree, and (5) Strongly agree. The average of the approval scores across the 14 questions was multiplied by 0.2 to acquire the approval rating (max 100%).

6.7.3 Results

Eleven participants started and seven participants completed the assessment. The completed responses are included in this analysis. The participants (3 male, 4 female; average ± standard deviation age: 24.5 ± 4.0 – one participant's age was unknown) all worked in the food service industry (e.g., barista, food runner, restaurant manager) for an average ± standard deviation of 7.7 ± 7.6 years. Four of the participants reported regularly wearing SR shoes, one reported that they wore SR shoes sometimes, and two reported not wearing SR shoes. Overall, the scanner received an average approval score of 3.9 (out of 5) with a standard deviation of 1.2 (Table 6.4). This score corresponds to an approval rating of 78% which is just below the target rating of 80%. There were three questions, one from each section, which received scores less than 4 on average (questions 4, 10, and 13). The usability, usefulness, and desirability sections received average scores of 4.1, 4.1, and 3.4, respectively.

Four of the participants offered suggestions for improvement. Participant #1 suggested implementing a support bar near the scanner to make it safer. Participant #3 stated, “The quicker it is to use, the more likely people are to check on a regular basis”. Participant #4 suggested adding marking on the device to help with correct shoe placement on the waveguide. Lastly, Participant #5 who works at a “fast-paced coffee shop” said “the scanner is very easy to use”, but they did not know how often they would be able to use it.

Table 6.4 Questionnaire Results

Results from discussion are separated by UUD section. The average score across all participants is shown for each question and by section. Average scores less than 4 are bolded signifying an approval of less than 80% for that question.

No.	Section	Question	Average score	Score standard deviation	Score within section
1	Usability	The instructions were clear and I know how to use the scanner.	4.9	0.4	4.1
2		I believe I would feel safe standing on the scanner without additional support (besides the support box for the other foot).	4.1	1.5	
3		The time it would take to use the scanner (~5 minutes) is reasonable.	4.1	1.1	
4		The time it takes to use the scanner would fit well into my work schedule daily	**2.0**	1.0	
5		The time it takes to use the scanner would fit well into my work schedule once a week	4.0	1.2	
6		The time it takes to use the scanner would fit well into my work schedule once a month	4.7	0.5	
7		The time it takes to use the scanner would fit well into my work schedule once every 3 months	4.9	0.4	
8	Usefulness	I feel that is it important to know when to replace my shoes.	4.0	0.0	4.1
9		Rate the scanner recommendations (good, replace soon, replace now) *	4.3	0.8	
10		If I do not receive money from my employment for new shoes, I would pay out-of-pocket to replace my shoes if I received a 'replace now' indication.	**3.0**	1.3	
11		The lights/shapes to recommend replacement are easy to understand	5	0	
12	Desirability	The overall size of the scanner is good.	4.0	0.6	3.4
13		The look of the scanner is important to me.	**2.3**	1.4	
14		I would use the scanner to know that my shoes are safe.	4.0	1.2	
			3.9	1.2	

*Response options were (1) Not at all useful, (2) Slightly useful, (3) Moderately useful, (4) Very useful, (5) Extremely useful

6.7.4 Discussion

The results show that the tool received an approval rating of 78% which just undershoots the targeted goal of 80%. Eleven questions across the three sections received approval scores of 4 or higher. Therefore, three questions – one in each section – were responsible for the low rating with individual scores below 4.

The structure and results of the assessment are consistent with previous research. UCD and specifically UUD approaches were used to gather user feedback consistent with previous research techniques (ISO, 2019; Sanders, 1992). The UUD questions within the questionnaire used simple language and scoring, and there was space for participants to give open-ended feedback. Furthermore, the video demonstration followed UCD practices by using written words and verbal communication along with images and graphics (Unnava & Burnkrant, 1991). The quantitative responses to the questions give useful information for areas to improve the scanner. For example, questions 4-7 give proposed timeframes for which the scanner could be used. The scores from these questions give quantifiable data from which recommendations for use frequency could be derived. Furthermore, the qualitative responses provide valuable recommendations for implementation improvements.

The rating fell below the proposed objective goal for several reasons. Questions 4, 10, and 13 were responsible for achieving a score below 80%. Results from question 4 (usability section) indicated that participants did not feel that the scanner would fit well in their daily schedule. This information is useful for indicating that such a device may work better if used within the other 3 timeframes presented (i.e., once a week, month, or every 3 months) which all received scores equal to or higher than 4. Furthermore, this question's score is supported by free-form responses from Participant 3 and 5 which suggested that a tool that is quicker to use is more likely to be used more

often. Question 10 inquired of the importance of a ‘replace now’ indication; participants indicated that if they did not receive money from their employer to replace their shoes, they would be less likely to spend money out-of-pocket. Given the importance of replacing shoes to prevent slip-risk, these findings support the importance of employer subsidization of footwear costs which aligns with past research (Bell et al., 2018). Question 13 did not give useful information regarding the scanner itself, but rather the importance of aesthetics to the overall use. This question did not necessarily imply a good or poor approval rating of the tool itself. As such, when disregarding the score of this question, the overall approval score increased to 4.1 which corresponds to an approval rating of 82%, exceeding the objective threshold.

There are a few limitations that should be acknowledged for this analysis. Only seven participants were able to complete the assessment. A larger sample size would give more generalizable results, though the low standard deviation across the questions (range 0-1.5) supports that these responses may be common responses from food service employees. Furthermore, due to restrictions from the COVID-19 pandemic, participants were not able to use and assess the scanner in person which would have allowed for more thorough feedback. However, the online approach allowed for a faster turnaround for results and more standardized presentation of the assessment compared to in-person testing.

Overall, the user feedback assessment gave valuable feedback for future iterations of the scanner. The scores from each section show that the scanner is usable and useful. By re-evaluating and disregarding question 13, the scanner is desirable to potential users as well. Future iterations of the scanner may seek to expedite the scanning process, specify an appropriate frequency of use, decrease ambiguity of foot placement, and perhaps provide additional support via a bar to improve user safety and balance confidence.

6.8 Conclusions & Future Work

The scanner was able to accurately determine the size of the shoe tread in contact with the waveguide, achieved an acceptable user feedback score, and was able to predict under-shoe peak fluid pressures and slip outcome. This tool has potential to act as a good indicator for when shoes should be replaced.

This tool has potential through future development to be used to prevent slip and fall accidents. As the original human slipping study combined SR and non-SR shoes to find that the worn region size predicted slip risk, future work may include assessing the tool's accuracy at predicting slips for non-SR shoes, starting with the non-SR shoes from the human slipping study. Two improvements could be made to eliminate user interaction during image processing: 1) the waveguide could be covered except for a designated region such that cropping the image within the image processing technique would become unnecessary, and 2) an algorithm could be used to measure and control for the color of the tread. The first improvement also aligns with feedback from Participant #4 which suggested making it easier for the user to know where to place the foot during testing. The information from the user feedback assessment as well as the limiting features addressed in this prototype provide a thorough basis for future prototype iterations.

7.0 Conclusion & Future Vision

In this section, the conclusion of this dissertation work and potential future directions are discussed. This section may be of particular value to slip and fall prevention strategists, footwear companies and designers, and researchers examining the impact of footwear on reducing slips and falls in the workplace.

7.1 Finding Implications

7.1.1 Key Points

This dissertation identified several key points that will be discussed in this chapter. Given the importance of UCD practices in effectively relaying information, the following summary will follow UCD practices by using a graphic with some or no wording for each key point. The key points are listed below with graphic and elaboration in the following sections:

1. Traction performance measurements at baseline are insufficient for assessing long-term safety of footwear.
2. Hydrodynamic modeling and specifically, the application of the tapered-wedge bearing solution offers a valid, theory-based approach to assess slip risk of worn footwear.
3. Worn region size (WRS) is a valuable indicator for traction performance.
4. Shoes should be designed with wear in mind with a goal to slow the growth of the WRS.
5. RCOF can indicate wear rate and may be useful for targeting shoe distribution and design.
6. Hardness does not indicate wear rate and may be more useful for other design elements.
7. The developed scanner identifies WRS and predicts slipping.
8. Increased awareness of shoe tread condition and policy change is needed. Current shoes should be replaced more often than is recommended.
9. UCD practices are essential for effective product development.

7.1.1.1 Point 1 – Traction performance & long-term safety

Traction performance measurements at baseline are insufficient for assessing long-term safety of footwear.

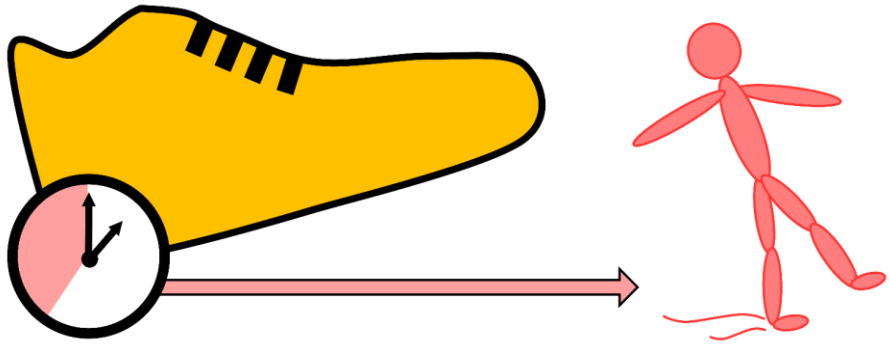

Figure 7.1 Point 1 – Traction performance & long-term safety

Traction performance changes with shoe outsole wear.

This research mapped shoe-floor traction performance with progressive wear which informs slip risk that is associated with increased wear. Previous research has focused on shoe friction and fluid drainage at new or completely worn stages. This research fills the gap to understand how a shoe's ability to prevent a slip via under-shoe friction and fluid drainage changes over time. Research in Aim 1 showed that as shoes become worn artificially and naturally, there may be a slight increase in ACOF followed by steadily decreasing ACOF. Fluid drainage was quantified via fluid force (decreased fluid drainage is associated with increased fluid force) that generally increased from baseline as tread became worn. Both the steady decrease in ACOF and increase in fluid force show that shoes do not perform as well when worn as when new. These effects were progressively seen as the distance shoes were worn and time spent using the shoes increased. Therefore, there need to be metrics to assess footwear traction performance at multiple wear stages, especially during the footwear design process. Furthermore, it would be beneficial for footwear manufacturers who present information on shoe traction performance in the new

condition to also provide footwear monitoring instructions so that users know when that performance data no longer applies to their shoes. A potential metric of worn region size is discussed in Section 7.1.1.3 - Point 3.

7.1.1.2 Point 2 – Hydrodynamic modeling to assess slip risk

Hydrodynamic modeling and specifically, the application of the tapered-wedge bearing solution offers a valid, theory-based approach to assess slip risk of worn footwear.

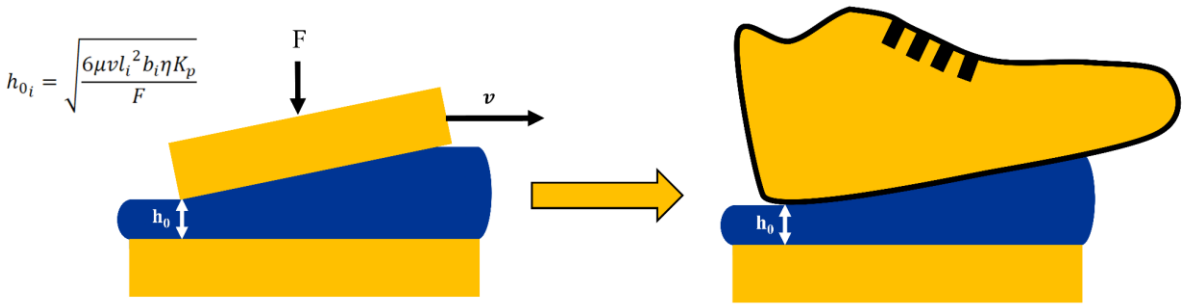

Figure 7.2 Point 2 – Hydrodynamic modeling to assess slip risk

The tapered-wedge bearing solution can be applied to footwear to understand under-shoe hydrodynamics changes with wear.

Sections 3.2 and 4.1.3.5 within Aim 1 showed that the tapered-wedge bearing solution can be used to explain under-shoe hydrodynamics. Specifically, this model applied the shoe worn region dimensions as the size of the wedge to determine the predicted film thickness between the shoe and the contaminated flooring. This application indicated that the predicted film thickness is positively correlated with the measured under-shoe fluid force. This finding gives unique insight regarding how progressively worn shoe outsole geometry can be used to predict under-shoe hydrodynamics.

7.1.1.3 Point 3 – Value of worn region size

Worn region size (WRS) is a valuable indicator for traction performance.

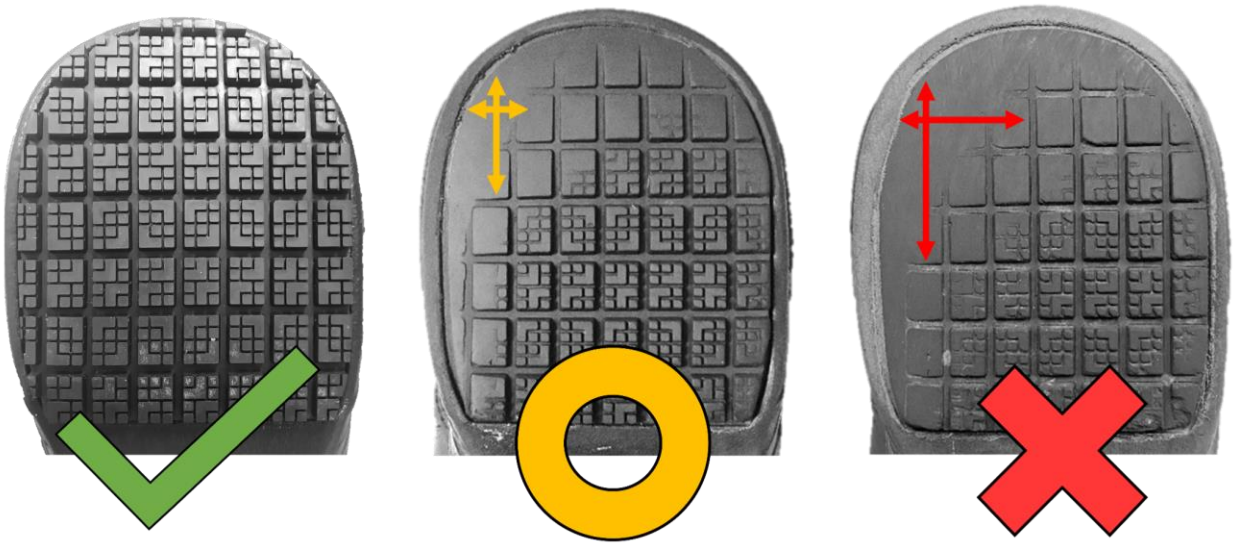

Figure 7.3 Point 3 – Value of worn region size

Worn Region Size Indications: (Left) The completely intact tread and green check mark indicate the shoe is effective in protecting from a potential slip. (Middle) The slightly worn shoe and yellow 'O' indicate that the shoe is becoming worn and should be considered being replaced soon. (Right) The more severely worn shoe and red 'X' indicate that the shoe has become too worn and should be replaced as soon as possible.

Results presented in this dissertation supported the use of WRS as a valid metric for determining loss in traction performance due to wear (confirmed in accelerated worn shoes, modeling of worn shoes, and naturally worn shoes). However, the methods used to capture WRS evolved throughout the research leading to some discrepancies across the studies regarding the thresholds of WRS that necessitate replacement. Results from the accelerated wear procedure in Aim 1 revealed that a WRS of 800 mm^2 was an appropriate estimate at which to replace shoes. This estimate was obtained using the caliper (length/width measurement and multiplication) technique. In Aim 3, the WRS was detected using the portable scanner. This imaging technique showed that WRSs of 136 mm^2 and 331 mm^2 were associated with slip risks of 80% and 95%,

respectively. One reason for the lower threshold in Aim 3 is because the imaging technique could not detect the entire WRS, but rather the portion of the WRS that was in contact of the portable scanner. Another reason may have been that the caliper method assumed a rectangular worn region, while the scanner measured the true area of the worn region regardless of its shape. While the exact threshold varied across studies, this research produced consistent evidence that the WRS contributes to a decrease in traction performance and an increase in slip risk. Therefore, future recommendations for shoe replacement may need to further refine the method of measuring the WRS. Parallel work to this dissertation used a common ergonomic tool – a AA and AAA battery – against the WRS to accurately determine slip risk (Beschorner et al., 2020). Notably, the AA battery (surface area = 165 mm^2) has an area that fell within the range of WRS associated with a loss in traction performance observed in Aim 3.

7.1.1.4 Point 4 – Worn region size consideration for shoe design

Shoes should be designed with wear in mind with a goal to slow the growth of the WRS.

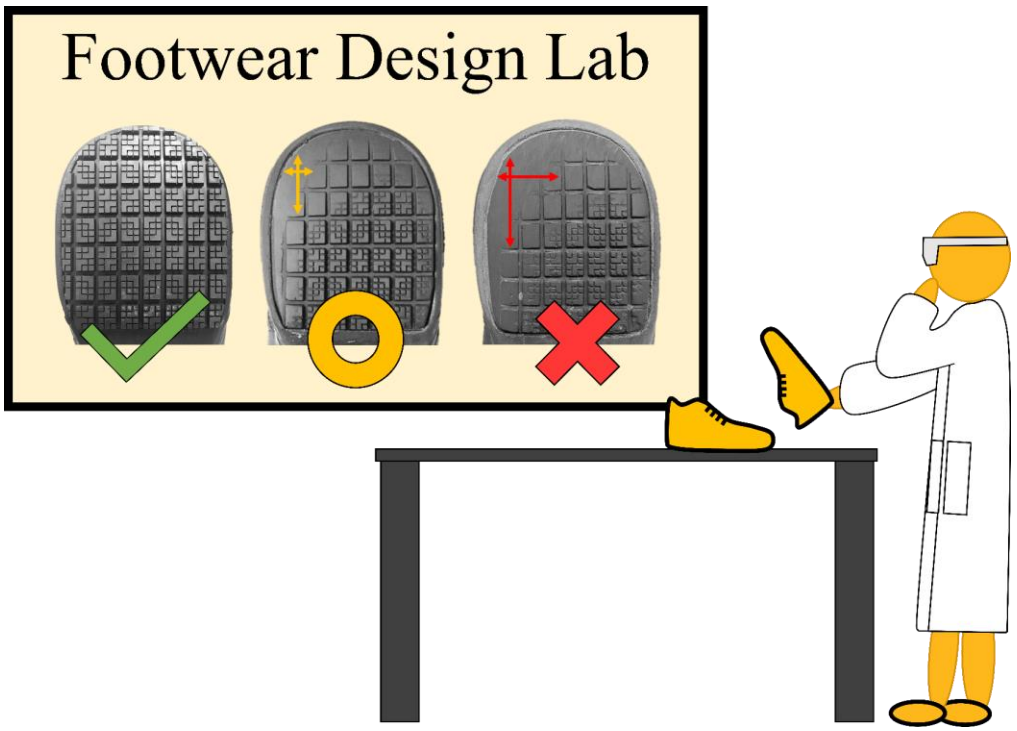

Figure 7.4 Point 4 – Worn region size consideration for shoe design

Shoes can be designed to slow the growth of the WRS.

The WRS growth is an important aspect of determining slip risk. Footwear, especially SR shoes, should be designed to reduce the speed at which the WRS grows. This could be done practically by varying the tread depth of adjacent treads to allow for channels to be present even with normal wear. Furthermore, results in Aim 1 found that higher tread proportions led to slower wear on shoes. Therefore, shoes with increased tread proportion may help to minimize the speed at which the worn region grows.

The size of tread blocks is an important factor for traction performance. Patterns consisting of small tread blocks – as is customary of SR shoes – have increased fluid drainage ability (Hemler, Sundaram, et al., 2020). Alternatively, shoes with large tread blocks (lugs) on the rear of the shoes as seen with shoes I and J in Aim 2 (Section 5.2) have been found to have high initial under-shoe

fluid pressures even though the risk of slipping due to ACOF measurements was low when new (Walter et al., 2021). Therefore, work boots should consider alternative designs that break up the large lug designs and allow for fluid dispersion under the shoe even if ACOF testing passes current standards when new.

7.1.1.5 Point 5 – RCOF & wear rate indication

RCOF can indicate wear rate and may be useful for targeting shoe distribution and design.

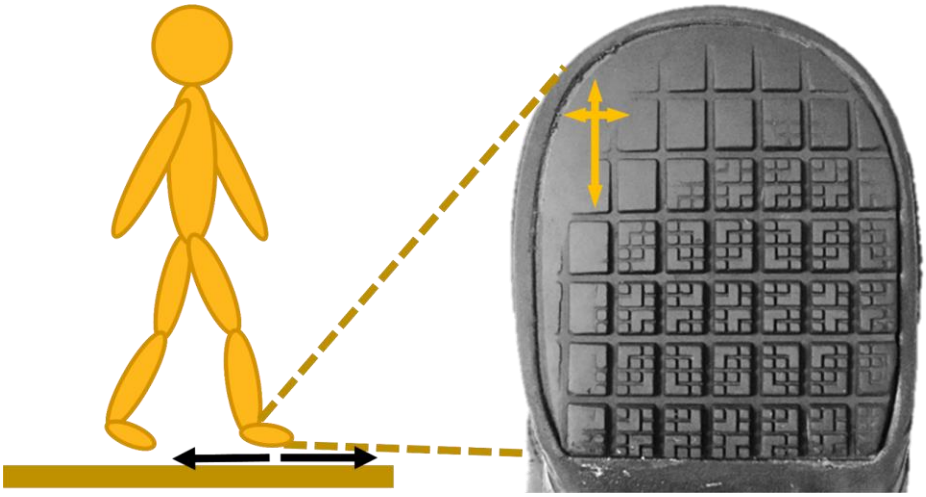

Figure 7.5 Point 5 – RCOF & wear rate indication

This research added to the knowledge that slips and falls are impacted by an individual's RCOF. Previous work has shown that a higher RCOF is linked to increased risk of slipping (Beschorner et al., 2016). This work showed that higher RCOF is also linked to increased shoe wear rate which leads to increased slip risk.

Footwear design could be carefully constructed to accommodate ranges of RCOF. For example, individuals with a higher RCOF, signifying a faster wear rate, may be safer from slips and falls with footwear tread designs that emphasize durability. On the other hand, individuals with lower RCOF signifying a slower wear rate may be safer from slips and falls with footwear

tread designs that emphasize higher friction and fluid dispersion capabilities when newer. The development of inexpensive methods for calculating RCOF may improve shoe selection for individuals. Therefore, the development of various tread designs considering RCOF implications accompanied by the development of inexpensive methods for calculating RCOF will reduce shoe wear which reduces slip risk, but will consequently improve individual shoe tread knowledge and awareness (as discussed in Point 8).

7.1.1.6 Point 6 – Hardness did not indicate wear rate

Hardness does not indicate wear rate and may be more useful for other design elements.

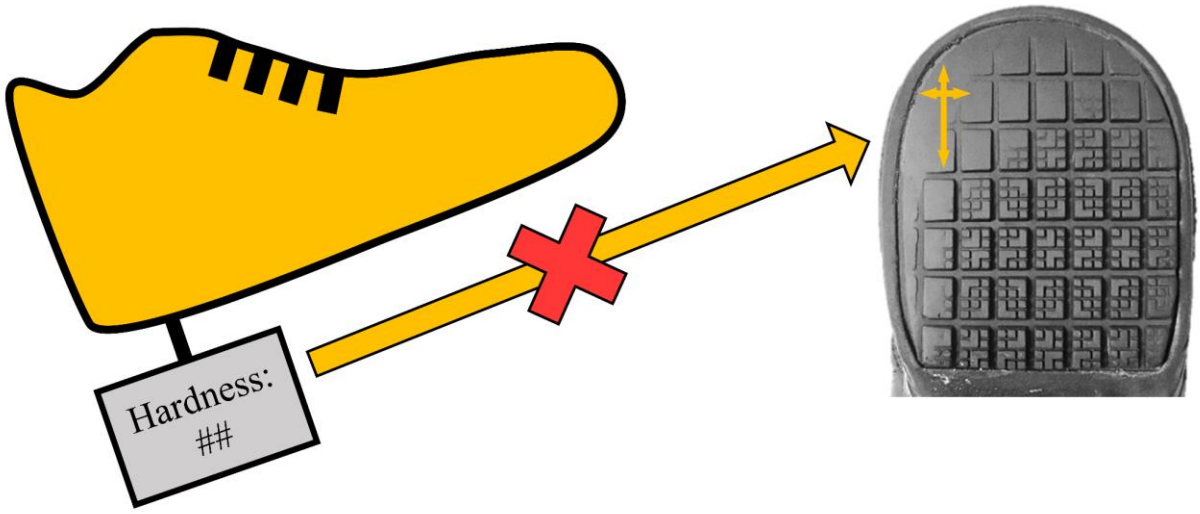

Figure 7.6 Point 6 – Hardness did not indicate wear rate

The footwear design analysis within Aim 2 showed that shoe tread material hardness did not affect shoe tread wear rate across multiple shoe designs and across natural and simulated wear. Therefore, hardness may not be an important factor for how fast or slow tread wears down. However, previous work has shown that hardness is an important factor for slip initiation in young adults (Tsai & Powers, 2008). Footwear companies that are interested in reducing slip and fall occurrence via footwear design may lower shoe hardness within an acceptable range to reduce slip

likelihood. Furthermore, previous research has found that certain outsole materials may decrease slip likelihood (Yamaguchi & Hokkirigawa, 2014; Yamaguchi et al., 2012). In addition to reducing slip likelihood from outsole material innovation, footwear companies may explore using materials that are more resistant to abrasion to reduce wear rate.

7.1.1.7 Point 7 – Benefit of the scanner

The developed scanner identifies WRS and predicts slipping.

Figure 7.7 Point 7 – Benefit of the scanner

The scanner accurately identifies WRS & predicts slipping.

The scanner was verified to measure tread block size with moderate accuracy and was subsequently validated to predict slip risk from the scanned WRS. The WRS best predicted slip risk when measured at a waveguide angle (angle between shoe and scanner surface) of 7°. The scanner was able to measure the WRS for SR shoes with varied tread shape, size, and color. Some of the scanned shoes possessed outsole tread atypical to the conventional SR patterns of uniform, small tread blocks which suggests that the scanner would also work on non-SR shoes. Furthermore, the results of this research found that a slip risk of 80% on the scanner corresponded with a WRS of 136 mm^2 which is just slightly less than the WRS detected by a different tool that recommended

replacement (Beschorner et al., 2020). As such, the scanner provides a practical, verified, and validated tool for identifying shoe outsole WRS and recommending replacement.

7.1.1.8 Point 8 – Shoe tread condition awareness

Increased awareness of shoe tread condition and policy change is needed. Current shoes should be replaced more often than is recommended.

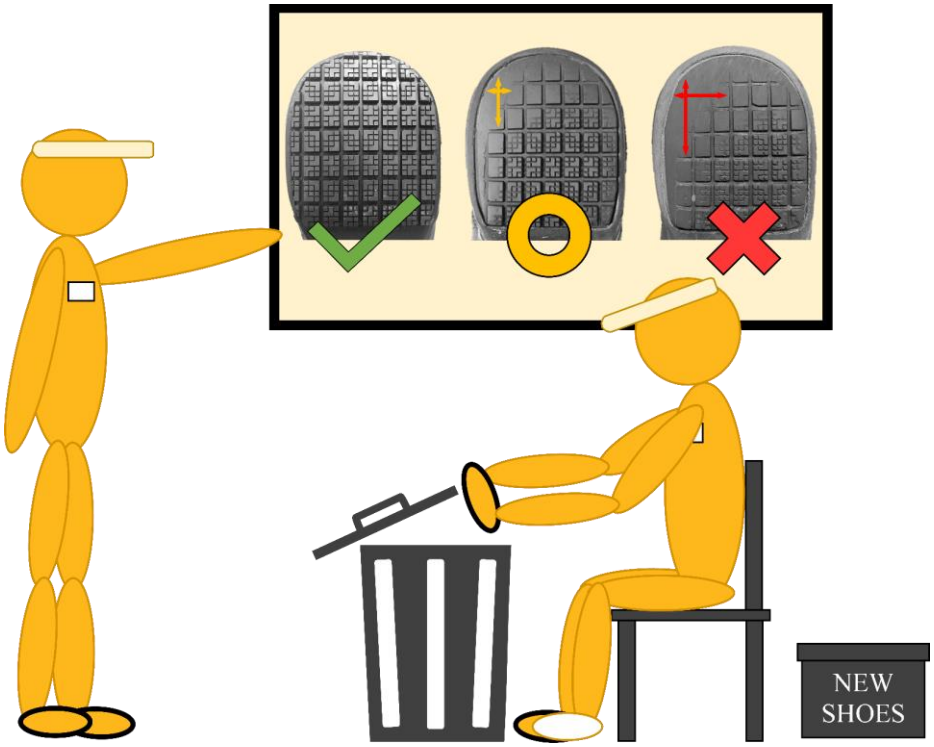

Figure 7.8 Point 8 – Shoe tread condition awareness

Increased safety awareness of shoe condition and policy change is needed.

The SME interviews and the user feedback assessment revealed important aspects of developing a usable, useful, and desirable shoe tread monitoring tool. Overall, Aim 3 showed that involving the potential user in the design process made the product designer aware of information that may have been overlooked otherwise. For example, one SME stated that if it is not a requirement to use a workplace tool, then it will not be used (Manager of Fast Food Restaurant B

& C - SME #2, 2020). Furthermore, Question 10 from the user feedback assessment showed that employees are less likely to replace their shoes after they have been told that the condition of their shoes was unsatisfactory if they had to pay for the shoes with their own money. These responses gave insight into the importance of involving workplace managers and providing funding for intervention programs.

This dissertation informs some recommendations for shoe tread awareness and workplace policy changes:

1. This research supports previous work that has shown that SR shoes are important for reducing slips and falls in the workplace. Therefore, workplaces that do not already require the use of SR shoes should consider implementing this requirement for worker safety.
2. The SME interviews showed that, of the small sample size, knowledge about the importance of shoe tread was minimal. SR shoes have small tread blocks that increase friction and fluid drainage capacity. Footwear companies may consider strategically providing this and other information on the shoe box or other marketing materials to improve customer shoe knowledge and buy-in.
3. This research showed that policies that supply incentive or funding for shoe replacements may help employees to replace shoes more often and in turn, keep employees safer. Previous work has shown that shoe replacement programs in which employers pay for new shoes have been effective for reducing slips and falls in the workplace (Bell et al., 2018). Employers could implement similar programs and also use a tool such as the proposed scanner in Aim 3 so that employees would be encouraged to check the condition of their shoes. If the condition is unsatisfactory, the employer should supply incentive or funding to replace their shoes. Presumably, at least some of the cost of such programs would be offset by reducing the

occurrence of slips and falls. However, future research would need to perform return on investment analyses to assess the economics of such an intervention.

4. Current standards for shoe replacement rely on time the shoes are used or distance walked. This research shows that the size of the worn region is a better indicator. As such, some of this data collected for this dissertation informed two posters (one for food service and one for healthcare) generated by the National Occupational Research Agenda (NORA) (National Occupational Research Agenda (NORA) Traumatic Injury Prevention Cross-Sector Council, 2021). These posters share the technique and goal behind using a simple ergonomic tool of a battery against the worn region of the shoe outsole (Beschorner et al., 2020). Similar media such as these posters may be beneficial for increasing awareness of shoe wear and the dangers associated. They may consequently reduce slip and fall injuries when employees replace their shoes in a timely manner.

7.1.1.9 Point 9 – Effectiveness of UCD

UCD practices are essential for effective product development.

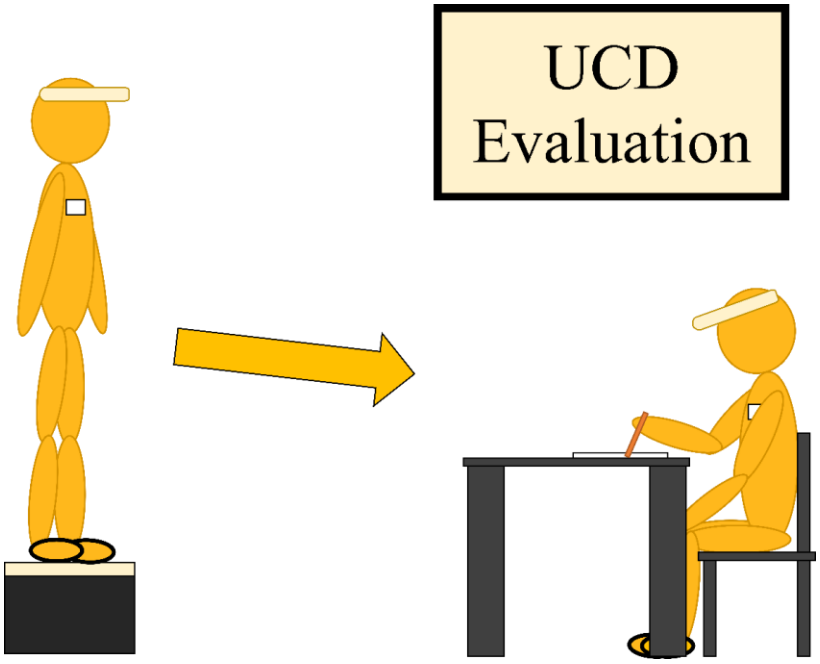

Figure 7.9 Point 9 – Effectiveness of UCD

Implementing UCD practices is essential for effective product develoment.

This research showed that eliciting the potential user of a product is important for development. One SME stated that they had tried to use an existing tool that tracked shoe tread depth which could be used to recommend replacement (Manager of Fast Food Restaurant A - SME #3, 2020; Shoes For Crews, 2019a). However, the SME expressed confusion as to how and where to apply the tread depth gauge. The SMEs confusion is consistent with work in Section 3.1 which showed that once a worn region starts to form, the minimum tread depth goes to zero. Therefore, there is ambiguity as to where to apply the tread depth tool after the worn region has formed. Involving UCD practices for the development of this tool across the life of the shoe may have mitigated this confusion and led to a more understandable wear gauge that takes shoe wear into

account. Overall, engaging with the potential users of a product is important to understand and mitigate possible pitfalls.

Product design and customizing the intended use would benefit from UCD practices. Results from Aim 3 indicate that involving the potential user in the product design process is beneficial. Furthermore, one SME stated that the potential scanner they were shown would need to be placed in an "easily tangible" location for use (Team Member of Full Service Restaurant A and Grocery Store A - SME #4, 2020). This knowledge is valuable to show that the product design should then be completely portable to be able to accommodate a variety of workplace settings. Additionally, conducting further research to determine the best way to advertise intervention tools such as the one presented in Aim 3 would increase tool use.

7.1.2 Mechanistic Model Overview

The work in this dissertation provided answers to the mechanistic model first proposed in Section 2.5. Aims 1 and 3 showed that increased footwear usage led to increased slip risk. Specifically, the pathway of increased footwear usage to increased tread wear was mediated by peak shear forces and RCOF, but not by peak normal force or outsole hardness as shown in Aim 2. The increased tread wear led to the formation of a worn region as seen in Aims 1 and 3. This increased worn region size indicated decreased ACOF which has been shown to lead to increased under-shoe fluid pressures as supported in Aim 1. Work in Aim 3 supports previous work that found that increased worn region formation is indicative of slip risk.

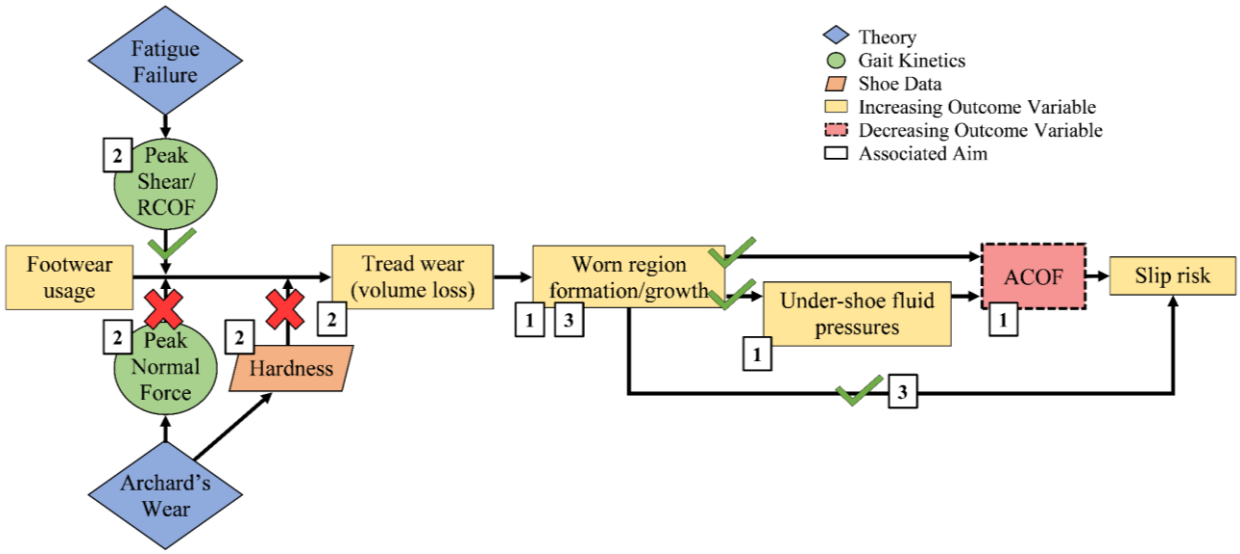

Figure 7.10 Mechanistic Model with Implemented Findings

Pathways with check marks indicate that research proved the pathway to be valid. Pathways with 'X' marks indicate that the research proved the pathway to be invalid.

7.2 The Future of the Scanner

The scanner presented in Aim 3 has potential to effectively inform timely shoe replacement, as briefly mentioned in Section 6.8. This dissertation shows the success of the scanner to predict slip risk based on shoe outsole wear. Given this success, future iterations of the scanner could streamline the process of scanning the shoes and providing a slip risk metric (i.e., the replacement recommendations presented in previous sections). Furthermore, future versions could incorporate a digital display to create and save user profiles. Adding a user profile option could enable employers to track employees' progressive shoe wear to provide timely shoe replacement.

The inexpensive nature of the scanner could be optimized even further. The materials for the scanner cost less than $200 which is less than 2% of a single fall (Washington State Department

of Labor & Industries, 2020). Future tools may be able to reduce that cost more and provide a portable power source making the scanner portable. A portable scanner would allow for companies with diverse floorplans to use the scanner wherever is best suited for the employees. Furthermore, using a more durable waveguide that does not get scratched easily would improve the long-term durability of the scanner.

Given the success of FTIR technology in the scanner, the technology has great potential for success in other applications of footwear- and foot-floor contact. For example, such technology could be applied in dynamic settings to understand the shoe-floor contact of a variety of footwear and individuals. Furthermore, this scanner and technology could be expanded to inform athletes of the most appropriate footwear according to their anatomical structure and foot-floor contact (e.g., RCOF measurements, medial lateral foot contact measurements).

Overall, the scanner has great potential to impact many fields. The food service and safety industries may benefit from reduced occurrences of slips and falls. The footwear industry may benefit from increased understanding of shoe-floor contact and opportunity for improved detection of individual shoe-floor interactions which could be applied in retail stores. Lastly, the technology industry may benefit from another optics technology with broad implications.

Appendix A Progressive Accelerated Wear – Changes in and Application of Traction Performance and Geometry

Appendix A.1 Copyright Permission

Appendix A.1.1 Section 3.1 – Accelerated Shoe Wear

This section was published as “Changes in under-shoe traction and fluid drainage for progressively worn shoe tread” in Applied Ergonomics, 80, Hemler, S.L., Charbonneau, D.N., Iraqi, A., Redfern, M.S., Haight, J.M., Moyer, B.E., & Beschorner, K.E., pg 35-42, Copyright Elsevier (2019).

Appendix A.1.2 Section 3.2 – Shoe Wear Geometry Predicts Under-Shoe Hydrodynamics

This section was published as “Predicting hydrodynamic conditions under worn shoes using the tapered-wedge solution of Reynolds equation” in Tribology International, 145, Hemler, S.L., Charbonneau, D.N., & Beschorner, K.E., Copyright Elsevier (2020).

Appendix B Impact of Gait Kinetics and Shoe Outsole Hardness on Wear

Appendix B.1.1 Section 5.1 – Gait Kinetics

This section was published as “Gait Kinetics Impact Shoe Tread Wear Rate” in Gait & Posture, 86, Hemler, S.L., Sider, J.R., Redfern, M.S., & Beschorner, K.E., 157-161, Copyright Elsevier (2021).

Appendix C Development of a Tool to Assess Outsole Worn Region Size and Determine Slip Risk

Appendix C.1 SME Interview Guide

Intro: Thank you for taking time for me to interview you. I am a researcher at the Human Movement and Balance Lab at the University of Pittsburgh and my goal is to determine factors that contribute to slips and falls in the workplace to develop strategies for preventing slips and falls. The goal of this interview is to get your perspective as the expert in your field, so I will ask you questions regarding your workplace activities and ask for your input on potential slip and fall prevention strategies. I'll be recording this conversation to be able to reference your information, but you can request to have the recording paused if you are uncomfortable answering a certain question with the recording active. Do you have any questions before we get started?

1. **Introduction to SF in workplace**:
    a. Have you ever slipped/witnessed a slip in the workplace? To what extent are slips and falls a problem at your site on a scale from 1 to 10 with 1 being not a problem at all and 10 being a serious issue?
    b. What are some of the factors contributing that might make someone slip in your workplace?
    c. What kind of slip-prevention techniques (if any) are in place at your site?
2. **Perspective on footwear**:
    a. What kind of apparel requirements are there (e.g. particular clothing, aprons)? Footwear specifically?

b. Do you think footwear is important for preventing slips and falls? Why?

c. How are decisions made to replace footwear? (e.g. is it up to you, your employer, management)

d. Have you ever suspected that you or others are wearing shoes that need to be replaced? If yes, what made you come to that decision?

3. **Footwear questions**:

a. When do you decide to buy new shoes? For example, consider the last time you bought new shoes - what was the determining factor that led you to buy new shoes? (e.g. after a certain number of months of wear? Comfort? Wear?)

b. Are your shoes SR?

c. Without looking at your shoes and off the top of your head, what can you tell me about the bottom of your shoes?

d. Now look at the bottom of your shoes. What do you notice about it? (e.g. tread design, wear, color, markings) Do you think that your shoes need to be replaced? What features would lead you to make this conclusion?

e. Are these shoes SR?

f. If your shoes would be replaced because of wear on the bottom of your shoes, when do you think you would replace them and why? (e.g. Is there a time?)

g. *Show progressively worn shoe pictures* – At which wear option would you recommend replacing shoes?

4. Tool presentation:

a. I will present three tools for you to determine the size of the worn region and will ask some questions for each [*randomize order of presentation to minimize bias*]

i. Option 1 (Figure 6.3) – Low tech option – handheld indicator – *the user would hold up the indicator against the worn region of the shoe. When the entire worn region fits within the red transparent region, it is recommended to replace the shoes.*

ii. Option 2 (Figure 6.4)– New tech option – phone app – *the user would take picture of the shoe outsole along with some sort of scale and then the app would indicate if shoe replacement is recommended.*

iii. Option 3 (Figure 6.5) – Existing tech option – portable FTIR mechanism – *the user would stand on the shoebox-sized scanner. The tool would then scan the bottom of the shoe and indicate via a light on the side if the shoe should be replaced or not.*

b. Questions for each tool (*after explaining each tool and asking if they understand the tool*):

   i. What do you like about the tool?

   ii. What would make it challenging to use this tool?

   iii. If you could change the tool to make it better, what would you do?

   iv. Do you have any thoughts that might be valuable for the development of this tool?

5. Overall workplace:

a. When developing the tool, integration into the workplace is an important factor to make sure that the tool is used effectively.

i. Can you tell me about the process of entering/exiting your workplace when you start/end your shift? For example, do you clock in for each shift? Is there a place where you leave your personal items?

ii. If you were to use the tools above, when might be an appropriate time to use the tool? Consider both convenience and a time that would be easy to remember.

iii. Can you rate each of the tools to how well they might integrate into your work environment on a scale from 1-10 with 1 being integrated poorly and 10 integrating very well? [*Go through each tool*]

iv. If you had each of these tools, how often would you be willing to use it? *Alternate* phrasing: how often would it be reasonable for your supervisor to require you to use the tool? Follow-up: If recommended, would you be willing to use it every day? Would you be willing to use it every week? Would you be willing to use it every 2 weeks?

6. **Additional information**: Is there anything else that might be helpful for me to know when I'm creating a tool? (e.g., perceptions of tools, workplace environment needs, benefits that might help use)

Appendix C.2 User Feedback Assessment

Appendix C.2.1 User Feedback Eligibility Screening

Study: User Experience Assessment of Portable Shoe Scanner

Principal Investigator: Kurt Beschorner, PhD

The purpose of this research study is to assess the user experience with a portable shoe scanner to be used in the service industry. As such, we are recruiting people who currently work or have worked in the service industry.

If you decide to participate in the study, you will be asked to complete one online session will consist of watching a demonstration video of the potential device and then completing a questionnaire; the entire study will last no more than 20 minutes. If you decide to participate, the only risk is possible breach of confidentiality. There are no direct benefits to you. You will not receive any payment for participation.

Before enrolling people in this study, we need to determine if they are eligible. The following questions and information will assess your overall health to participate in the study. The information will be kept confidential. The purpose of these questions is only to determine whether you are eligible for our study. Remember that your participation is voluntary. This study is being conducted by Sarah Hemler, who can be reached at SLH148@pitt.edu for further questions.

After this eligibility assessment, you will be directed as to the next steps for participation in the study.

Eligibility Criteria

Answer to ALL questions must be YES, otherwise subject is not eligible to participate in the study:

1. Are you 18 years old or older? YES NO

2. Do you currently work in the service industry (e.g. restaurant) OR did you work in the service industry since January 2020? YES NO
3. Are you available for one, 20-minute online session? YES NO

If any answer is 'no', display:

Based on your answer(s), you are/are not eligible for this study. Thank you for your time.

If all answers are 'yes', display:

Based on your answers, you are eligible for this study. Please proceed to the next page to begin the study.

Appendix C.2.2 User Feedback Questionnaire

Please watch this video and then continue to the questionnaire. Note, the video will be available to re-watch at the top of each segment of the questionnaire: [*insert video*]

The following questions will refer to the portable shoe scanner that was introduced. Please answer as if you are being asked to use the scanner in your workplace. Please complete the survey in one sitting; it should take less than 10 minutes.

Video will be available on each page of the questionnaire so that the participant may re-watch at any point.

Usability

1. The instructions were clear and I know how to use the scanner.

Strongly Disagree	*Disagree*	*Neither agree nor disagree*	*Agree*	*Strongly Agree*
1	*2*	*3*	*4*	*5*

2. I believe I would feel safe standing on the scanner without additional support (besides the support box for the other foot).

Strongly Disagree	*Disagree*	*Neither agree nor disagree*	*Agree*	*Strongly Agree*
1	*2*	*3*	*4*	*5*

3. The time it would take to use the scanner (~5 minutes) is reasonable.

Strongly Disagree	*Disagree*	*Neither agree nor disagree*	*Agree*	*Strongly Agree*
1	*2*	*3*	*4*	*5*

4. The time it takes to use the scanner would fit well into my work schedule daily.

Strongly Disagree	*Disagree*	*Neither agree nor disagree*	*Agree*	*Strongly Agree*
1	*2*	*3*	*4*	*5*

5. The time it takes to use the scanner would fit well into my work schedule once a week.

Strongly Disagree	*Disagree*	*Neither agree nor disagree*	*Agree*	*Strongly Agree*
1	*2*	*3*	*4*	*5*

6. The time it took to use the scanner would fit well into my work schedule once a month.

Strongly Disagree	*Disagree*	*Neither agree nor disagree*	*Agree*	*Strongly Agree*
1	*2*	*3*	*4*	*5*

7. The time it takes to use the scanner would fit well into my work schedule once every 3 months.

Strongly Disagree	*Disagree*	*Neither agree nor disagree*	*Agree*	*Strongly Agree*
1	*2*	*3*	*4*	*5*

Usefulness

8. I feel that it is important to know when to replace my shoes.

Strongly Disagree	*Disagree*	*Neither agree nor disagree*	*Agree*	*Strongly Agree*
1	*2*	*3*	*4*	*5*

9. Rate the scanner recommendations (good, replace soon, replace now).

Strongly Disagree	*Disagree*	*Neither agree nor disagree*	*Agree*	*Strongly Agree*
1	*2*	*3*	*4*	*5*

10. If I do not receive money from my employment for new shoes, I would pay out-of-pocket to replace my shoes if I received a ‘replace now’ indication.

Strongly Disagree	*Disagree*	*Neither agree nor disagree*	*Agree*	*Strongly Agree*
1	*2*	*3*	*4*	*5*

11. The lights/shapes to recommend replacement are easy to understand.

Strongly Disagree	*Disagree*	*Neither agree nor disagree*	*Agree*	*Strongly Agree*
1	*2*	*3*	*4*	*5*

Desirability

12. The overall size of the scanner is good.

Strongly Disagree	*Disagree*	*Neither agree nor disagree*	*Agree*	*Strongly Agree*
1	*2*	*3*	*4*	*5*

13. The look of the scanner is important to me.

Strongly Disagree	*Disagree*	*Neither agree nor disagree*	*Agree*	*Strongly Agree*
1	*2*	*3*	*4*	*5*

14. I would use the scanner to know that my shoes are safe.

Strongly Disagree	*Disagree*	*Neither agree nor disagree*	*Agree*	*Strongly Agree*
1	*2*	*3*	*4*	*5*

Is there anything else you'd like to share that could make your experience with the portable shoe scanner better?

_____

_____

_____

_____

_____

Additional Information

1. What is your age: _____
2. What is your sex: M F prefer not to share
3. At what type(s) of service facility(ies) have you worked? (select all that apply):

Restaurant Café Grocery Store Other None of the above

If ‘other’, please list ‘other’ workplace(s): _____

4. What is the total length of time you were/have been employed in the service industry (enter time in years): _____
5. List the position(s) you worked in the service industry (e.g. barista, manager): _____
6. Do you regularly wear slip-resistant shoes at work? (circle one)

   Yes Sometimes No

Bibliography

Albert, D. L., Moyer, B. E., & Beschorner, K. E. (2017). Three-Dimensional Shoe Kinematics During Unexpected Slips: Implications for Shoe–Floor Friction Testing. *IISE Transactions on Occupational Ergonomics and Human Factors, 5*(1), 1-11.

Archard, J. (1953). Contact and rubbing of flat surfaces. *Journal of applied physics, 24*(8), 981-988.

Aschan, C., Hirvonen, M., Mannelin, T., & Rajamäki, E. (2005). Development and validation of a novel portable slip simulator. *Applied ergonomics, 36*(5), 585-593.

ASTM, A. S. f. T. a. M. (2011). ASTM F2913-11: Standard Test method for Measuring the Coefficient of Friction for Evaluation of Slip performance of Footwear and Test Surfaces/Flooring Using a Whole Shoe Tester. In. West Conshohocken, PA: ASTM International.

ASTM, A. S. f. T. a. M. (2015). ASTM D2240-15: Standard Test Method for Rubber Property-Durometer Hardness. In: ASTM International.

Békési, N. (2012). Modelling Friction and abrasive wear of elastomers. *Advanced Elastomers-Technology, Properties and Applications*. Retrieved from https://books.google.com/books?hl=en&lr=&id=nOecDwAAQBAJ&oi=fnd&pg=PA341&dq=Modelling+friction+and+abrasive+wear+of+elastomers&ots=1EianqlYdN&sig=9v2bikAvbXKSyhaP-9C8sIz1REA#v=onepage&q=Modelling%20friction%20and%20abrasive%20wear%20of%20elastomers&f=false

Békési, N., & Váradi, K. (2010). Wear simulation of a reciprocating seal by global remeshing. *Periodica Polytechnica. Engineering. Mechanical Engineering, 54*(2), 71.

Békési, N., Váradi, K., & Felhős, D. (2011). Wear simulation of a reciprocating seal. *Journal of Tribology, 133*(3).

Bell, J. L., Collins, J. W., & Chiou, S. (2018). Effectiveness of a no-cost-to-workers, slip-resistant footwear program for reducing slipping-related injuries in food service workers: a cluster randomized trial. *Scandinavian Journal of Work, Environment & Health*.

Beschorner, K. E., Albert, D. L., Chambers, A. J., & Redfern, M. S. (2014). Fluid pressures at the shoe–floor–contaminant interface during slips: Effects of tread & implications on slip severity. *Journal of Biomechanics, 47*(2), 458-463.

Beschorner, K. E., Albert, D. L., & Redfern, M. S. (2016). Required coefficient of friction during level walking is predictive of slipping. *Gait & posture, 48*, 256-260.

Beschorner, K. E., Jones, T. G., & Iraqi, A. (2017). *The Combined Benefits of Slip-Resistant Shoes and High Traction Flooring on Coefficient of Friction Exceeds Their Individual Contributions.* Paper presented at the Proceedings of the Human Factors and Ergonomics Society Annual Meeting.

Beschorner, K. E., Lovell, M., Higgs III, C. F., & Redfern, M. S. (2009). Modeling mixed-lubrication of a shoe-floor interface applied to a pin-on-disk apparatus. *Tribology Transactions, 52*(4), 560-568.

Beschorner, K. E., Redfern, M. S., Porter, W. L., & Debski, R. E. (2007). Effects of slip testing parameters on measured coefficient of friction. *Applied ergonomics, 38*(6), 773-780.

Beschorner, K. E., Siegel, J. L., Hemler, S. L., Sundaram, V. H., Chanda, A., Iraqi, A., . . . Redfern, M. S. (2020). An observational ergonomic tool for assessing the worn condition of slip-resistant shoes. *Applied ergonomics, 88*, 103140.

Beschorner, K. E., & Singh, G. (2012). *A novel method for evaluating the effectiveness of shoe-tread designs relevant to slip and fall accidents.* Paper presented at the Proceedings of the Human Factors and Ergonomics Society Annual Meeting.

Betts, R. P., Franks, C. I., Duckworth, T., & Burke, J. (1980). Static and dynamic foot-pressure measurements in clinical orthopaedics. *Medical and biological Engineering and Computing, 18*(5), 674.

Bharthi, R., Sukinik, J., Hemler, S. L., & Beschorner, K. E. (2020). *Correlation Between the Locations of Shoe Wear Region and Center of the Contact Region at Peak Friction.* Paper presented at the Biomedical Engineering Society Annual Conference, Virtual.

Blanchette, M. G., & Powers, C. M. (2015). The influence of footwear tread groove parameters on available friction. *Applied ergonomics, 50*, 237-241.

Bridgestone. (2021). HOW TO CHECK TIRE TREAD DEPTH. Retrieved from https://www.bridgestonetire.com/tread-and-trend/drivers-ed/how-to-check-your-tire-tread-penny-test

Brooks Sports, I. (2020). When to replace your running shoes.

Burnfield, J. M., & Powers, C. M. (2006). Prediction of slips: an evaluation of utilized coefficient of friction and available slip resistance. *Ergonomics, 49*(10), 982-995.

Cagan, J., & Vogel, C. M. (2020). *Creating Breakthrough Products: Revealing the Secrets that Drive Global Innovation (Special Second Edition)* (Second Edition ed.). Pittsburgh, PA.

Cham, R., & Redfern, M. S. (2002). Changes in gait when anticipating slippery floors. *Gait & posture, 15*(2), 159-171.

Chanda, A., Jones, T. G., & Beschorner, K. E. (2018). Generalizability of Footwear Traction Performance across Flooring and Contaminant Conditions. *IISE Transactions on Occupational Ergonomics and Human Factors*(just-accepted), 1-23.

Chanda, A., Reuter, A., & Beschorner, K. E. (2019). Vinyl Composite Tile Surrogate for Mechanical Slip Testing. *IISE Transactions on Occupational Ergonomics and Human Factors, 7*(2), 132-141.

Chang, W.-R., Chang, C.-C., & Matz, S. (2011). The effect of transverse shear force on the required coefficient of friction for level walking. *Human factors, 53*(5), 461-473.

Chang, W.-R., Grönqvist, R., Leclercq, S., Brungraber, R. J., Mattke, U., Strandberg, L., . . . Courtney, T. K. (2001). The role of friction in the measurement of slipperiness, Part 2: Survey of friction measurement devices. *Ergonomics, 44*(13), 1233-1261.

Chang, W.-R., Grönqvist, R., Leclercq, S., Myung, R., Makkonen, L., Strandberg, L., . . . Thorpe, S. C. (2001). The role of friction in the measurement of slipperiness, Part 1: Friction mechanisms and definition of test conditions. *Ergonomics, 44*(13), 1217-1232.

Chang, W.-R., Leclercq, S., Lockhart, T. E., & Haslam, R. (2016). State of science: occupational slips, trips and falls on the same level. *Ergonomics, 59*(7), 861-883.

Cook, A., Hemler, S., Sundaram, V., Chanda, A., & Beschorner, K. (2021). Differences in friction performance between new and worn shoes. *IISE Transactions on Occupational Ergonomics and Human Factors, Taylor & Francis*, 1-8. doi:10.1080/24725838.2021.1925998

Courtney, T. K., Sorock, G. S., Manning, D. P., Collins, J. W., & Holbein-Jenny, M. A. (2001). Occupational slip, trip, and fall-related injuries–can the contribution of slipperiness be isolated? *Ergonomics, 44*(13), 1118-1137.

Darragh, A. R., Lavender, S., Polivka, B., Sommerich, C. M., Wills, C. E., Hittle, B. A., . . . Stredney, D. L. (2016). Gaming Simulation as Health and Safety Training for Home Health Care Workers. *Clinical simulation in nursing, 12*(8), 328-335. doi:10.1016/j.ecns.2016.03.006

De, S. K., & White, J. R. (2001). *Rubber technologist's handbook* (Vol. 1): iSmithers Rapra Publishing.

Dwyer-Joyce, R. S., Drinkwater, B. W., & Donohoe, C. J. (2003). The measurement of lubricant–film thickness using ultrasound. *Proceedings of the Royal Society of London. Series A: Mathematical, Physical and Engineering Sciences, 459*(2032), 957-976.

Firestone - Complete Auto Care. HOW TO TELL IF YOU NEED NEW TIRES? Retrieved from https://www.firestonecompleteautocare.com/penny-tire-test/

Fryar, C. D., Carroll, M. D., & Ogden, C. L. (2018). Prevalence of overweight, obesity, and severe obesity among adults aged 20 and over: United States, 1960–1962 through 2015–2016.

Fuller, D. (1956). *Theory and Practice of Lubrication for Engineers*. New York: John Wiley & Sons, Inc.

Gent, A. N., & Pulford, C. T. R. (1983). Mechanisms of rubber abrasion. *Journal of Applied Polymer Science, 28*(3), 943-960. doi:10.1002/app.1983.070280304

Goodyear Auto Service. (2021). How to Check Tire Tread Depth. Retrieved from https://www.goodyearautoservice.com/en-US/tire-basics/tread-depth

Grönqvist, R. (1995). Mechanisms of friction and assessment of slip resistance of new and used footwear soles on contaminated floors. *Ergonomics, 38*(2), 224-241.

Hamrock, B. J. (1994). *Fundamentals of fluid film lubrication*: McGraw-Hill, Inc.

Han, J. Y. (2005). *Low-cost multi-touch sensing through frustrated total internal reflection.* Paper presented at the Proceedings of the 18th annual ACM symposium on User interface software and technology.

Hanson, J. P., Redfern, M. S., & Mazumdar, M. (1999). Predicting slips and falls considering required and available friction. *Ergonomics, 42*(12), 1619-1633.

Harrick, N. J. (1962). Use of Frustrated Total Internal Reflection to Measure Film Thickness and Surface Reliefs. *Journal of applied physics, 33*(9), 2774-2775. doi:10.1063/1.1702547

Health and Safety Laboratory U.K. (2009). HSE/HSL Footwear slip resistance testing results - updated April 2009. Retrieved from http://web.archive.org/web/20090612113348/http://www.hse.gov.uk/slips/research/footwear-results-april09.pdf

Hemler, S. L., & Beschorner, K. E. (2019a). *Effect of Progressive Shoe Wear and Heel Type on Traction Performance Changes.* Paper presented at the Society of Tribologists and Lubrication Engineers Annual Meeting, Nashville, TN.

Hemler, S. L., & Beschorner, K. E. (2019b). *Predicting Slip Risk Based on Footwear.* Paper presented at the Society of Tribologists and Lubrication Engineers, Nashville, TN.

Hemler, S. L., & Beschorner, K. E. (2020). *Influence of individual gait and shoe design factors on tread wear*. Paper presented at the Slips, Trips and Falls Conference, Madrid, Spain.

Hemler, S. L., Charbonneau, D. N., & Beschorner, K. E. (2017). *Effects of Shoe Wear on Slipping–Implications for Shoe Replacement Threshold.* Paper presented at the Proceedings of the Human Factors and Ergonomics Society Annual Meeting.

Hemler, S. L., Charbonneau, D. N., & Beschorner, K. E. (2020). Predicting hydrodynamic conditions under worn shoes using the tapered-wedge solution of Reynolds equation. *Tribology International, 145*, 106161.

Hemler, S. L., Charbonneau, D. N., Iraqi, A., Redfern, M. S., Haight, J. M., Moyer, B. E., & Beschorner, K. E. (2019). Changes in under-shoe traction and fluid drainage for progressively worn shoe tread. *Applied ergonomics, 80*, 35-42.

Hemler, S. L., Pliner, E. M., Redfern, M. S., Haight, J. M., & Beschorner, K. E. (2020). Traction performance across the life of slip-resistant footwear: preliminary results from a longitudinal study. *Journal of Safety Research*.

Hemler, S. L., Pliner, E. M., Redfern, M. S., Haight, J. M., & Beschorner, K. E. (2021). *Traction Performance during Wear Varies Across Shoes.* Paper presented at the International Ergonomics Association, Vancouver, CA.

Hemler, S. L., Redfern, M. S., Haight, J. M., & Beschorner, K. E. (2018a). *Influence of Natural Wear Progression on Shoe Floor Traction–A Pilot Study.* Paper presented at the Proceedings of the Human Factors and Ergonomics Society Annual Meeting.

Hemler, S. L., Redfern, M. S., Haight, J. M., & Beschorner, K. E. (2018b). *Mapping the traction performance of work shoes during natural progressive wear.* Paper presented at the CDC - National Occupational Injury Research Symposium, Morgantown, WV.

Hemler, S. L., Sider, J. R., & Beschorner, K. E. (2019). *Influence of Required Coefficient of Friction on Rate of Shoe Wear.* Paper presented at the International Society of Posture & Gait Research World Congress, Edinburgh, Scotland.

Hemler, S. L., Sider, J. R., Redfern, M. S., & Beschorner, K. E. (2021). Gait Kinetics Impact Shoe Tread Wear Rate. *Gait & posture, 86*, 157-161.

Hemler, S. L., Sundaram, V. H., & Beschorner, K. E. (2019). *Influence of slip-resistant shoe classification and shoe age on under-shoe hydrodynamics during human slips.* Paper presented at the International Society of Biomechanics & American Society of Biomechanics, Calgary, Alberta, Canada.

Hemler, S. L., Sundaram, V. H., & Beschorner, K. E. (2020). *A hydrodynamics model to predict under-shoe fluid pressures based on the dimensions of a worn region.* Paper presented at the American Society of Biomechanics, Virtual.

Hemler, S. L., Tushak, C. M., Walter, P. J., & Beschorner, K. E. (2020). *Shoe tread wear rate may not necessarily be associated with material hardness.* Paper presented at the Society of Tribologists and Lubrication Engineers, Conference cancelled due to COVID-19 pandemic; abstract accepted.

Hunter, J. G., Miller, R. H., & Suydam, S. (2017). *Accuracy of a shoe-worn device to measure running mechanics*.

Ido, T., Yamaguchi, T., Shibata, K., Matsuki, K., Yumii, K., & Hokkirigawa, K. (2019). Sliding friction characteristics of styrene butadiene rubbers with varied surface roughness under water lubrication. *Tribology International, 133*, 230-235.

Imbimbo, M., & De Luca, A. (1998). FE stress analysis of rubber bearings under axial loads. *Computers & structures, 68*(1), 31-39.

Iraqi, A., & Beschorner, K. E. (2017). *Vertical Ground Reaction Forces During Unexpected Human Slips*. Paper presented at the Proceedings of the Human Factors and Ergonomics Society Annual Meeting.

Iraqi, A., Cham, R., Redfern, M. S., & Beschorner, K. E. (2018). Coefficient of friction testing parameters influence the prediction of human slips. *Applied ergonomics, 70*, 118-126.

Iraqi, A., Cham, R., Redfern, M. S., Vidic, N. S., & Beschorner, K. E. (2018). Kinematics and kinetics of the shoe during human slips. *Journal of Biomechanics, 74*, 57-63.

Iraqi, A., Vidic, N. S., Redfern, M. S., & Beschorner, K. E. (2020). Prediction of coefficient of friction based on footwear outsole features. *Applied ergonomics, 82*, 102963.

ISO. (2019). ISO 9241-210: Ergonomics of human-system interaction - Part 210: Human-centred design for interactive systems. In.

ISO/DIS. (2020). ISO/DIS 20345: Personal protective equipment - safety footwear.

ISO/IEC. (2001). ISO 20871:2001 Footwear - Test methods for outsoles - Abrasion resistance. In. Geneva, Switzerland: ISO/IEC.

James, S. L., Lucchesi, L. R., Bisignano, C., Castle, C. D., Dingels, Z. V., Fox, J. T., . . . Liu, Z. (2020). The global burden of falls: global, regional and national estimates of morbidity and mortality from the Global Burden of Disease Study 2017. *Injury prevention*.

Jones, T. G., Iraqi, A., & Beschorner, K. E. (2018). Performance testing of work shoes labeled as slip resistant. *Applied ergonomics, 68*, 304-312. doi:10.1016/j.apergo.2017.12.008

Jordan, P. W. (1998). *An introduction to usability*: CRC Press.

Kadaba, M. P., Ramakrishnan, H. K., & Wootten, M. E. (1990). Measurement of lower extremity kinematics during level walking. *Journal of orthopaedic research, 8*(3), 383-392.

Kajdas, C., Wilusz, E., & Harvey, S. (1990). *Encyclopedia of tribology* (Vol. 15): Elsevier.

Kim, I.-J. (2000). *Wear progression of shoe heels during slip resistance measurements.* Paper presented at the Proceedings of the Human Factors and Ergonomics Society Annual Meeting.

Kim, S., Lockhart, T., & Yoon, H.-Y. (2005). Relationship between age-related gait adaptations and required coefficient of friction. *Safety Science, 43*(7), 425-436.

Kummer, H. W. (1966). Unified theory of rubber and tire friction.

Leamon, T. B., & Li, K. W. (1990). *Microslip length and the perception of slipping.* Paper presented at the Proceedings of 23rd International Congress on Occupational Health.

Li, K. W., & Chen, C. J. (2004). The effect of shoe soling tread groove width on the coefficient of friction with different sole materials, floors, and contaminants. *Applied ergonomics, 35*(6), 499-507.

Li, K. W., & Chen, C. J. (2005). Effects of tread groove orientation and width of the footwear pads on measured friction coefficients. *Safety Science, 43*(7), 391-405.

Li, K. W., Wu, H. H., & Lin, Y.-C. (2006). The effect of shoe sole tread groove depth on the friction coefficient with different tread groove widths, floors and contaminants. *Applied ergonomics, 37*(6), 743-748.

Liberty Mutual Insurance. (2018). *2018 Liberty Mutual Workplace Safety Index*. Retrieved from https://business.libertymutualgroup.com/business-insurance/Documents/Services/Workplace%20Safety%20Index.pdf

Liberty Mutual Insurance. (2020). 2020 workplace safety index: the top 10 causes of disabling injuries. Retrieved from https://viewpoint.libertymutualgroup.com/article/2020-workplace-safety-index-the-top-10-causes-of-disabling-injuries/?extcmp=BLMG_mod_WSI2020

Liberty Mutual Research Institute for Safety. (2016). *2016 Liberty Mutual Workplace Safety Index*. Retrieved from www.libertymutualgroup.com

Liberty Mutual Research Institute for Safety. (2017). *2017 Liberty Mutual Workplace Safety Index*. Retrieved from https://www.libertymutualgroup.com/about-liberty-mutual-site/news-site/Pages/2017-Liberty-Mutual-Workplace-Safety-Index.aspx

Lowe, B., Dempsey, P., & Jones, E. (2018). Assessment Methods Used by Certified Ergonomics Professionals. *Proceedings of the Human Factors and Ergonomics Society Annual Meeting, 62*(1), 838-842. doi:10.1177/1541931218621191

Lupker, H., Cheli, F., Braghin, F., Gelosa, E., & Keckman, A. (2004). Numerical prediction of car tire wear. *Tire Science and Technology, 32*(3), 164-186.

Maegawa, S., Itoigawa, F., & Nakamura, T. (2016). A role of friction-induced torque in sliding friction of rubber materials. *Tribology International, 93*, 182-189.

Manager of Fast Food Restaurant A - SME #3. (2020) *Subject Matter Expert Interview/Interviewer: S. L. Hemler*.

Manager of Fast Food Restaurant A - SME #7. (2020) *Subject Matter Expert Interview/Interviewer: S. L. Hemler*.

Manager of Fast Food Restaurant B & C - SME #2. (2020) *Subject Matter Expert Interview/Interviewer: S. L. Hemler*.

Manning, D., Jones, C., & Bruce, M. (1985). Boots for oily surfaces. *Ergonomics, 28*(7), 1011-1019.

Manning, D. P., Jones, C., & Bruce, M. (1990). Proof of shoe slip-resistance by a walking traction test. *Journal of Occupational Accidents, 12*(4), 255-270.

Mars, W. V., & Fatemi, A. (2002). A literature survey on fatigue analysis approaches for rubber. *International Journal of fatigue, 24*(9), 949-961.

Mars, W. V., & Fatemi, A. (2004). Factors that affect the fatigue life of rubber: a literature survey. *Rubber Chemistry and Technology, 77*(3), 391-412.

Maslow, A. H. (1943). A theory of human motivation. *Psychological review*, *50*(4), 370.

Meng, H. C., & Ludema, K. C. (1995). Wear models and predictive equations: their form and content. *Wear, 181-183*, 443-457. doi:10.1016/0043-1648(95)90158-2

Moghaddam, S. R. M. (2018). *Computational Models for Predicting Shoe Friction and Wear.* (Doctor of Philosophy). University of Pittsburgh,

Moghaddam, S. R. M., Acharya, A., Redfern, M. S., & Beschorner, K. E. (2018). Predictive multiscale computational model of shoe-floor coefficient of friction. *Journal of Biomechanics, 66*, 145-152.

Moghaddam, S. R. M., Hemler, S. L., Redfern, M. S., Jacobs, T. D. B., & Beschorner, K. E. (2019). Computational model of shoe wear progression: Comparison with experimental results. *Wear, 422*, 235-241.

Moghaddam, S. R. M., Iraqi, A., & Beschorner, K. E. (2014). *Finite Element Model of Wear Progression in Shoe Soles*. Paper presented at the STLE Tribology Frontiers Conference, Chicago.

Moghaddam, S. R. M., Redfern, M. S., & Beschorner, K. E. (2015). A microscopic finite element model of shoe–floor hysteresis and adhesion friction. *Tribology letters*, *59*(3), 42.

Moore, D. F. (1975). The friction of pneumatic tyres.

Moriyasu, K., Nishiwaki, T., Shibata, K., Yamaguchi, T., & Hokkirigawa, K. (2019). Friction control of a resin foam/rubber laminated block material. *Tribology International, 136*, 548-555.

Moyer, B. E. (2006). *Slip and fall risks: Pre-slip gait contributions and post-slip response effects.* University of Pittsburgh,

Myshkin, N. K., Petrokovets, M. I., & Kovalev, A. V. (2006). Tribology of polymers: adhesion, friction, wear, and mass-transfer. *Tribology International, 38*(11), 910-921.

National Center for Injury Prevention and Control, C. (2018). 10 Leading Causes of Nonfatal Emergency Department Visits, United States. Retrieved from https://webappa.cdc.gov/sasweb/ncipc/nfilead.html

National Occupational Research Agenda (NORA) Traumatic Injury Prevention Cross-Sector Council. (2021). Posters: Slip Resistant Shoe Tread Wear. Retrieved from https://www.cdc.gov/nora/councils/ti/posters.html

Needham, J. A., & Sharp, J. S. (2016). Watch your step! A frustrated total internal reflection approach to forensic footwear imaging. *Scientific reports*, *6*, 21290.

Newton, I. (1952). *Opticks, or, a treatise of the reflections, refractions, inflections & colours of light*: Courier Corporation.

Nighswonger, T. (2020). If the Shoe Fits the Hazard, Wear It - Matching the correct footwear to a specific work environment can improve safety and reduce risks. Retrieved from https://www.ehstoday.com/ppe/foot-protection/article/21907466/if-the-shoe-fits-the-hazard-wear-it

Norman, D. A. (1988). OF EVERYDAY THINGS. In: New York City, NY, USA: Doubleday.

Occupational Health & Safety. (2018). A Guide to Safety Footwear Regulations - Good shoes make better employees. Retrieved from https://ohsonline.com/Articles/2018/04/01/A-Guide-to-Safety-Footwear-Regulations.aspx

Optimum Safety Management. Workplace Injury Prevention: Using the Right Footwear. Retrieved from https://www.optimumsafetymanagement.com/blog/workplace-injury-prevention-footware/

Pahl, G., & Beitz, W. (2013). *Engineering design: a systematic approach*: Springer Science & Business Media.

Paivio, A., Rogers, T. B., & Smythe, P. C. (1968). Why are pictures easier to recall than words? *Psychonomic Science*, *11*(4), 137-138. doi:10.3758/bf03331011

Pascoe, M., & Tabor, D. (1956). The friction and deformation of polymers. *Proceedings of the Royal Society of London. Series A. Mathematical and Physical Sciences*, *235*(1201), 210-224. Retrieved from https://royalsocietypublishing.org/doi/abs/10.1098/rspa.1956.0077?casa_token=nGBpAdfOvFsAAAAA:izEXydIznHRIENDlZx-hgpjeJcFigtDcLYX_mLhbKxTvIZn5z8maWF8uBbQ1vIaZrZ-QQ9M0O4dB

Pea, R. D. (1987). User centered system design: new perspectives on human-computer interaction. *Journal educational computing research, 3*(1), 129-134.

Perkins, P. J. (1978). Measurement of slip between the shoe and ground during walking. In *Walkway surfaces: Measurement of slip resistance*: ASTM International.

Pliner, E. M., Hemler, S. L., & Beschorner, K. E. (2019). *Gait Parameters of Shoe Wear: A Case Study of the Shoe Wear Rate by Individual Gait Parameters.* Paper presented at the Society of Tribologists and Lubrication Engineers Annual Meeting, Nashville, TN.

Polivka, B. J., Anderson, S., Lavender, S. A., Sommerich, C. M., Stredney, D. L., Wills, C. E., & Darragh, A. R. (2019). Efficacy and usability of a virtual simulation training system for health and safety hazards encountered by healthcare workers. *Games for health journal, 8*(2), 121-128.

Power, C. (1992). Will it sell in Podunk? Hard to say. *Business Week, 10*, 46-47.

Proctor, T. D., & Coleman, V. (1988). Slipping, tripping and falling accidents in Great Britain—present and future. *Journal of Occupational Accidents, 9*(4), 269-285.

Razzaghi-Kashani, M., & Padovan, J. (1998). Simulation of surface flaw propagation associated with the mechanical fatigue wear of elastomers. *Rubber Chemistry and Technology, 71*(2), 214-233.

Redfern, M. S., Cham, R., Gielo-Perczak, K., Grönqvist, R., Hirvonen, M., Lanshammar, H., . . . Powers, C. (2001). Biomechanics of slips. *Ergonomics, 44*(13), 1138-1166.

Sanders, E. B. N. (1992). Converging perspectives: product development research for the 1990s. *Design Management Journal (Former Series), 3*(4), 49-54.

Sato, S., Yamaguchi, T., Shibata, K., Nishi, T., Moriyasu, K., Harano, K., & Hokkirigawa, K. (2020). Dry sliding friction and Wear behavior of thermoplastic polyurethane against abrasive paper. *Biotribology*, 100130.

Savkoor, A. (1965). On the friction of rubber. *Wear, 8*(3), 222-237. Retrieved from https://www.sciencedirect.com/science/article/abs/pii/0043164865901614

Schallamach, A. (1958). Friction and abrasion of rubber. *Wear, 1*(5), 384-417. Retrieved from https://www.sciencedirect.com/science/article/abs/pii/0043164858901133

Schallamach, A. (1971). How does rubber slide? *Wear, 17*(4), 301-312. Retrieved from https://www.sciencedirect.com/science/article/abs/pii/0043164871900330

Shoes For Crews. (2013). SHOES FOR CREWS® $5,000 Slip & Fall Warranty: Limitations, Conditions & Exceptions. Retrieved from https://web.archive.org/web/20110708152954/http://www.shoesforcrews.com/sfc3/index.cfm?route=inserts.warranty/warranty5k.cfm

Shoes For Crews. (2019a). Outsole Care. In.

Shoes For Crews. (2019b). Shoe Care and Cleaning Tips. . Retrieved from https://www.shoesforcrews.com/sfc3/index.cfm?changeWebsite=US_en&route=inserts.QA/cleaning_caring

Shoes For Crews (Europe). (2019). How Often Should You Replace Work Shoes? Retrieved from https://blog.sfceurope.com/how-often-should-you-replace-work-shoes

Singh, G., & Beschorner, K. E. (2014). A Method for Measuring Fluid Pressures in the Shoe–Floor–Fluid Interface: Application to Shoe Tread Evaluation. *IIE Transactions on Occupational Ergonomics and Human Factors, 2*(2), 53-59.

Skechers. (2013). SKECHERS USA, INC.'S ("SKECHERS")
$5,000 SLIP & FALL WARRANTY. Retrieved from http://sh.skechers.com/skechers/skechers-direct/pdf/SlipandFallWarrantyandProcedures.pdf

Sommerich, C. M., Evans, K. D., Lavender, S. A., Sanders, E., Joines, S., Lamar, S., . . . Park, S. (2019). Collaborating With Sonographers and Vascular Technologists to Develop Ergonomics Interventions to Address Work-Related Musculoskeletal Disorders. *Journal of Diagnostic Medical Sonography, 35*(1), 23-37.

Southern, E., & Thomas, A. (1979). Studies of rubber abrasion. *Rubber Chemistry and Technology, 52*(5), 1008-1018. Retrieved from https://meridian.allenpress.com/rct/article-abstract/52/5/1008/91300

SR Max Slip Resistant Shoe Company. (2017). Get a Grip! Quick tips to stop slips. Retrieved from https://www.srmax.com/education/blog/when-should-you-replace-your-work-

shoes#:~:text=You'll%20Have%20to%20Replace%20Them%20Eventually&text=Generally%2C%20slip%20resistant%20shoes%20will,has%20to%20be%20replaced%20eventually.

Sridharan, K., & Sivaramakrishnan, R. (2012). Dynamic behavior of tyre tread block. *American Journal of Engineering and Applied Sciences, 5*(2).

Stachowiak, G., & Batchelor, A. W. (2013). *Engineering Tribology*. Oxford, UNITED STATES: Elsevier Science & Technology.

Strandberg, L. (1983). On accident analysis and slip-resistance measurement. *Ergonomics, 26*(1), 11-32.

Strandberg, L. (1985). The effect of conditions underfoot on falling and overexertion accidents. *Ergonomics, 28*(1), 131-147.

Sukinik, J., Bharthi, R., Hemler, S. L., & Beschorner, K. E. (2020). *Relationship Between Center of Pressure and Contact Region During Gait: Implication for Shoe Wear and Slipping Risk.* Paper presented at the Biomedical Engineering Society Annual Conference, Virtual.

Sundaram, V. H., Hemler, S. L., Chanda, A., Haight, J. M., Redfern, M. S., & Beschorner, K. E. (2020). Worn Region Size of Shoe Outsole Impacts Human Slips: Testing a Mechanistic Model. *Journal of Biomechanics*, 109797.

Sundaram, V. H., Hemler, S. L., Chanda, A., Haight, J. M., Redfern, M. S., & Beschorner, K. E. (2020). Worn Region Size of Shoe Outsole Impacts Human Slips: Testing a Mechanistic Model. *Journal of Biomechanics, 105*(109797).

Team Member of Fast Food Restaurant A & B - SME #5. (2020) *Subject Matter Expert Interview/Interviewer: S. L. Hemler*.

Team Member of Fast Food Restaurant B - SME #1. (2020) *Subject Matter Expert Interview/Interviewer: S. L. Hemler*.

Team Member of Full Service Restaurant A and Grocery Store A - SME #4. (2020) *Subject Matter Expert Interview/Interviewer: S. L. Hemler*.

Team Member of Grocery Store B - SME #6. (2020) *Subject Matter Expert Interview/Interviewer: S. L. Hemler*.

The Texas Department of Insurance. Footwear Safety FactSheet. Retrieved from https://www.tdi.texas.gov/pubs/videoresource/fsfootwear.pdf

Thomas, S., Gupta, B. R., & De, S. K. (1987). Tear and wear of thermoplastic elastomers from blends of poly(propylene) and ethylene vinyl acetate rubber. *Journal of Materials Science, 22*(9), 3209-3216. doi:10.1007/bf01161184

Tisserand, M. (1985). Progress in the prevention of falls caused by slipping. *Ergonomics, 28*(7), 1027-1042.

Torkki, M., Malmivaara, A., Reivonen, N., Seitsalo, S., Laippala, P., & Hoikka, V. (2002). Individually fitted sports shoes for overuse injuries among newspaper carriers. *Scandinavian Journal of Work, Environment & Health, 28*(3), 176-183. doi:10.2307/40967193

Tracy, R. H., Reeves, E. H., Radclyffe, N. J., & Longden, R. M. (2004). Hand held probe for measuring tire tread wear. In: Google Patents.

Trkov, M., Yi, J., Liu, T., & Li, K. (2018). Shoe–floor interactions in human walking with slips: Modeling and experiments. *Journal of biomechanical engineering, 140*(3), 031005.

Tsai, Y. J., & Powers, C. M. (2008). The influence of footwear sole hardness on slip initiation in young adults. *Journal of forensic sciences, 53*(4), 884-888.

U.S. Department of Health & Human Services. (2020). User-Centered Design Basics. Retrieved from https://www.usability.gov/what-and-why/user-centered-design.html

U.S. Department of Labor - Bureau of Labor Statistics. (2020). *Nonfatal Occupational Injuries and Illnesses Requiring Days Away From Work, 2018*. Retrieved from Washington, D.C.:

U.S. Department of Labor - Bureau of Labor Statistics. (2021). *Nonfatal Occupational Injuries and Illnesses Requiring Days Away From Work, 2019*. Retrieved from

Unnava, H. R., & Burnkrant, R. E. (1991). An imagery-processing view of the role of pictures in print advertisements. *Journal of Marketing Research, 28*(2), 226-231.

Verma, S. K., Chang, W. R., Courtney, T. K., Lombardi, D. A., Huang, Y.-H., Brennan, M. J., . . . Perry, M. J. (2011). A prospective study of floor surface, shoes, floor cleaning and slipping in US limited-service restaurant workers. *Occupational and environmental medicine, 68*(4), 279-285.

Verma, S. K., Zhao, Z., Courtney, T. K., Chang, W.-R., Lombardi, D. A., Huang, Y.-H., . . . Perry, M. J. (2014). Duration of slip-resistant shoe usage and the rate of slipping in limited-service restaurants: results from a prospective and crossover study. *Ergonomics, 57*(12), 1919-1926.

Walter, P. J., Tushak, C. M., Hemler, S. L., & Beschorner, K. E. (2021). Effect of tread design and hardness on interfacial fluid force and friction in artificially worn shoes. *Footwear Science, in review*.

Washington State Department of Labor & Industries. (2020). *Claim counts and costs by OIICS Accident Type*.

Yamaguchi, T., & Hokkirigawa, K. (2014). Development of a High Slip-resistant Footwear Outsole Using a Hybrid Rubber Surface Pattern. *Industrial Health, 52*(5), 414-423. doi:10.2486/indhealth.2014-0105

Yamaguchi, T., Katsurashima, Y., & Hokkirigawa, K. (2017). Effect of rubber block height and orientation on the coefficients of friction against smooth steel surface lubricated with glycerol solution. *Tribology International, 110*, 96-102.

Yamaguchi, T., Umetsu, T., Ishizuka, Y., Kasuga, K., Ito, T., Ishizawa, S., & Hokkirigawa, K. (2012). Development of new footwear sole surface pattern for prevention of slip-related falls. *Safety Science, 50*(4), 986-994.

Zhang, S.-W. (2004). *Tribology of elastomers*: Elsevier.

Zhu, S., Yu, A. W., Hawley, D., & Roy, R. (1986). Frustrated total internal reflection: A demonstration and review. *American Journal of Physics, 54*(7), 601-607. doi:10.1119/1.14514